TOPOLOGICAL ORGANIZATION, FUNCTIONAL CHARACTERIZATION AND LOCALIZATION OF THE BOVINE ROD PHOTORECEPTOR Na/Ca-K EXCHANGER

by

Tom Sang-Yong Kim

B.Sc., University of British Columbia, 1992

A THESIS SUBMITTED IN PARTIAL FULFILLMENT OF

THE REQUIREMENTS FOR THE DEGREE OF

Doctor of Philosophy

in

THE FACULTY OF GRADUATE STUDIES

Department of Biochemistry and Molecular Biology

We accept this thesis as conforming

to the required standard

THE UNIVERSITY OF BRITISH COLUMBIA

October 1998

In presenting this thesis in partial fulfilment of the requirements for an advanced degree at the University of British Columbia, I agree that the Library shall make it freely available for reference and study. I further agree that permission for extensive copying of this thesis for scholarly purposes may be granted by the head of my department or by his or her representatives. It is understood that copying or publication of this thesis for financial gain shall not be allowed without my written permission.

Department of Biochemistry & Molecular Biology

The University of British Columbia
Vancouver, Canada

Date Feb 26/99

ABSTRACT

The Na/Ca-K exchanger in vertebrate photoreceptors plays an essential role in regulating the calcium concentration in photoreceptor outer segments. The structural and functional properties of the bovine rod photoreceptor Na/Ca-K exchanger were examined in this study using eight, anti-exchanger monoclonal antibodies.

Experimental evidence for the topological organization of the exchanger was provided by mapping the epitopes of the antibodies using glutathione S-transferase fusion proteins containing specific regions of the exchanger. Five antibodies were mapped to the large N-terminal hydrophilic domain and shown to label the extracellular surface of the rod outer segment (ROS) plasma membrane by immunogold labeling for electron microscopy. Three antibodies were mapped to the hydrophilic domain connecting the two putative transmembrane domains and shown to label the cytoplasmic surface.

The antibodies were also used to determine subcellular localization of the exchanger and to purify the exchanger by immunoaffinity chromatography. The exchanger was localized to the plasma membrane of rod photoreceptor outer segments. When the ROS membrane proteins were solubilized in CHAPS detergent, the exchanger did not appear to co-purify with other ROS membrane proteins. Treatment of the immunoaffinity-purified exchanger with deglycosylating enzymes indicated that the exchanger possesses a large amount of O-linked oligosaccharides in the large N-terminal hydrophilic domain.

Limited proteolysis was used to determine the importance of the large extracellular and intracellular domains for ion transport. Trypsin degraded the extracellular domain, and kallikrein degraded a large part of the cytoplasmic domain. Following the removal of either of these hydrophilic domains, the exchanger exhibited Na^+ and K^+-dependent Ca^{2+} efflux activity similar

to that of the untreated exchanger. The Vmax for the protease treated exchangers, however, increased ~2 fold. These results indicate that the ion binding and transport sites are located within or near the transmembrane domains and the removal of the bulky hydrophilic domain enables the exchanger to undergo a faster conformational change during ion transport.

The oligomeric nature of the exchanger was determined using velocity sedimentation and size exclusion chromatography. Hydrodynamic properties of the detergent solubilized exchanger suggested that the exchanger is a monomer. Chemical crosslinking and velocity sedimentation studies, however, indicated that the exchanger exists as a dimer within the plasma membrane.

These studies provide insight into the structural and functional properties of the exchanger. The O-glycosylated exchanger is exclusively localized in the ROS plasma membrane as a dimer, and the large hydrophilic domains of the exchanger do not appear to play a role in ion transport.

TABLE OF CONTENTS

LIST OF TABLES

LIST OF FIGURES

LIST OF ABBREVIATIONS

BCA	bicinchoninic acid
BES	N,N-*bis*-(2-hydroxyethyl)-2-aminoethanesulfonic acid
β-ME	β-mercaptoethanol
BSA	bovine serum albumin
bp	base pairs
cDNA	complementary deoxyribonucleic acid (reverse-transcribed from mRNA)
cGMP	guanosine 3`,5`-cyclic monophosphate
CB	Coomassie Blue
CHAPS	3-[(cholamidopropyl)-dimethylammonio]-1-propanesulfonate
Ci	Curie
CNBr	cyanogen bromide
CY3	carboxymethyl indocarbocyanine
DEAE	diethyl aminoethyl
DMEM	Dulbecco`s modified Eagle medium
DNA	deoxyribonucleic acid
DIC	differential interference contrast
DTT	dithiothreitol
ECL	enhanced chemiluminescence
EDTA	ethylaminediamine tetraacetic acid
ELISA	enzyme-linked immunosorbant assay
FBS	fetal bovine serum
FCCP	carbonyl cyanide *p*-trifluoromethoxyphenylhydrazone
GC	guanylate cyclase
GCAP	guanylate cyclase activating protein
GCL	ganglion cell layer
GTP	guanosine 3`-triphosphate
HBS	Hepes buffered saline
HEPES	N-[2-hydroxyethyl] piperazine—N`-[2-ethanesulfonic acid]
Ig	immunoglobulin

INL	inner nuclear layer
IPL	inner plexiform layer
kDa	kilodalton
mRNA	messenger ribonucleic acid
NP-40	nonidet P-40
ONL	outer nuclear layer
OPL	outer plexiform layer
pA	picoAmpere
PAGE	polyacrylamide gel electrophoresis
PBS	phosphate buffered saline
PDE	phosphodiesterase
PMc 1D1	anti- alpha subunit of the cGMP-gated channel monoclonal antibody
PMSF	phenylmethyl sulfonyl fluoride
PNGase F	peptide N-glycosidase F
pPDM	N,N-para-phenylene-dimaleimide
RNA	ribonucleic acid
ROS	rod outer segment
RK	rhodopsin kinase
SBTI	soybean trypsin inhibitor
SDS	sodium dodecyl sulfate
T	transducin
TCPK	N-tosyl-L-phenylalanine chloromethyl ketone
Tris	Tris [hydroxymethyl]aminomethane
TX-100	Triton X-100 detergent
Vi	initial velocity
Vmax	maximum velocity

ACKNOWLEDGEMENTS

I would like to give my warmest thanks to my supervisor, Dr. Bob Molday, for giving me the opportunity to work in his lab. His patience and guidance has helped me to successfully complete my degree. I am grateful to my committee members, Dr. Michel Roberge and Dr. Ian Clarke-Lewis for their advice on my thesis.

I would like to give a very special thanks to Yi-Te Hsu for teaching me the basic lab techniques, especially the functional reconstitution assay and Orson Moritz for helping me with pretty much everything in the lab. I would also like to thank Laurie Molday for generating the antibodies and helping with the microscopy studies, Andy Goldberg for teaching me the sedimentation protocol, Delyth Reid for performing the electron microscopy studies on retina, Michelle Illing for helping with the peptide synthesis and Andy Williams for teaching me the basic molecular biological techniques.

I would also like to thank other members of the lab: Andréa Dosé, Shu-Chan Hsu, Carol Colville, Chris Loewen, Theresa Hii, Tatjana Lukic, Igor Nasonkin, Nancy Mah, René Warren, Natalie Rundle, Jinhi Ahn and Jason Wong.

I would like to thank Dr. Helmut Reiländer and Dr. Kenneth Philipson for providing the bovine rod photoreceptor exchanger cDNA and canine cardiac exchanger cytoplasmic loop fusion protein construct, respectively. I am also grateful to Dr. Paul Bauer for sharing his work on the crosslinking studies.

Finally, I would like to thank the members of my family especially my parents.

INTRODUCTION

1.1 The Retina:

Vision is one of the five senses that permit us to obtain information about our immediate surroundings. Images of the outside world are interpreted by the brain when light reflects off objects and enters the vertebrate eye through the pupil (Fig. 1). Depending on the intensity of the surrounding illumination, the iris dilates or contracts to regulate the amount of light entering the eye. The light is then focused by the lens onto the retina, located at the posterior end of the eye. The retina is composed of several different neuronal cells (Fig. 2). Interestingly, light passes through the ganglion cell layer and inner nuclear layer and interacts with rod and cone photoreceptor cells. Specifically, the outer segments of the photoreceptors absorb and convert light energy into an electrical potential. This signal is transmitted to the other neuronal cells of the retina and then, through the optic nerve to the visual cortex, where the information is processed into an image.

1.2 Photoreceptor Cells:

1.2.1 Structure:

Vertebrate retinas have two types of sensory cells called rod and cone photoreceptors (Fig. 3). Cone photoreceptors can be further classified as short, medium or long wavelength absorbing cells and function in color vision. Rod photoreceptors, on the other hand, are responsible for mediating vision under conditions of dim illumination. In the human retina, cone photoreceptors are mostly concentrated in the macular (central) region of the retina while rod photoreceptors are distributed throughout the peripheral region.

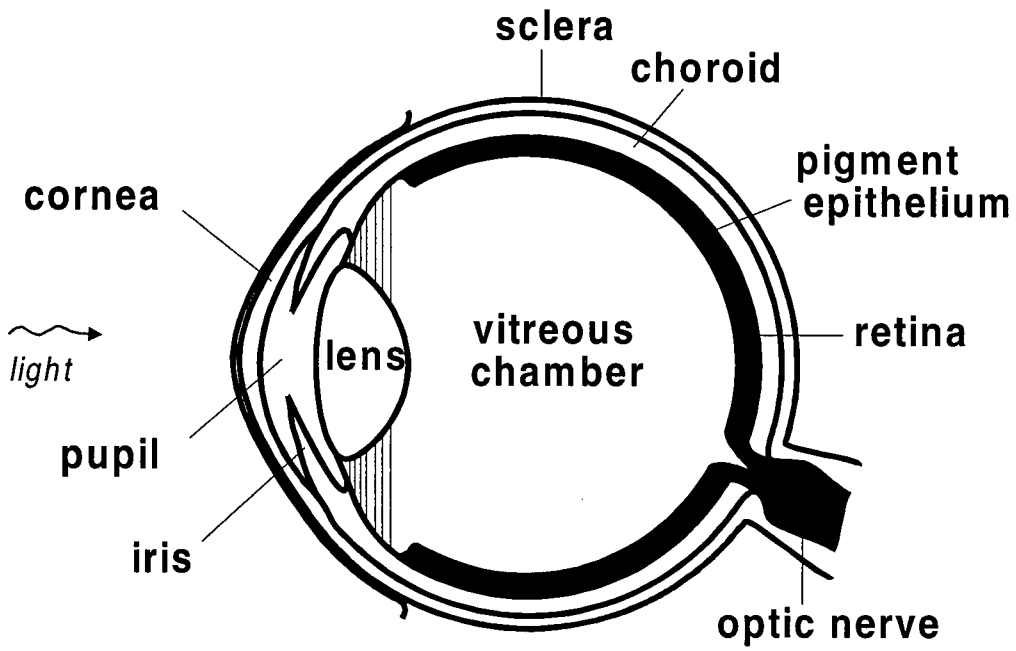

Fig. 1: Diagram of a sagittal section of a vertebrate eye.
Light passes through the transparent cornea and enters the eye through the pupil. The lens focuses the light onto to the retina where the photoreceptors absorb the light and transmit the signal via the optic nerve to the brain. The eye is protected by the hard outer sclera, which is continuous with the cornea. The vascular layer at the back of the eye called the choroid provides the nutrients for the retina via the pigment epithelium. (Figure modified from Dosé, 1995.)

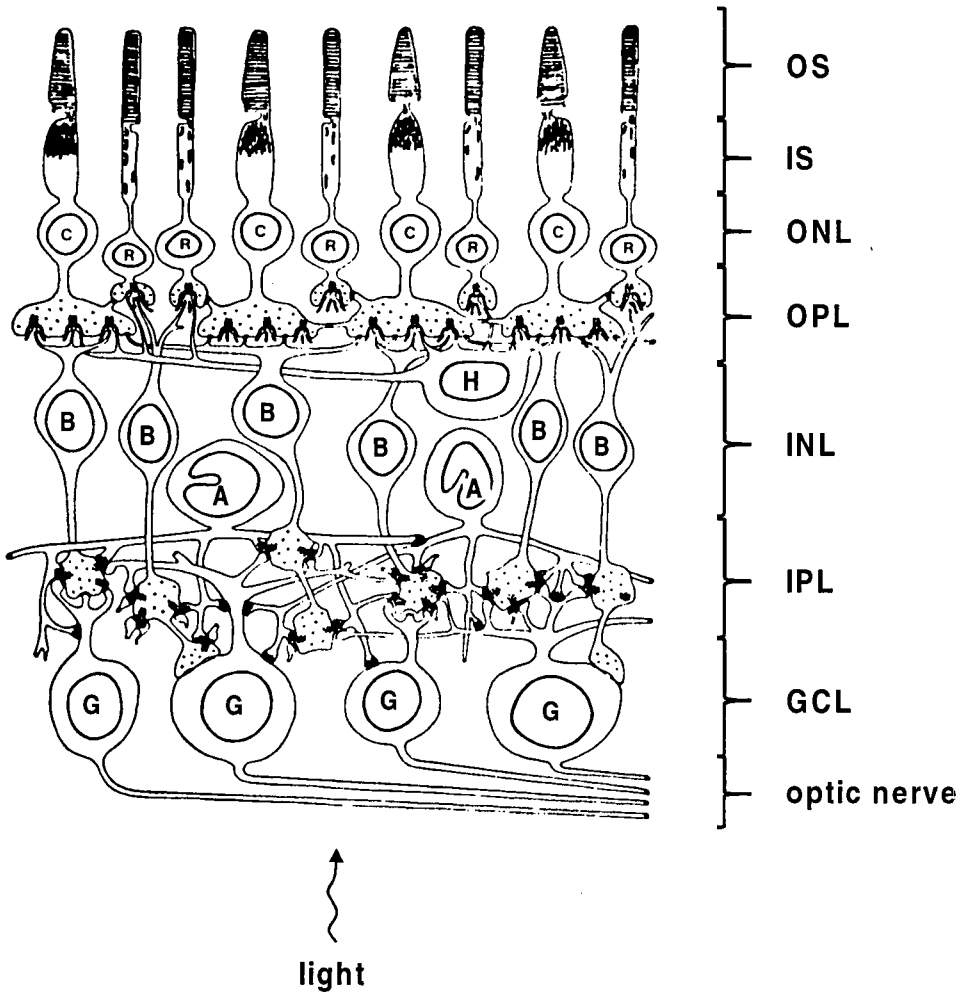

Fig. 2: Different cell layers of the retina and their neurocircuitry.
The rod (R) and cone (C) photoreceptors are the closest to the sclera and make up the first layer of cells. The photoreceptor outer segments (OS) and inner segments (IS) are followed by the photoreceptor nuclei, the outer nuclear layer (ONL). The bipolar (B), amacrine (A) and horizontal (H) cells make up the inner nuclear layer (INL), the second layer of cells. The outer plexiform layer (OPL) is the site of synapse between the photoreceptors and the bipolar and horizontal cells. The inner plexiform layer (IPL) contains the synapse between the bipolar and amacrine cells and ganglion cell layer (GCL). The ganglion (G) cells make up the third layer of cells and its axons form the optic nerve. (Shichi, 1983.)

Both polarized neuronal cells, which have been named after their morphological shape, can be structurally divided into four sections: the synaptic terminal, cell body, the inner segment and outer segment (Fig. 3). The outer segment is the site of visual transduction and is connected to the inner segment by a non-motile cilium. The structural property of the cilium allows for the easy detachment and isolation of the rod outer segments for the study of visual transduction. The inner segment contains the protein synthesis and metabolic organelles such as the endoplasmic reticulum, golgi and mitochondria. The cell body contains the nucleus, and the synaptic terminus is the site of neurotransmitter release. Under non-stimulatory conditions, the neurotransmitter, glutamate (Copenhagen and Jahr, 1989), is continuously released from the synaptic terminal and upon excitation the release of this neurotransmitter is inhibited.

The outer segment of a rod cell contains a stack of hundreds of membranous disks enveloped by a plasma membrane. In contrast, the cone outer segment lacks separate disks, but the continuous folding of the cone outer segment plasma membrane forms the equivalent disk-like structures. In many species the disks become shorter towards the apical end giving the outer segment a tapered appearance. Thus, the surface area of the cone plasma membrane is several times larger than rods, even though anatomically, the cone outer segment is smaller than the rod outer segment. The rod outer segment disks are formed by the evagination of the ciliary plasma membrane (Steinberg *et al.*, 1980). Filamentous structures connect the disks to adjacent disks and to the plasma membrane (Roof and Heuser, 1982; Sjostrand and Kreman, 1978). The disks are highly organized and oriented perpendicular to the incident light. This orientation enables rhodopsin in rods and cone opsins in short, medium and long wavelength cones to efficiently absorb light.

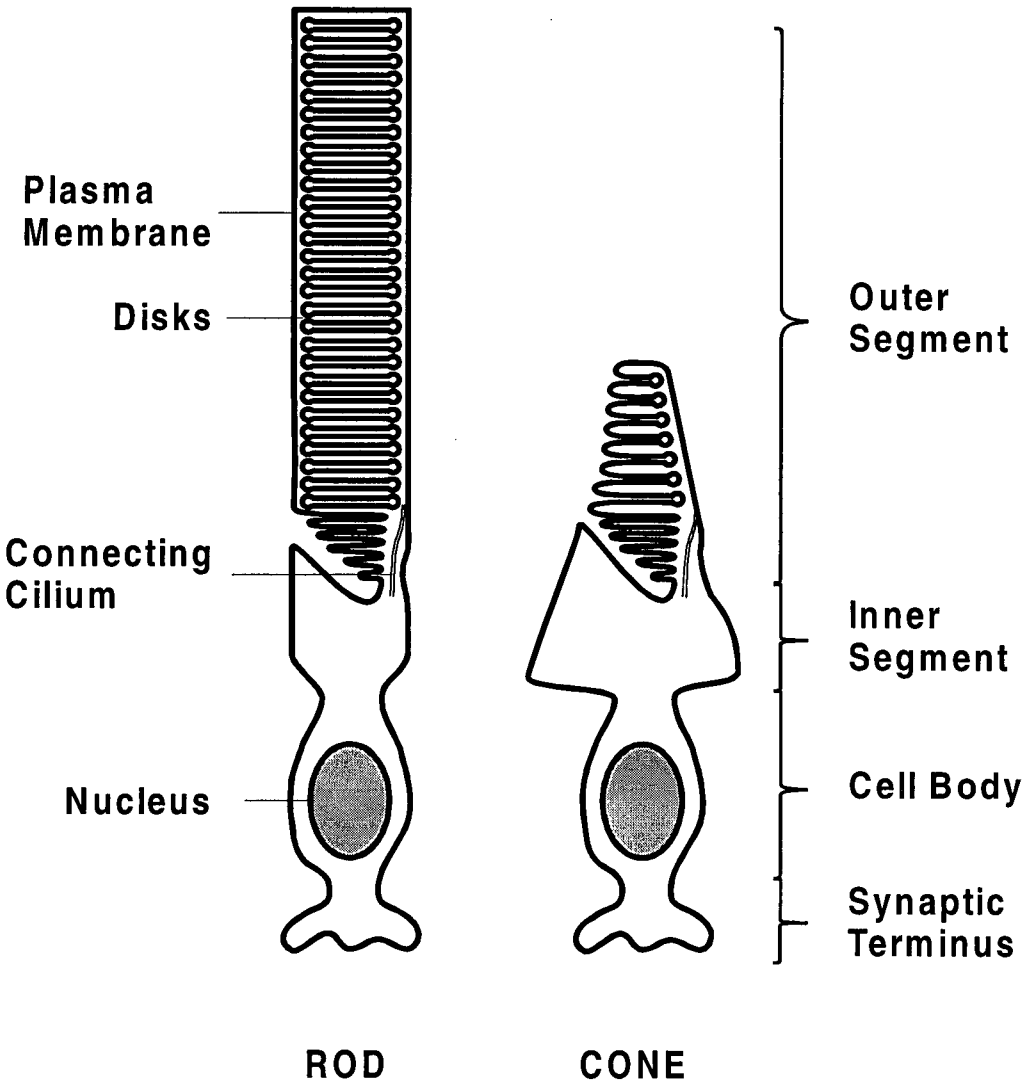

Fig. 3: Vertebrate photoreceptors.
Rods and cones are the two types of vertebrate photoreceptor cells (not drawn to scale). Morphologically both photoreceptors can be divided into four compartments: the outer segment, inner segment, cell body and synaptic terminus. The disks in the rod outer segment are surrounded by a separate plasma membrane whereas the disks in the cone outer segment are continuous with the plasma membrane. The outer segment is connected to the inner segment by a cilium. (Figure modified from Dosé, 1995.)

The protein composition between the ROS plasma membrane and disk membrane was suggested to be different, since the plasma membrane displayed Ca^{2+} efflux activity whereas disk membranes did not (Bauer, 1988). With the advent of a technique to separate the disks from the plasma membrane (Molday and Molday, 1987), the protein and lipid composition between the ROS disks and plasma membrane have been shown to be different. Immunoelectron microscopy studies have localized the Na/Ca-K exchanger (Reid *et al.*, 1990), cGMP-gated channel complex (Cook *et al.*, 1989) and glucose transporter (Hsu and Molday, 1991) to the plasma membrane, whereas peripherin (Molday *et al.*, 1987), rom-1 (Moritz and Molday, 1996; Bascom *et al.*, 1992) and the frog 290 kDa or bovine 220 kDa glycoproteins (Papermaster *et al.*, 1978; Illing *et al.*, 1997) have been localized to the rim regions of the disks. Rhodopsin, however, is present in both membrane fractions (Hsu *et al.*, 1993; Nir *et al.*, 1984). In terms of lipids, the disks have a higher content of unsaturated fatty acids and more cholesterol than the plasma membrane (Boesze-Battaglia and Albert, 1989). The unsaturated fatty acids are thought to facilitate the high curvature of the disk rim regions.

1.2.2 Phagocytosis of the Outer Segments:

A process unique to the photoreceptors is the continuous replacement of the outer segment. Packets of rod and cone outer segments are phagocytosed by the retinal pigment epithelium cells at the apical end and new outer segment membrane is assembled at the base (reviewed by Spalton *et al.*, 1994). Elegant metabolic radioactive-labeling experiments have shown that the entire rod outer segment is renewed every 10-14 days (Fig. 4). Although the mechanism of phagocytosis by RPE cells has yet to be determined, a defective phagocytic process has been shown to result in photoreceptor degeneration (reviewed by Bok, 1989).

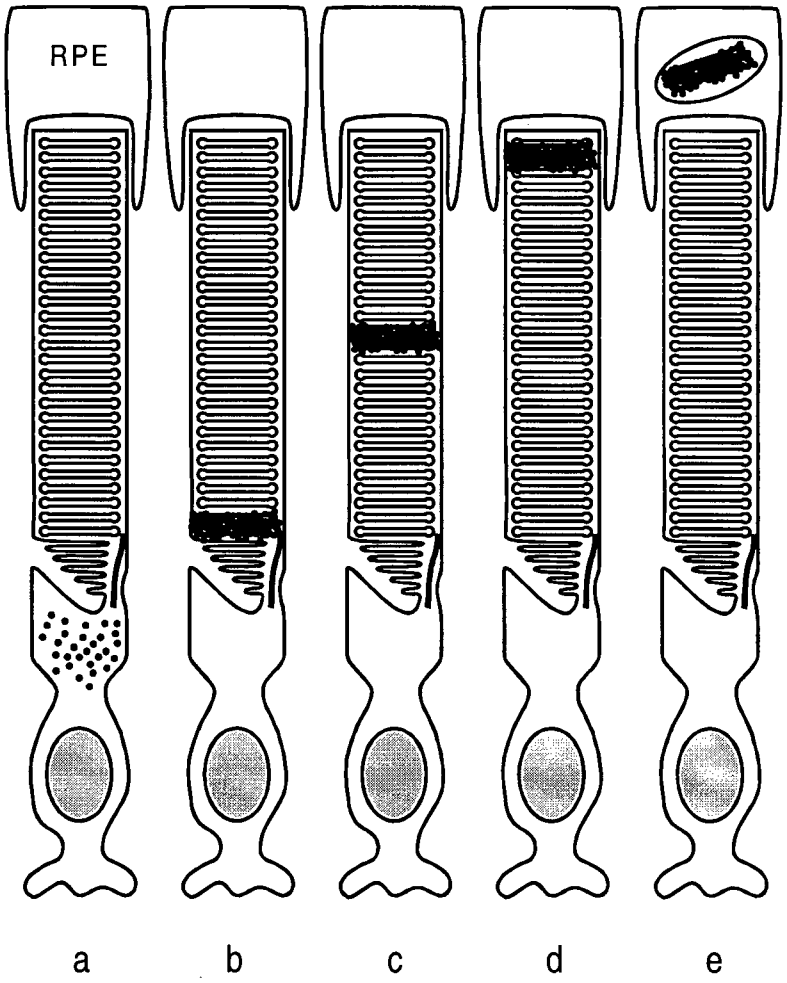

Fig. 4: A diagram illustrating the rod photoreceptor outer segment renewal.
The radioactive amino acids are incorporated into proteins destined for the rod outer segment in the inner segment (a). The proteins are then transported to the base of the ROS plasma membrane, which evaginates to form the disks (b). The continuous formation of new disks displaces the radioactive disks along the length of the ROS (c). Once the disks reach the apical end of the rod (d), the disks are phagocytized by the retinal pigment epithelium (RPE) (e). Over a period of a week or two the outer segment is completely renewed (Young, 1976).

1.3 Visual Transduction:

Most of the work on visual transduction has been studied on rod photoreceptors for a couple of reasons. First, the rod cells are more abundant than cone cells in most mammalian retinas: a ratio of 20 rod cells to 1 cone cell in human retinas (Osterber, 1935). Second, a straightforward isolation procedure for ROS has allowed for the preparation of large amounts of ROS for biochemical studies (Papermaster and Dreyer, 1974). The complex photo-excitation cascade and the subsequent light adaptation or recovery process in rod photoreceptors have been studied extensively (reviewed by Yau 1994, Palczewski, 1994, Koch 1995, Polans *et al.*, 1996).

1.3.1 Dark Current:

In the dark-adapted state, rod photoreceptors have a circulating dark current which has a value of 20-50 pA per vertebrate rod cell (Baylor *et al.*, 1979a, b). The inward current is due to the cations that enter through the cGMP-gated channel in the outer segment and the outward current is composed of K^+ ions that exit through the voltage-gated K^+ channel in the inner segment (Fig. 5) (Beech and Barnes, 1989). The inward dark current, contributed by Na^+ but also to a lesser extent Ca^{2+} and Mg^{2+} ions (Nakatani and Yau, 1988), keeps the photoreceptors depolarized near – 40 mV. Most other neuronal cells have a resting potential of – 60 mV to – 70 mV, determined by the K^+ ion distribution. The Na^+/ K^+ ATPase in the inner segment and Na/Ca-K exchanger in the outer segment maintain the dark current by preserving the Na^+, K^+ and Ca^{2+} ion concentration gradients across the photoreceptor cell membrane. The efflux of Mg^{2+} is currently unknown.

The depolarized state of the photoreceptor causes the voltage-sensitive Ca^{2+} channels in the synaptic region to remain open. The resulting high local Ca^{2+} concentration causes the

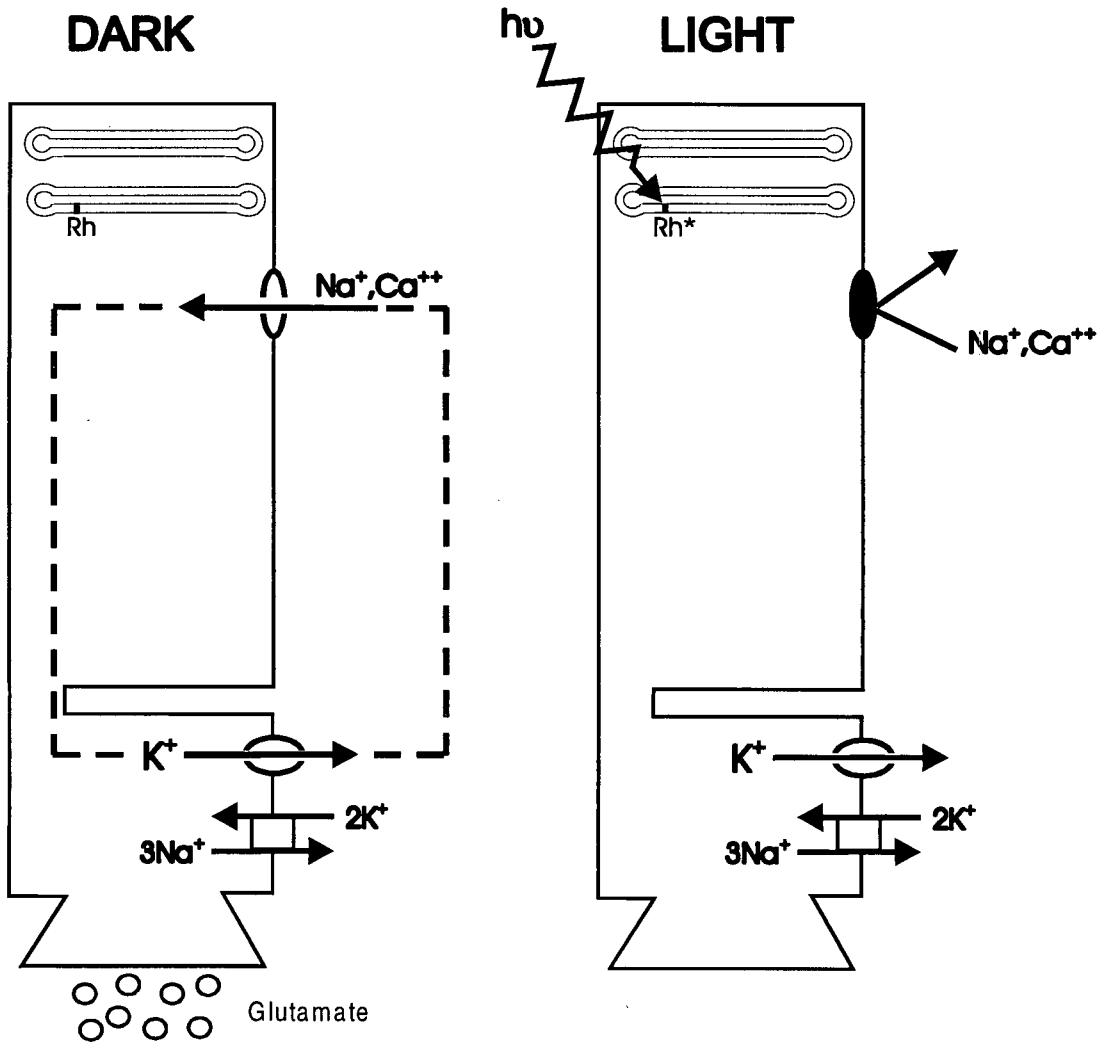

Fig. 5: Dark current in the photoreceptors.
The dark current consists of the influx of cations through the cGMP-gated channel in the outer segment and the efflux of K^+ through the voltaged-gated K^+ channel in the inner segment. This dark current maintains the photoreceptor resting membrane potential at –40 mV. Activation of rhodopsin (Rh) with light (hυ) results in the disruption of the dark current, due to the closure of the cGMP-gated channel, and the subsequent hyperpolarization of the cell to –70 mV. The Na^+/ K^+ ATPase in the inner segment maintains the transmembrane Na^+ and K^+ gradients, thereby preserving the dark current. (Figure modified from Dosé, 1995.)

continuous release of neurotransmitters (Fig. 6) (Morgan *et al.*, 1998). The absorption of a photon(s) initiates a cascade of reactions leading to the closure of the cGMP-gated channels in a restricted area of the plasma membrane. Due to the compartmentalization of photoreceptors, photoexcitation has a graded response rather than an all or none response. The inhibition or decrease of the inward dark current and the continued efflux of K^+ ions via the K^+ channel in the inner segment result in the hyperpolarization of the photoreceptor cell (Fig. 5). Upon hyperpolarization, the voltage-gated Ca^{2+} channels in the synaptic region close, but the Ca^{2+} ATPase continues to pump Ca^{2+} out. The subsequent decrease in the Ca^{2+} concentration suppresses neurotransmitter release at the synaptic region (Fig. 6) (Morgans *et al.*, 1998).

1.3.2 Visual Transduction Cascade:

The visual transduction cascade for vertebrate rod outer segments is shown in Fig. 7. The cascade of events is initiated when a photon of light isomerizes the 11-*cis*-retinal chromophore of rhodopsin to its all-*trans*-retinal isomer. This causes rhodopsin to undergo a series of conformational changes leading to its active state, metarhodopsin II (R*) (Lamola *et al.*, 1974). R* amplifies the signal by activating several hundred molecules of the heterotrimeric G-protein, transducin, composed of a $T\alpha$, $T\beta$ and $T\gamma$ subunit (Gray-Keller *et al.*, 1990). R* catalyzes the GTP for GDP exchange on the $T\alpha$ subunit. In turn, $T\alpha$ dissociates from $T\beta\gamma$ and binds to the phosphodiesterase (PDE) complex (Hurley and Stryer, 1982), composed of two catalytic subunits, α and β, and two inhibitory γ subunits. As a result, PDE is activated and further amplifies the signal by hydrolyzing ~4 x 10^5 cGMP molecules per second (Yee and Liebman, 1978). Depletion of the local intracellular free cGMP concentration causes the cGMP-gated channel to close (Fesenko *et al.*, 1985) and the conductance across the plasma membrane to

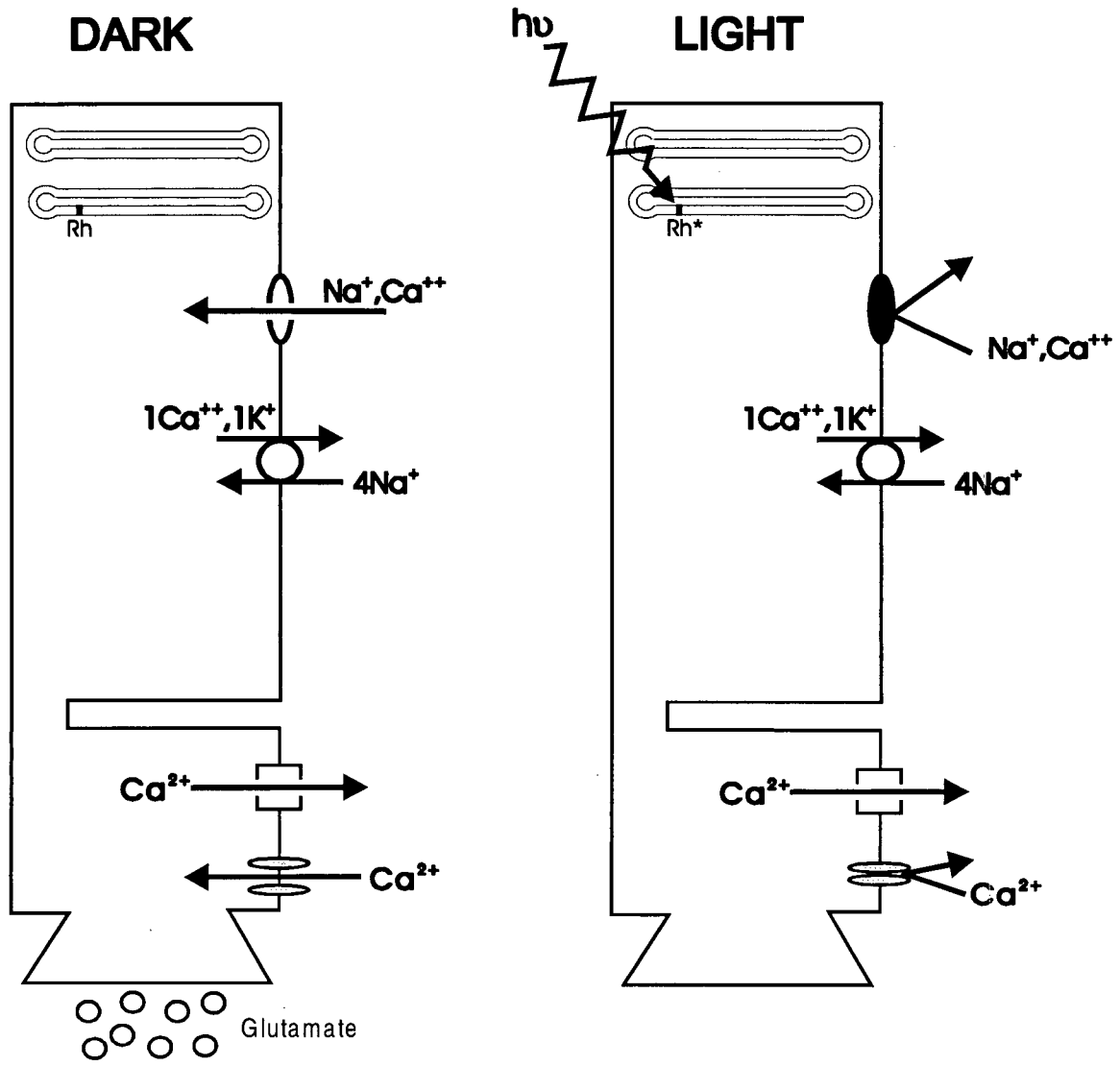

Fig. 6: Regulation of neurotransmitter release by the intracellular calcium levels in the photoreceptor.

The Ca^{2+} concentration in the outer segment is regulated by the influx of Ca^{2+} through the cyclic GMP-gated channel and the efflux via the Na/Ca-K exchanger whereas in the synaptic region the Ca^{2+} enters via the voltage-gated Ca^{2+} channel and the exits via the Ca^{2+} ATPase. In the dark, the depolarized state of the photoreceptor permits the influx of Ca^{2+} in the synaptic region through the voltage sensitive Ca^{2+} channel. The resulting increase in local Ca^{2+} concentration causes the continuous release of neurotransmitters. Upon illumination, the cGMP-gated channel in the outer segment and the voltage-gated Ca^{+} channel in the synaptic region close, but the exchanger and the Ca^{2+} ATPase continue to transport Ca^{2+} out of the cell, thereby lowering the intracellular Ca^{2+} concentration and inhibiting neurotransmitter release. Rh represents rhodopsin and hυ represents a photon of light. (Morgans et al., 1998.)

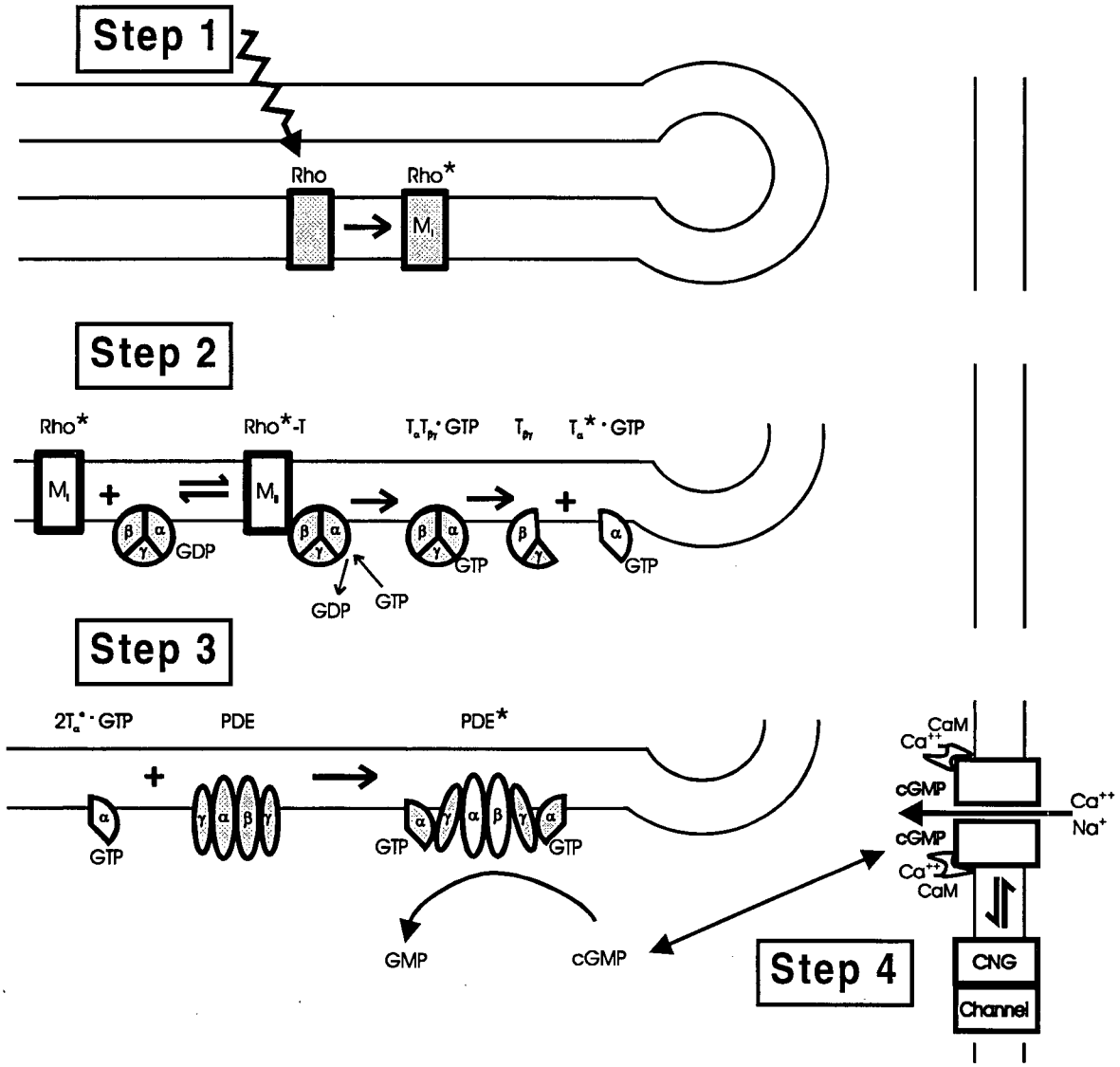

Fig. 7: Schematic diagram of the phototransduction cascade.
Excitation of photoreceptors begins when light initiates rhodopsin (Rho) to undergo several conformational changes starting with metarhodopsin I (M_I) (Step 1). Metarhodopsin II (M_{II}), which is in equilibrium with M_I, then catalyzes the exchange of GDP for GTP in transducin (T) and the dissociation of Tα from T$\beta\gamma$ (Step 2). The α-subunit of transducin then activates phosphodiesterase (PDE) (Step 3). The resulting decrease in cGMP causes the calmodulin (CaM) modulated cGMP-gated channel (CNG) to close, preventing the influx of cations (Step 4). (Figure modified from Dosé, 1995.)

decrease. The absorption of one photon translates into a decrease of 1 pA of the inward dark current (Baylor *et al.*, 1979b).

1.3.3 Recovery:

For recovery to the dark state, the inactivation of rhodopsin, transducin and phosphodiesterase must coincide with the activation of guanylyl cyclase (GC) (Fig. 8). The intracellular free calcium concentration facilitates the inactivation of the visual transduction cascade through calcium binding proteins.

First, the calcium binding protein, recoverin, has been shown to indirectly modulate the activity of rhodopsin (Gray-Keller *et al.*, 1993; Kawamura, 1993). Low Ca^{2+} levels disrupt the Ca^{2+}–dependent association and inhibition of rhodopsin kinase (RK) by recoverin (Klenchin *et al.*, 1995; Chen *et al.*, 1995). The subsequent phosphorylation of rhodopsin by RK followed by the binding of arrestin results in the inactivation of rhodopsin (Palczewski *et al.*, 1991;Gurevich and Benovic, 1992). In the end, the chromophore is removed from the phosphorylated rhodopsin. This form of rhodopsin is not capable of binding Tα, RK or arrestin.

The quenching of activated rhodopsin prevents further activation of downstream biochemical reactions. Tα-GTP activity is slowly inactivated by the intrinsic GTPase activity, which converts GTP to GDP. The Tα GTPase activity is stimulated by its interaction with PDE and by a membrane bound GTPase activating protein (Antonny *et al.*, 1993; Angleson and Wensel, 1993). Recently, two G protein signaling regulators have been cloned (Chen *et al.*, 1996; Faurobert and Hurley, 1997), and one or both of these proteins are likely candidates for stimulating GTPase activity. After hydrolysis of GTP, Tα dissociates from the PDEγ inhibitory subunit and reassociates with the Tαβ complex. Phosphorylation of PDEγ subunit by

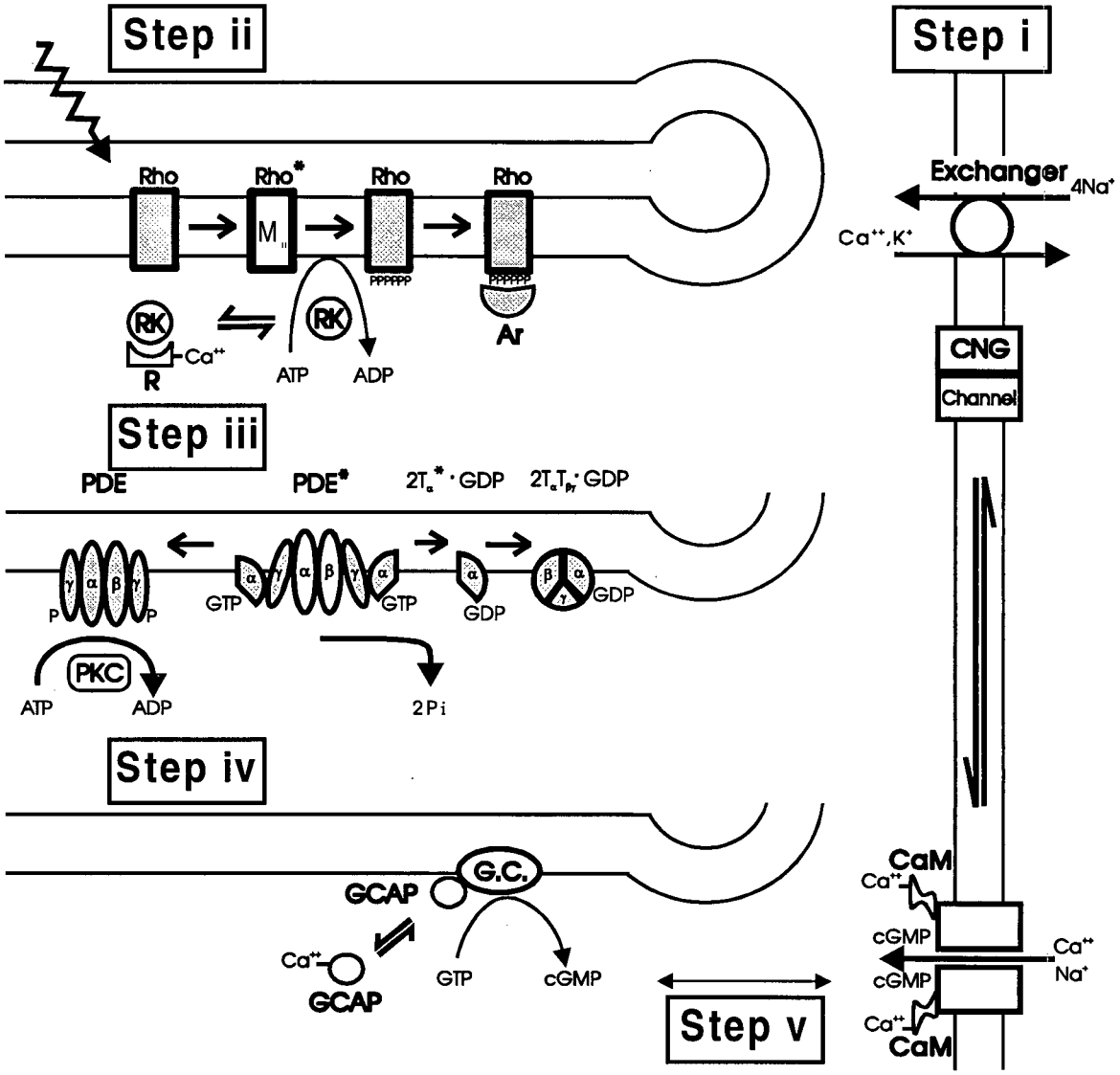

Fig. 8: Schematic diagram of the recovery process.
Recovery of photoreceptors following excitation begins when the intracellular calcium levels decrease due to the closed cGMP-gated channel and the continued efflux of Ca^{2+} by the Na/Ca-K exchanger (Step i). At low intracellular Ca^{2+} levels, the Ca^{2+} dependent inhibition of rhodopsin kinase (RK) by recoverin (R) is relieved; rhodopsin is then inhibited by rhodopsin kinase and arrestin (Ar) (Step ii). Phosphodiesterase (PDE) is inactivated by the dissociation of the α-subunit of transducin (T) due to the hydrolysis of GTP and the phosphorylation of the γ-subunit of PDE by protein kinase C (PKC) (Step iii). At low Ca^{2+} levels, the guanylyl cyclase activating protein (GCAP) activates guanylyl cyclase (GC) (Step iv) and the resulting increase in cGMP opens the channel, re-establishing the calmodulin dependent modulation (Step v). (Figure modified from Dosé, 1995.)

protein kinase C has been shown to increase the ability of this subunit to inhibit the catalytic PDE$\alpha\beta$ subunits (Udovichenko *et al.*, 1994).

Second, lowering the level of Ca^{2+} stimulates guanylyl cyclase (GC) to synthesize cGMP. Increased cGMP levels in turn re-open the cGMP-gated channel and re-establishes the inward current. Two soluble Ca^{2+} binding proteins called guanylyl cyclase activating protein or GCAP1 (Palczewski *et al.*, 1994) and GCAP2, (Dizhoor *et al.*, 1995) have been shown to regulate the activity of ROS GC. In the retina, two GC enzymes, retGC1 (Shyjan *et al.*, 1992) and retGC2 (Lowe *et al.*, 1995), have been cloned and localized to the photoreceptor outer segments (Yang and Garbers, 1997). The functional significance of having two retGCs and two GCAPs in the outer segments of photoreceptors requires further investigation.

Third, the Ca^{2+} binding protein, calmodulin, regulates the cGMP-gated channel (Hsu and Molday, 1993). At high Ca^{2+} concentrations, calmodulin binds to the cGMP-gated channel and decreases the apparent affinity of the channel for cGMP. At low Ca^{2+} levels, however, calmodulin dissociates from the cGMP-gated channel complex, and the channel has a higher apparent affinity for cGMP. The increased sensitivity of the channel at low cGMP concentrations allows for an expeditious return of the cell to its depolarized resting state.

1.3.4 Visual Transduction in Cone Photoreceptors:

Phototransduction in cone cells follow a similar cascade of reactions. However, cone photoreceptors are less sensitive to light, about 1/50 to $1/100^{th}$ of rods, (Schnapf and McBurney, 1980). Cones also exhibit a faster photoresponse (Hestrin and Korenbrot, 1990) and faster recovery or adaptation following excitation (reviewed by Yau, 1994).

Light adaptation has been suggested to be mediated by the light-induced decrease in intracellular calcium (Matthews *et al.* 1988; Nakatani and Yau, 1988b). The faster decrease of intracellular Ca^{2+} in the cone outer segment, mediated by the Na/Ca exchanger, is consistent with the faster adaptation of cones (Yau and Nakatani, 1985; Cobbs and Pugh, 1986).

The lower sensitivity of cones, however, is not due to the faster Ca^{2+} feedback mechanism in cones (Nakatani and Yau, 1989). The faster regeneration of the cone opsins from 11-cis retinal and opsin and the faster formation and shorter lifetime of active cone opsins (Shichida *et al.*, 1994; Yoshizawa, 1994) may, in part, be responsible for the difference in light sensitivity and photoresponse.

Rods are more sensitive to light for three additional possibilities (Tovée, 1996). First, the persistence of the photoresponse in rod photoreceptors compared to cones is longer. This may increase the probability that a second photon will be absorbed while the rod is still excited, resulting in the excitation of a bipolar cell. Second, the larger anatomical size of rod photoreceptors compared to cones may increase the probability of rods to adsorb photons. Finally, a greater number of rod cells innervates a single ganglion cell compared to cone cells. The larger receptive field covered by rod cells may increase the probability of rod cells to absorb light and stimulate the ganglion cell.

The identification and biochemical characterization of other cone specific isoforms such as transducin (Lerea *et al.*, 1986), PDE (Piriev *et al.*, 1995; Shimizu-Matsumoto *et al.*, 1996), and cGMP-gated channel (Bönigk *et al.*, 1993) may provide some insight into the differences between cone and rod photoresponses.

1.4 Calcium Homeostasis:

Integral membrane proteins that transport Ca^{2+} regulate the intracellular Ca^{2+} levels. To date, only two proteins have been shown to transport Ca^{2+} out of the cell: the Ca^{2+} ATPase and the Na/Ca exchanger (reviewed by Carafoli, 1987). On the other hand, voltage-gated or ligand-gated Ca^{2+} ion channels facilitate the entry of Ca^{2+} into the cell or its release from internal stores. In the rod outer segment, the influx of Ca^{2+} through the cGMP-gated channel and the efflux via the Na/Ca-K exchanger dictates the intracellular Ca^{2+} levels.

1.5 Properties of Na/Ca Exchangers:

Two classes of protein are responsible for the Na/Ca exchange activity in cells. One class includes the Na/Ca exchanger isoforms (NCX1, NCX2, NCX3)(Nicoll *et al.* 1996a), and the other class is the Na/Ca-K exchanger in the rod photoreceptor outer segment (Reiländer *et al.* 1992). NCX1 is expressed in most tissues, whereas NCX2 and NCX3 are selectively expressed in the skeletal muscle and brain (Nicoll *et al.* 1996a, Li *et al.* 1994). Sequence alignment of the Na/Ca exchanger isoforms shows a significant degree of similarity (Fig. 9). When the putative leader peptide and the alternatively spliced regions (N-terminal region of the cytoplasmic domain) are discounted, NCX1 and NCX2 share 68%, NCX1 and NCX3 share 73% and NCX2 and NCX3 share 75% identity. However, the rod exchanger and Na/Ca exchanger isoforms share very little sequence similarity.

The two classes of Na/Ca exchangers do share some similar structural and functional features but also exhibit some notable differences. Of the three Na/Ca exchangers, the cardiac exchanger, NCX1, has been the best characterized, so a comparison of the properties between the cardiac and rod exchanger will be summarized in the introduction.

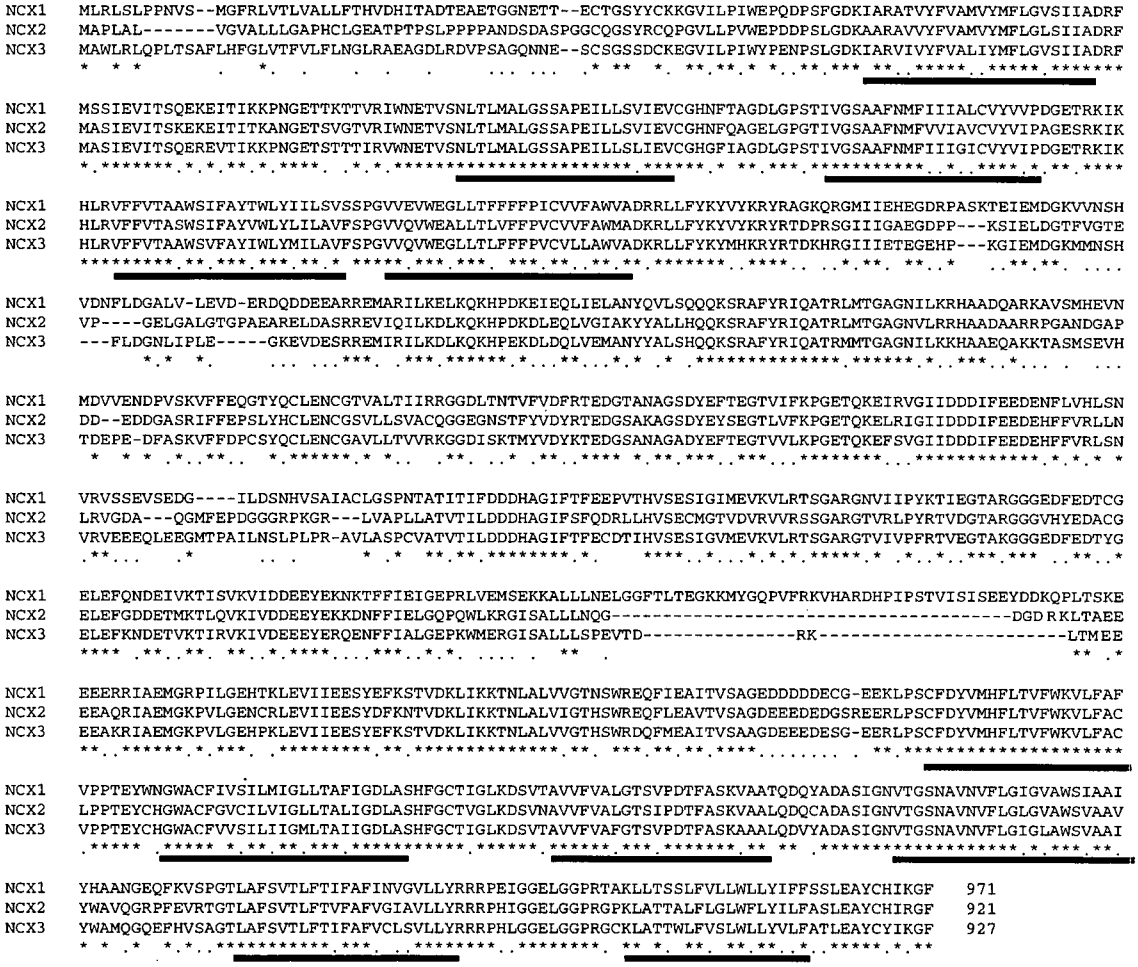

Fig. 9: Comparison of the rat Na/Ca exchangers, NCX1, NCX2 and NCX3, protein sequence.

The protein sequences of NCX1 (Low *et al.*, 1993), NCX2 (Li *et al.*, 1994) and NCX3 (Nicoll *et al.*, 1996a) were aligned with the Clustal program (PC Gene, Intelligenetics). When the putative leader sequence is not included in the alignment, NCX1 and NCX2 have 68% identity, NCX1 and NCX3 have 73% identity, and NCX2 and NCX3 have 75% identity. Identical residues are indicated by an *asterisk* whereas similar residues are indicated by a *dot*. The alignment gaps are indicated by *dashes* and the putative membrane spanning segments are *underlined.*

1.5.1 Thermodynamics:

Functionally, both the rod and cardiac exchangers utilize the Na^+ electrochemical gradient for the efflux of Ca^{2+} against its electrochemical gradient. The rod exchanger, however, also couples the free energy of the K^+ transmembrane gradient to transport Ca^{2+} with an exchange stoichiometry of $4Na^+$ for $1Ca^{2+}$ and $1K^+$ (Cervetto *et al.*, 1989; Schnetkamp *et al.*, 1989). The cardiac exchanger transports $3Na^+$ for $1Ca^{2+}$ (Reeves and Hale, 1984; Kimura *et al.* 1987; Bridge *et al.* 1990; Crespo *et al.* 1990). Coupling an extra Na^+ and K^+ for the efflux of Ca^{2+} enables the rod exchanger to attain lower intracellular Ca^{2+} concentrations than would be possible with a $3Na^+$ for $1Ca^{2+}$ exchange stoichiometry according to the following equations:

(1) $$[Ca^{2+}]_i/[Ca^{2+}]_o = ([Na^+]_i/[Na^+]_o)^4([K^+]_o/[K^+]_i)\exp(V_m zF/RT)$$

(2) $$[Ca^{2+}]_i/[Ca^{2+}]_o = ([Na^+]_i/[Na^+]_o)^3\exp(V_m zF/RT)$$

where subscripts i and o refer to intracellular and extracellular concentrations, respectively, V_m is the membrane potential, z is the net charge transported after each transport cycle, *F* is the Faraday's constant, R is the Gas constant, and T is the temperature.

Although earlier studies have suggested that the Na^+ for Ca^{2+} exchange mechanism is electrogenic (reviewed by Eisner and Lederer, 1985), the first clear experimental evidence for a membrane current associated with the Na^+-dependent transport of Ca^{2+} was shown in the rod outer segment by Yau and Nakatani (1984). The cloned cardiac exchanger also displays charge movement during Na/Ca exchange activity (Hilgemann *et al.* 1991). Thus, for every Ca^{2+} transported out of the cell a net positive charge enters.

The membrane potential of the cell also influences the exchange activity. Depolarization decreases the activity of the Na^+-dependent Ca^{2+} efflux of both the cardiac (Kimura *et al.*, 1987; Matsuoka and Hilgemann, 1992; Khananshvili, 1991) and rod exchanger (Lagnado *et al.*, 1988;

Schnetkamp and Szerencsei 1991; Perry and McNaughton, 1993). Conversely, hyperpolarization increases the efflux of Ca^{2+} from the cell. Since photoexcitation causes photoreceptors to hyperpolarize, stimulation of the Na/Ca-K exchanger upon hyperpolarization would facilitate light adaptation in photoreceptors by rapidly lowering the intracellular Ca^{2+}.

Voltage sensitivity of the rod exchanger is not observed when the exchange is initiated with saturating Na^+ concentrations (Lagnado *et al.*, 1988). This result suggests that the membrane potential affects the binding of Na^+ and that the translocation of ions across the membrane is not voltage-dependent. Neither the Km for K^+ nor Ca^{2+} is affected by the membrane potential (Perry and McNaughton, 1993). The voltage-dependent binding of Na^+ but not K^+ or Ca^{2+} suggests that the binding site for Na^+ is most likely within the membrane domain that senses the transmembrane potential (Lagnado and McNaughton, 1990).

Recently, site-directed mutagenesis studies of the cardiac exchanger have shown that mutations of Gly-138 or Gly-837, located within the transmembrane segment 3 and 9, respectively, altered the current-voltage relationship (Nicoll *et al.* 1996b). The authors suggest that these residues may play a role in the binding of Na^+. Mutations of other nearby residues in transmembrane segments 2, 3, 8 and 9 rendered the exchanger inactive. This suggests that these transmembrane segments play an important role in ion transport function. Further studies are required to determine whether the inactivity of the mutant exchangers is due to the importance of the residue in transport function or to the proper folding of the exchanger.

1.5.2 Kinetics:

Kinetic analysis of the exchange mechanism has provided a range of Km values for each ion transported due to differences in experimental conditions and sample preparations. The

Na/Ca exchange activity of the cardiac exchanger has a cooperative dependence for Na^+ with a Hill coefficient of 2-3 and Km_{Na} of 13-30 mM (reviewed by Reeves, 1990; Philipson, 1990). The cardiac exchanger has a higher affinity for Ca^{2+} on the cytoplasmic surface (Km_{Cai} = 0.6-10 μM) than on the extracellular surface (Km_{Cao} = 0.15-0.4 mM) (reviewed by Philipson and Nicoll, 1993).

The exchange activity of the rod exchanger, like the cardiac exchanger, has a cooperative dependence for Na^+ with a Km of 35-93 mM (Table 1). The rod exchanger shows Michealis-Menten kinetics for Ca^{2+} and K^+ dependent exchange activity with Km_{Ca} of 1-34 μM and Km_K of 0.1-3 mM, respectively (Table 1). Unlike the cardiac exchanger, the rod exchanger has the same affinity for Ca^{2+} on both sides of the membrane (Schnetkamp, 1989).

Table 1. Transport properties of the ROS Na/Ca-K Exchanger

Species	$Km_{,Na}$ and n	$Km_{,Ca}$	$Km_{,K}$	Reference
Bovine	36 mM & 2.0	1.1 μM	N	Schnetkamp, 1989,1991
Bovine	35 mM	N	N	Cook & Kaupp, 1988
Bovine	70 mM & 2.0	N	3 mM	Huppertz & Bauer, 1994
Salamander	93 mM & 2.3	2.3 μM	N	Lagnado *et al.*, 1988
Salamander	N	1.6 μM	N	Lagnado *et al.*, 1992
Bovine	N	5 μM	1 mM	Nicoll *et al.*, 1991
Bovine	N	N	1.2 mM	Schnetkamp *et al.*, 1989
Bovine	26 mM & 3.0	N	1 mM	Friedel *et al.*, 1991
Salamander	N	34 μM	151 μM	Perry & McNaughton 1993

Km is the ion concentration for ½ maximal activation of the exchange current
n is the Hill coefficient
N not available

The turnover rates for the rod and cardiac exchangers are different. The rod exchanger transports 60-120 Ca^{2+} ions per second after correcting for the molecular mass of the exchanger to 130 kDa (Cook and Kaupp, 1988; Nicoll and Applebury, 1989). A number of turnover rates

have been estimated for the cardiac exchanger: 350 (Powell *et al*, 1993), 1000 (Cheon and Reeves, 1988) and 2500 (Niggli and Lederer, 1991) ions per second.

1.5.3 Effect of Cations on Exchange Activity:

The distribution of the cations can affect the exchange activity. Na^+ and Ca^{2+} have been shown to compete for the same ion-binding site on the cardiac exchanger (Philipson and Nishmoto, 1981; Miura and Kimura, 1989; Matsuoka and Hilgemann, 1992). Likewise, K^+ and Ca^{2+} have both stimulatory and inhibitory effects on the activity of the rod exchanger (Schnetkamp and Szerencsei, 1991; Schnetkamp *et al.*, 1991b). When either K^+ or Ca^{2+} is present on the external side of the membrane, the Na^+ dependent Ca^{2+} efflux activity of the exchanger decreases. Both Ca^{2+} and K^+ compete for the same cation-binding site as Na^+. Under physiological conditions, the distribution of cations across the cell membrane – the high internal K^+ and external Na^+ concentrations – favours the forward exchange mode for both the cardiac and rod exchangers.

1.5.4 Modes of Exchange:

The cardiac and rod exchangers have several modes of exchange activity as illustrated in Fig. 10. The forward and reverse modes of exchange are dictated by the distribution of the cations across the membrane (Kimura *et al.* 1986; Kimura *et al.* 1987; Schnetkamp *et al.* 1989; Cervetto *et al.* 1989) Both exchangers display Ca-Ca (Reeves, 1990; Schnetkamp, 1980) and

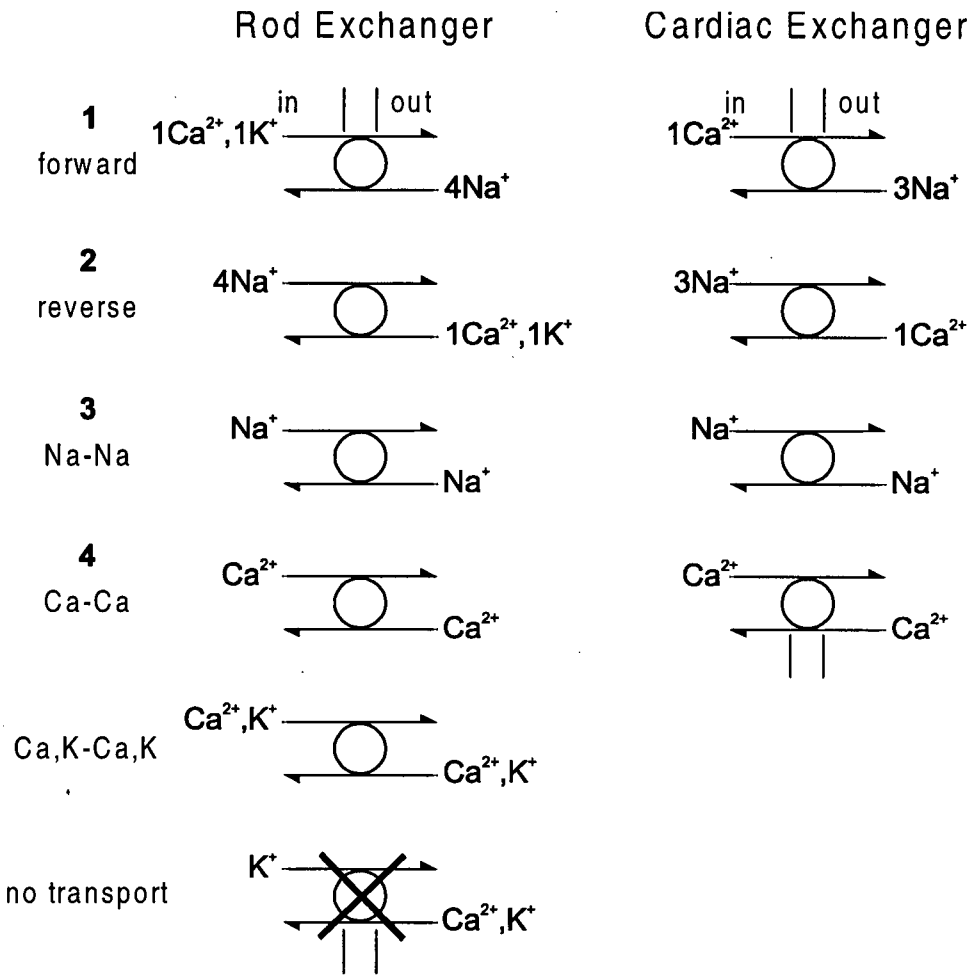

Fig. 10: Modes of cation exchange by the rod photoreceptor Na/Ca-K exchanger and the cardiac Na/Ca exchanger.

Both the rod and cardiac exchangers have four different exchange modes:

1. The forward mode is the efflux of Ca^{2+} coupled to the influx of Na^+.
2. The reverse mode is the influx of Ca^{2+} coupled to the efflux of Na^+.
3. The Ca^{2+}-Ca^{2+} self exchange mode is the equal exchange of Ca^{2+}.
4. The Na^+-Na^+ self exchange mode is the equal exchange of Na^+.

The rod exchanger has an additional mode of exchange, Ca^{2+},K^+-Ca^{2+},K^+, which requires the presence of K^+ on both sides of the membrane.

Na-Na (Reeves and Sutko, 1979; Schnetkamp, 1989) self-exchange modes, but the rod exchanger also exhibits Ca, K-Ca, K self exchange mode (Schnetkamp *et al.* 1991c). The Ca-Ca self-exchange mode of the rod exchanger can occur in the absence of K^+ whereas the K-K self-exchange mode is absolutely dependent on the presence of Ca^{2+} (Schnetkamp *et al.*, 1991c). Although initial studies have shown that the rod exchanger displays K^+-independent exchange activity (Cervetto *et al.*, 1989; Schnetkamp *et al.*, 1989; Friedel *et al.*, 1991), recent studies show that the rod exchanger is inactive in the absence of K^+ (Perry and McNaughton, 1993).

1.5.5 Regulation:

The cardiac exchanger is subject to regulation by a number of cytosolic factors. Na^+-dependent inactivation (Matsuoka *et al.*, 1997) and Ca^{2+}-dependent stimulation (Matsuoka *et al.*, 1995) of the exchanger have been localized to the N-terminal region of the cytoplasmic domain. Cytoplasmic H^+ (Doering and Lederer, 1994) and the exchange inhibitory peptide (XIP), a 20 amino acid sequence within the cytoplasmic loop (Li *et al.*, 1991), has been shown to inhibit exchange activity. In contrast, ATP has been shown to stimulate exchange activity by generating phosphatidylinositol -4,5- bisphosphate (PIP_2) (Hilgemann and Ball, 1996) or by protein kinase C phosphorylation (Iwamoto *et al.*, 1996).

Although increasing the pH has been shown to stimulate the activity of the rod exchanger (Schnetkamp, 1995), regulation of the rod exchanger by the other factors has yet to be shown.

1.5.6 Purification and Cloning:

Both proteins have been purified using ion exchange and lectin affinity chromatography. The purified bovine rod exchanger has a molecular mass of 230 kDa by SDS-PAGE (Cook and

Kaupp, 1988; Nicoll and Applebury, 1989) while the purified canine cardiac exchanger migrates at 120 kDa (Philipson *et al.*, 1988). The purified 230 kDa rod exchanger has been shown to exhibit K^+-dependent Na/Ca exchange activity (Friedel *et al.*, 1991). For the cardiac exchanger, it has been uncertain whether the Na/Ca exchange activity was associated with the 120 kDa protein or some other minor protein co-purifying with the exchanger. Cloning and functional expression of the cardiac exchanger has confirmed that the exchange activity is indeed due to the 120 kDa protein.

The cDNA of the canine cardiac exchanger encodes a protein of 970 amino acids having a calculated molecular mass of 110 kDa (Nicoll *et al.*, 1990). The cDNA of the bovine rod exchanger encodes a protein of 1199 amino acids having a calculated molecular mass of 130 kDa (Reiländer *et al.*, 1992). The difference between the calculated and the relative molecular mass by SDS-PAGE is due, in part, to the glycosylation of the cardiac and rod exchangers. The cardiac exchanger has a single glycosylation site at Asn 41 (Hryshko *et al.*, 1993). The glycosylation site(s) for the rod exchanger has yet to be determined, but removal of terminal sialic acid residues causes a shift in the mobility of the rod exchanger by SDS-PAGE (Reid *et al.*, 1990). The first transmembrane segment of both exchangers serves as the cleaved signal sequence (Hryshko *et al.*, 1993; Durkin *et al.* 1991; Reiländer *et al.*, 1992).

The cardiac and rod exchangers have little similarity in their primary sequence. Yet, hydropathy plots of both exchangers predict that a large negatively charged hydrophilic region connects the first transmembrane domain to the second transmembrane domain (Fig. 11). The rod exchanger, however, has a large hydrophilic N-terminal domain that is lacking in the cardiac exchanger.

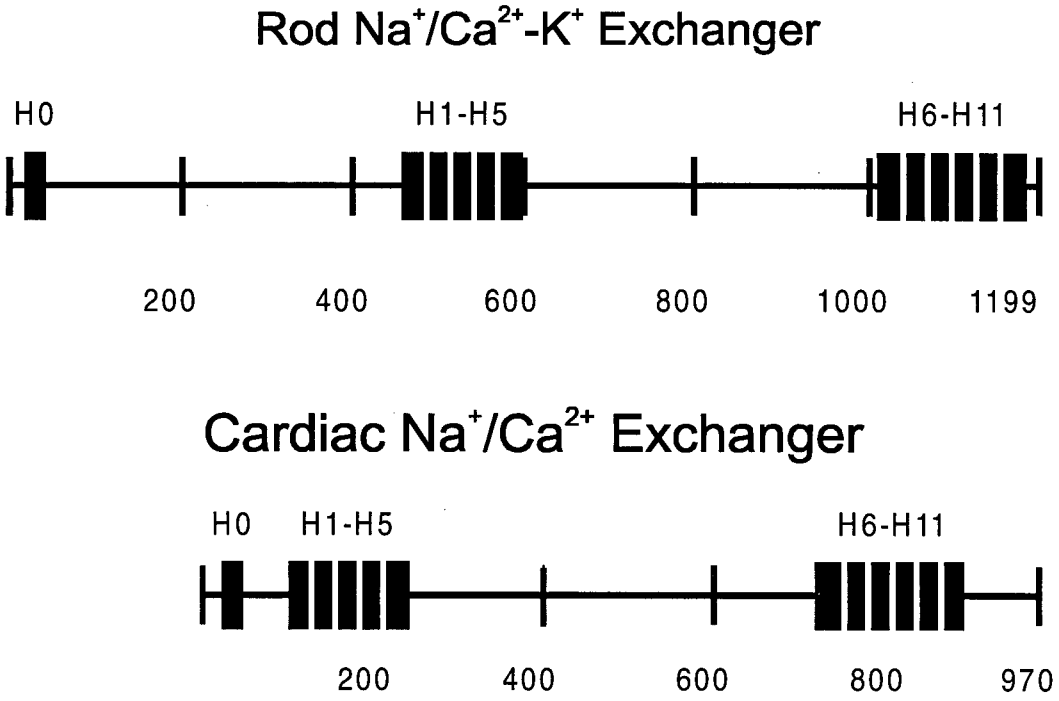

Fig. 11: Linear representation of the cardiac Na/Ca exchanger and the bovine rod photoreceptor Na/Ca-K exchanger.
The hydropathy plots for both exchangers predict a large hydrophilic region connecting two hydrophobic domains: one consisting of five transmembrane segments and the other consisting of 6 transmembrane segments. Both exchangers also have a predicted transmembrane segment at the N-terminus. However, the rod exchanger has a large N-terminal hydrophilic region, which is absent in the cardiac exchanger.

1.5.7 Protein Sequence Similarity of the Bovine Rod Photoreceptor Exchanger to other Na/Ca Exchangers:

Although K^+-dependent Na/Ca exchange activity has been observed in the rat brain (Dahan *et al.*, 1991) and in human platelets (Kimura *et al.*, 1993), the bovine rod exchanger had been the only the Na/Ca-K exchanger cloned. Recently, however, the human retina Na/Ca-K exchanger (Tucker *et al.*, 1998) and a novel rat brain Na/Ca-K exchanger (NCK2) (Tsoi *et al.*, 1998) have been cloned.

Sequence similarity searches of the rod exchanger using BLASTP (Altschul *et al.*, 1994) revealed a number of sequences. Sequences with the highest degree of similarity includes the human retina exchanger (NCK1), rat brain exchanger (NCK2), and a sequence from *C. elegans* (Kraev *et al.*, 1998). The similarity for these proteins is restricted to the two transmembrane spanning domains. The rod exchanger also shares limited but significant sequence similarity in the two α repeat regions of the Na/Ca exchanger isoforms. The α repeat regions were first identified by Schwarz and Benzer (1997); they suggested that this region might form the ion binding sites. The protein sequence similarity of the Na/Ca-K exchangers to the other Na/Ca exchangers is shown in the dendrogram (Fig. 12) and in the alignment of the α repeat regions (Fig. 13).

Sequences from bacteria, yeast, *C. elegans* and plant also have some sequence similarity in the α repeat regions but their function has yet to be determined.

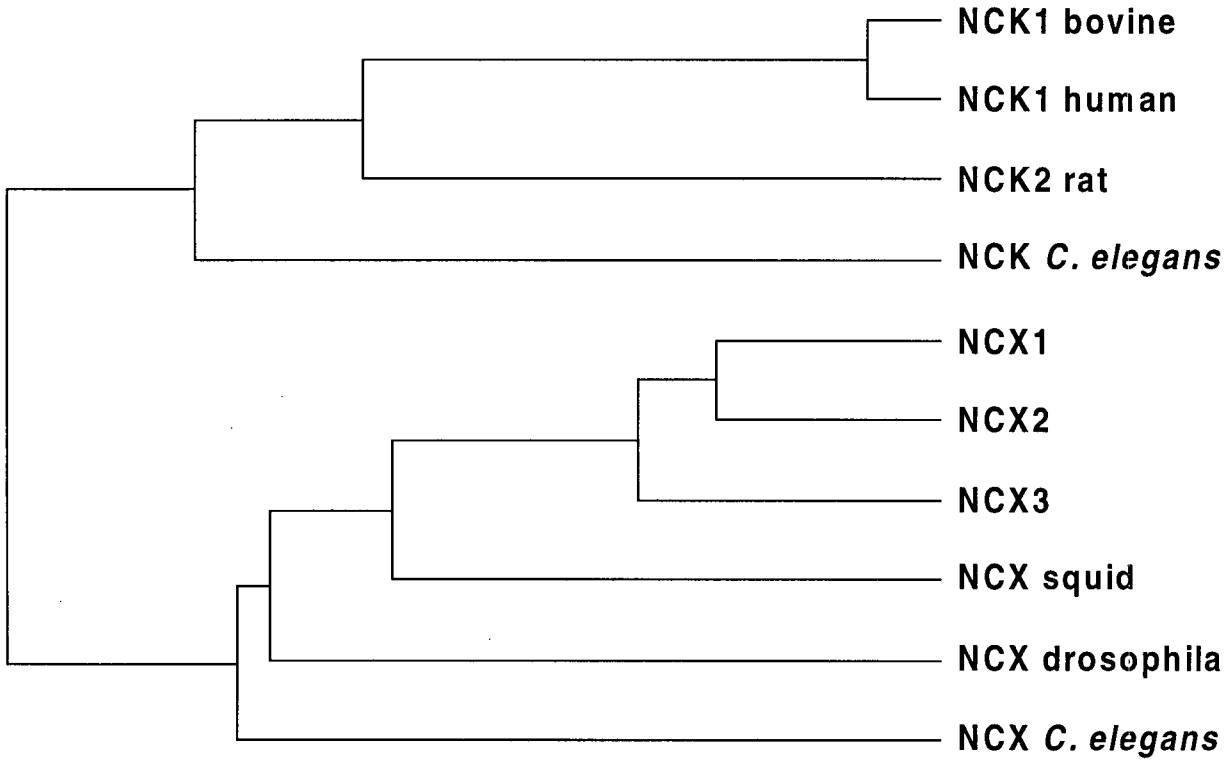

Fig. 12: Dendrogram of the Na^+-dependent Ca^{2+} exchangers.
Sequence similarity between the Na^+-dependent Ca^{2+} exchangers was determined using the Clustal program (PC gene, IntelliGenetics). The distance along the horizontal axis represents the similarity between the sequences (ie. a shorter distance indicates a higher degree of similarity). The sequences are as follows: NCK1 bovine (Reiländer *et al.*, 1992), NCK1 human (Tucker *et al.*, 1998), NCK2 (Tsoi *et al.*, 1998), NCK *C. elegans* (Kraev *et al.* 1998), NCX1 (Low *et al.*, 1993), NCX2 (Li *et al.*, 1994), NCX3 (Nicoll *et al.*, 1996a), NCX squid (He *et al.*, 1996), NCX drosophila (Schwarz and Benzer, 1997; Ruknudin *et al.* 1997), and NCX *C. elegans* (*Caenorhabditis elegans*) (Kraev and Carafoli, 1998).

```
                        TMS              α1 repeat              TMS
NCX1      NETVSNLTLMALGSSAPEILLSVIEVCGHNFTAGDLGPSTIVGSAAFNMFIIIAL  182
NCX2      NETVANLTLMALGSSAPEILLSVIEVCGHNFQAGELGPGTIVGSAAFNMFVVIAV  179
NCX3      NETVANLTLMALGSSAPEILLSLIEVCGHGFIAGDLGPSTIVGSAAFNMFIIIGI  184
SQUID     NETVSNLTLMALGSSAPEILLSVIEVVGQKFEAGQLGPSTIVGSAAFNLFIITAI  172
CalX      NETVANLTLMALGSSAPEILLSVIEIYAKDFESGDLGPSTIVGSAAYNLFMIIAV  231
CENCX1    NETVSNLTLMALGSSAPEILLSVIEICGNNFEAGELGPSTIVGSAAFNLFIIIAV  59

NCKX1     SEDVAGATFMAAGGSAPELFTSLIGV---FISHSNVGIGTIVGSAVFNILFVIGT  536
NCKX2     SDDVAGATFMAAGGSAPELFTSLIGV---FIAHSNVGIGTIVGSAVFNILFVIGM  223
CENCKX    SDDVAGATFMAAGGSAPEFFTSVIGV---FIAQNNVGIGTIVGSATFNILCVLAF  189

α1 CONSERVED

            V   T MA G SAPE   S I           G  TIVGSA FN

                        TMS              α2 repeat              TMS
NCX1      KDSVTAVVFVALGTSVPDTFASKVAA--TQDQYADASIGNVTGSNAVNVFLGIGV  882
NCX2      KDSVNAVVFVALGTSIPDTFASKVAA--LQDQCADASIGNVTGSNAVNVFLGLGV  832
NCX3      KDSVTAVVFVAFGTSVPDTFASKAAA--LQDQYADASIGNVTGSNAVNVFLGIGL  838
SQUID     KDAVTAVSFVALGTSVPDTFASKVAA--INDKYADSSIGNVTGSNAVNVFLGIGI  803
CalX      KDSVTAILFVALGTSIPDTFASMIAA--KHDEGADNCIGNVTGSNAVNVFLGIGL  861
CENCX1    KDSVTALTLVAMGTSLPDTFASRTAA--VGDQWADGSIGNVTGSNAVNVFLGIGI  790

NCKX1     SEEIMGLTILAAGTSIPDLITSVIVAR---KGLGDMAVSSSVGSNIFDITVGLPL  1120
NCKX2     SEEIMGLTILAAGTSIPDLITSVIVAR---KGLGDMAVSSSVGSNIFDITVGLPL  882
CENCKX    PTEIIGLTILAAGTSIPDLITSVIVAR---KGLGDMAVSSSVGSNIFDVCVGLPI  506

α2 CONSERVED
                    A GTS PD   S   A        D       GSN      G

CONSERVED BETWEEN α1 AND α2

                      G S P    S                    GS
```

Fig. 13: Amino acid alignment of α repeat regions.
The alignment includes the sequences of the rat NCX1 (Low et al., 1993), NCX2 (Li et al., 1994) and NCX3 (Nicoll et al., 1996a), squid NCX (He *et al.*, 1996), *Drosophilia* CalX (Schwarz and Benzer, 1997), *C. elegans* CENCX (Kraev and Carafoli, 1998) and CENCKX (Kraev *et al.*, 1998), bovine retina NCKX1 (Reiländer *et al.*, 1992) and rat brain NCKX2 (Tsoi *et al.*, 1997). The putative transmembrane segments are *overlined.* *Dashes* indicate gaps introduced to maximize the alignment.

1.6 Thesis Investigation:

The Na/Ca-K exchanger plays an important role in regulating the photoreceptor calcium concentration. The objective of the thesis was to characterize the bovine rod photoreceptor Na/Ca-K exchanger in order to gain insight into how the exchanger maintains calcium homeostasis in the ROS.

In the first part of the thesis, previously generated anti-Na/Ca, K exchanger monoclonal antibodies were used to study the structural and functional properties of the exchanger using biochemical and immunochemical methods. The antibodies were used to provide experimental evidence for the topological model of the Na/Ca-K exchanger. Localization of the large hydrophilic domains led to the structure-function relationship studies. Proteolysis and functional reconstitution were used to determine the regions of the exchanger that were essential for exchange activity. The antibodies were used to monitor the effect of limited proteolysis on the structure of Na/Ca-K exchanger. Ca^{2+} efflux assays were used to determine the effect of proteolysis to the Na/Ca exchange activity. The antibodies were also used to characterize the exchanger in terms of the cellular and subcellular localization within the bovine ROS and the type of glycosylation.

In the second part of the thesis, the hydrodynamic properties of the exchanger were used to examine the oligomeric nature of the Na/Ca-K exchanger. The oligomeric state of the detergent solubilized exchanger was examined by velocity sedimentation analysis and size exclusion chromatography, whereas the oligomeric state of the exchanger within the plasma membrane was determined by chemical cross-linking and velocity sedimentation studies.

METHODS AND MATERIAL

2.1 Preparation of ROS:

Bovine ROS were prepared by isopycnic density centrifugation on continuous sucrose gradients (Molday and Molday, 1987). Under dim red light, 100 freshly dissected retinas or previously frozen retinas were gently shaken in homogenization solution (20 mM Tris-HCl buffer, pH 7.4, containing 20% (w/v) sucrose, 10 mM β-D-glucose, 10 mM taurine and 0.25 mM $MgCl_2$). The homogenate was filtered through a fine Teflon screen, and the filtrate was layered on top of a 30%-50% (w/v) continuous sucrose gradient in homogenization solution with the indicated sucrose concentrations. The ROS were separated by centrifugation at 4°C for 1 h at 24,000 RPM in a Beckman SW 28 rotor. The ROS band was collected and washed in homogenization buffer. After centrifugation for 8 min at 8000 RPM in a SS 34 rotor, the ROS were suspended at ~8 mg/ml in homogenization buffer and used immediately or stored at -70°C.

2.2 Purification of the Exchanger:

ROS were hypotonically lysed by washing twice with 10 volumes of 10 mM Hepes-KOH buffer, pH 7.4, containing 1 mM DTT and 1 mM EDTA and twice in the same buffer without EDTA. Following each wash the membranes were collected by centrifugation at 4°C for 10 min at 40,000 RPM in a Beckman TLA 100.4 rotor. The membranes were suspended in 1/10 the solubilization volume with 10 mM Hepes-KOH buffer, pH 7.4, and solubilized at 1.0 mg/ml in 10 mM Hepes-KOH buffer, pH 7.4, containing 18 mM CHAPS, 150 mM KCl, 2 mM $CaCl_2$ and 2 mg/ml soybean L-α-phosphatidylcholine (Sigma type IV). The exchanger was purified from the CHAPS solubilized ROS membrane extract by DEAE-650S (Supelco) chromatography followed by AF Red Fractogel-TSK (Merck) chromatography (Cook and Kaupp, 1988). Briefly,

10 ml of solubilized ROS was applied to a DEAE column (3 ml) pre-equilibrated in solubilization buffer. After washing the column with 10 bed volumes of wash buffer (10 mM Hepes-KOH buffer, pH 7.4, containing 150 mM KCl, 2 mM $CaCl_2$ and 1 mM DTT), the bound proteins were eluted with wash buffer containing 0.7 M KCl, and 1 ml fractions were collected. The DEAE fractions containing the exchanger were pooled and applied to the AF Red Fractogel column (3 ml) pre-equilibrated in the 0.7 M KCl wash buffer. The unbound fraction of the AF Red Fractogel column was separated by SDS-PAGE for Coomassie Blue staining or for Western blotting.

2.3 Monoclonal Antibodies:

2.3.1 Generation of Monoclonal Antibodies:

Monoclonal antibodies were generated from Balb/c mice immunized with either ROS plasma membranes or the purified exchanger as described (Mackenzie and Molday, 1982). The monoclonal antibodies, PMe 4G1, PMe 2D9, PMe 7A5, PMe 3D12, PMe 6E2, PMe 4G7, PMe 1B3 and PMe 2A11, were generated by D.M. Reid, L.L. Molday and S.C. Hsu.

2.3.2 Purification of Monoclonal Antibodies:

The monoclonal antibodies were purified from ascites fluid by ammonium sulphate precipitation followed by DEAE anion exchange chromatography as previously described (Goding, 1986). Balb/C mice were pristane primed and then injected peritoneally with the desired hybridoma cells. The ascites fluid (2 ml) was mixed with an equal volume of saturated ammonium sulphate at 4°C for 1 h. The precipitated proteins were centrifuged at 12,000g for 20 min. The pellet, which contains the antibody, was resuspended in 2 ml of 20 mM Tris-HCl buffer, pH 7.4. The solution was then dialyzed overnight in 20 mM Tris-HCl buffer, pH 7.4,

containing 40 mM NaCl with 3 changes of 1 l each. The dialyzed solution was centrifuged at 12,000g for 10 min and filtered before applying the solution to a DEAE Sephacel column. The antibody was eluted using a continuous salt gradient from 20-300 mM NaCl and collected in one ml fractions. Purification of the antibody was monitored by SDS-PAGE followed by Coomassie Blue staining. The fractions containing the antibody were pooled and dialyzed in 10 mM borate-HCl buffer, pH 8.4, at 4°C overnight with 3 changes of 1 l each.

2.3.3 Preparation of Immunoaffinity Matrices:

The monoclonal antibodies were coupled to cyanogen bromide (CNBr) activated Sepharose 2B beads (Pharmacia) as previously described (Cuatrecasas, 1970). Typically, 8 ml of Sepharose beads in an equal volume of distilled water was adjusted to pH 10-11 with 0.2 M NaOH. CNBr (0.15 g Aldrich Chemical Company) was added to the beads, and the pH of the solution was maintained between 10-11 by the continuous addition of 0.2 M NaOH. After 30 min the excess CNBr was removed by washing the beads with 10 mM borate-HCl buffer, pH 8.4. The beads were centrifuged in a clinical table-top centrifuge following each wash. One ml of activated beads was incubated with one mg of purified antibody overnight at 4°C on a rocker.

2.4 Protein Assay:

For ROS, the protein concentration was determined using the BCA assay (Pierce). The assays were performed using a 96 well plate. Ten µl of sample was mixed with 200 µl of detection reagent and allowed to develop for 30 min at 37°C. The absorbance of the samples was taken at 540 nm in an ELISA plate reader (Bio-Tek instruments). For solubilized ROS membranes the protein concentration was determined using the modified Bradford assay (Read and Northcote, 1981). Samples (50 µl) were mixed with 950 µl of dye reagent (0.01% Serva

blue G (Interscience), 1.6 M phosphoric acid and 0.8 M ethanol). After 20 min, the colorimetric development of the samples was monitored at 595 nm using a LKB spectrophotometer with plastic cuvettes. For both protein assays bovine serum albumin was used as the standard.

2.5 SDS-PAGE and Western Blot Analysis:

SDS PAGE was performed using the discontinuous buffer system described by Laemmli (1970). The stacking gel contained 3.9% and 3.5% acrylamide for continuous and gradient polyacrylamide gels, respectively, and the separating gel contained the indicated amounts of acrylamide. Samples were prepared with an equal volume of SDS PAGE loading buffer (10 mM Tris buffer, pH 6.8, 40% sucrose, 4% SDS and 5% β-mercaptoethanol). After SDS PAGE, the gels were either stained with Coomassie Blue or electrophoretically transferred onto 0.45 μm Immobilon-P (Millipore) or 0.45 μm nitrocellulose filters in 25 mM Tris-HCl buffer, pH 8.4, containing 190 mM glycine (transfer buffer) (Towbin et al., 1979) using a semi-dry transfer apparatus (Biorad). ROS were transferred for 45 min in transfer buffer containing 5% methanol whereas fusion proteins were transferred for 20 min in transfer buffer containing 15% methanol.

For Western blot analysis, the membranes were first blocked in phosphate buffered saline (PBS: 0.01 M phosphate buffer, pH 7.5, 136 mM NaCl and 2 mM KCl) containing 0.5% milk and then incubated for 1 h with the MAb hybridoma culture fluid diluted 1:20 in PBS containing 0.05% milk. After washing the membranes in PBS, the blots were incubated for 30 min with sheep anti-mouse immunoglobulin (Ig) Fab' fragments conjugated to horseradish peroxidase diluted 1:5000 in PBS containing 0.05 % milk. Antibody labeling was detected by enhanced chemiluminescence (Amersham).

2.6 COS-1 Cell Expression:

The bovine rod photoreceptor Na/Ca-K exchanger cDNA in pBluescript KS (kindly provided by Dr. Helmut Reiländer) was digested with Bam HI and subcloned into the Bam HI site of the pAX 111 mammalian expression vector (kindly provided by Dr. Rob Kay at Terry Fox Laboratories, Vancouver). The transient transfection procedure used was a modified method of Chen and Okayama (1987). The solutions for the calcium phosphate precipitation method were stored at -20° C: CA (1.0 M $CaCl_2$) and BBS (50 mM BES-NaOH buffer, pH 6.95, containing 280 mM NaCl and 1.5 mM Na_2HPO_4). On day one, 2 x 10^5 COS-1 cells were plated onto a 60 x 15 mm petri dish and grown at 37°C in DMEM media containing 10% FBS and 10 U/ml penicillin/streptomycin. On the second day, 10 µg of plasmid DNA was mixed with 41 µl of CA, and the mixture was made up to a final volume of 165 µl. The DNA-calcium mixture was slowly added to BBS (165 µl) with a pipette, avoiding oxidation, and left at room temperature for 20 min. The DNA-calcium-phosphate mixture was then added to the COS-1 cells and placed in a 3% CO_2 incubator at 35°C overnight. On the third day, the media was changed and the cells were transferred to a 5% CO_2 incubator at 37°C. On the fourth day, cells were harvested by solubilizing the COS-1 cells in 200 µl PBS containing 18 mM CHAPS and 100 µg/ml phenylmethylsulfonylfluoride (PMSF). The cell extract was scrapped off the plate and centrifuged for 5 min at maximum speed in a microcentrifuge. The supernatant was mixed with an equal volume of the SDS loading buffer (5% SDS, 5% β-mercaptoethanol; 40% sucrose, 0.01M Tris-HCl, pH 6.8) and analyzed by SDS-PAGE followed by Western blot analysis.

2.7 Generation of Fusion Proteins:

2.7.1 Construction of Expression Plasmid:

The bovine rod photoreceptor Na/Ca-K exchanger cDNA was digested with the indicated restriction enzymes and subcloned into the appropriate pGEX expression vector (Pharmacia). The fusion proteins were constructed as follows: pbEX1 – a *Sau* 3AI to *Sca* I fragment (bp 95-449) was subcloned into the *Bam* HI/*Sma* I sites of pGEX 3X; pbEX2 – an *Alu* I fragment (bp 248- 524) was subcloned into the *Sma* I site of pGEX 2T; pbEX3 – an *Alu* I fragment (bp 524-872) was subcloned into the *Sma* I site of pGEX 2T; pbEX4 – a *Hind* III to *Sca* I fragment (bp 1010-1408) was blunted ended with Klenow and subcloned into the *Sma* I site of pGEX 2T; pbEX5 – a *Sau* 3AI fragment (bp1628 – 2184) subcloned into the *Bam* HI site of pGEX 2T was double digested with *Xho* I (bp 1798) (blunt ended with Klenow) and *Eco* RI (restriction site in the vector) and the resulting restriction fragment was inserted into the *Sma* I/*Eco* RI site of pGEX I; pbEX6 – an *Alu* I (bp 2266 – 2569) fragment was subcloned into the *Sma* I site of pGEX I; and pbEX7 – an *Alu* I (bp 2569 - 2620) fragment was subcloned into the *Sma* I site of pGEX I.

The constructs for fusion proteins, p630 (bp 1798-2427) and p430 (bp 1798-2997), were generated by nested deletion according to the manufacturer's protocol (Promega). After digesting the exchanger cDNA in pBluescript KS with *Kpn* I and *Sal* I, the linearized plasmid was sequentially treated with Exonuclease III, S1 nuclease, Klenow and calf intestinal alkaline phosphatase. The nested deleted plasmid was religated with a linker (5'-TGAGTGAGTGAGCGGCCGCTCACTCACTCA-3'), which contains a *Not* I site and introduces a stop codon in all three reading frames. The *Xho* I (bp 1798) to *Not* I (linker) fragment of the nested deleted plasmid was subcloned into the *Xho* I/ *Not* I site of pGEX 4T3 n2

vector. The reading frame of the inserts was confirmed by DNA sequencing using Sequenase version 2.0 (US Biochemical Corp.).

2.7.2 Expression and Purification of the Fusion Proteins:

GST exchanger fusion proteins were over expressed in *Escherichia coli* (XL-1 Blue) cells as described by Smith and Johnson (1988). Briefly, LB/Amp was inoculated with 1/10 the volume of the overnight culture. After the cells were incubated for 1.5 h on a shaker at 37°C, the expression of the fusion protein was induced by the addition of 0.1 mM IPTG and allowed to grow for an additional 3 h. The cells were centrifuged for 10 min at 5000 g in a SS-34 rotor and resuspended in PBS containing 1% Triton X-100 and 2 mM EDTA. The cells were lysed with a SLM Aminco French Press at 15,000 psi. After centrifugation of the cell lysate for 15 min at 27,000 g in a SS-34 rotor, the supernatant was incubated with glutathione-CL4 agarose at 25°C for 3 min. The immobilized fusion protein was eluted with 5 mM reduced-glutathione in 50 mM Tris-HCl buffer, pH 8.0. Alternatively, the cells were harvested by adding an equal volume of SDS loading buffer (5% SDS, 5% β-mercaptoethanol; 40% sucrose, 0.01M Tris-HCl, pH 6.8) and separated by SDS-PAGE for either Coomassie Blue staining or Western blot analysis.

2.8 Peptide Synthesis:

The epitopes for some of the mAbs were more precisely mapped using the Epitope Scanning kit (Cambridge Research Biochemicals, Northwich, UK). For these studies, nine amino acid peptides with seven amino acid overlap were synthesized by Fmoc chemistry for analysis by enzyme-linked immunosorbent assays. A large scale preparation of the peptide DEDEGEIQA, which corresponds to the PMe 2A11 epitope, was synthesized using the LKB Biolynx 4175 Peptide Synthesiser (LKB Biochom Ltd., Cambridge, UK).

2.9 Immunofluorescence Microscopy:

The cornea, lens and the majority of the vitreous humor were removed from fresh bovine eyes obtained ~3 h post mortem. The eye cups were fixed in 0.1 M sodium phosphate buffer, pH 7.4, containing 4% paraformaldehyde and 2 % sucrose for 2 h. The eye was then cut into 1 cm^2 sections and fixed for an additional 2 h. After washing the sections 4 times for 30 min each in sodium phosphate buffer, pH 7.4, containing 10% sucrose, the retina was detached and sliced into ~2x8 mm^2 sections. The tissue was embedded in O.C.T.™ compound (Tissue-Tek) by quick-freezing in liquid N_2 and sectioned at 10 μm thickness using a cryostat. The retina was blocked and made permeable by incubating in 0.1 M sodium phosphate buffer, pH 7.4, containing 0.2% TX-100 and 10% goat serum for 30 min. The tissue was then labeled overnight at 4°C with anti-exchanger MAb hybridoma culture fluid diluted 1:20 in the presence or absence of 0.5mg/ml competing peptide, DEDEGEIQA, followed by four 10 min washes with blocking buffer containing 3% goat serum. After incubation with 1:1000 diluted goat anti-mouse Ig conjugated to CY3 (Jackson) for 30 min, the tissue was washed as before. Both primary and secondary antibodies were diluted in blocking buffer containing 3% goat serum. The fluorescence was preserved with a drop of 10% Mowiol (Calbiochem), 25% glycerol in 0.1 M Tris-HCl buffer, pH 8.5 (Heimer and Taylor, 1974) and observed using a Zeiss Axiophot microscope.

2.10 Immunoelectron Microscopy:

A pre-embedding labeling protocol was used for electron microscopy studies. Intact ROS or hypotonically lysed ROS at 1.0 mg/ml protein concentration were prepared from fresh bovine eyes (section 2.1) and absorbed onto 13 mm Thermanox coverslips (Nunc, Inc.,

Naperville, IL) in homogenization buffer containing 5% sucrose. The coverslips were washed in 20 mM Tris-HCl buffer, pH 7.5, containing 5% sucrose and then blocked in 40 mM Tris-HCl buffer, pH 7.5, containing 4% BSA and 5% sucrose for intact ROS and 0.5% sucrose for lysed ROS for 30 min at 25°C. The samples were labeled overnight with anti-exchanger MAb hybridoma culture fluid diluted 2 fold followed by 3 washes for 10 min each in blocking buffer containing 0.1% BSA. The samples were then incubated for 30 min with 1:5 diluted goat anti-mouse Ig conjugated to 10 nm gold particles (British BioCell, Cardiff, UK) and washed 3 times for 10 min each in 0.1 M cocadylate-HCl buffer, pH 7.4, containing 0.2% sucrose (CW). Both the primary and secondary antibodies were diluted with blocking buffer containing 0.1% BSA.

The samples were fixed in 100 mM cocadylate-HCl buffer, pH 7.4, containing 2% gluteraldehyde and 0.2% sucrose for 1 h and washed as before in CW. The samples were then post-fixed in 0.1 M cocadylate-HCl buffer, pH 7.4, containing 1% osmium tetroxide and 0.2% sucrose for 1 h and dehydrated by successive 5 min incubations in 50%, 70%, 80% and 90% ethanol followed by 1 h in 100% ethanol. The samples were placed in rubber wells filled with Epon-Araldite resin (Polysciences, Inc., Warrington, PA) and allowed to solidify at 52°-55°C for 24-48 h. Ultrathin sections were cut from the resin block using a MT5000 Sorvall ultra microtome (Dupont) equipped with a diamond knife and collected on nickel grids.

The staining of the membranes was enhanced by sequentially treating the grids on small drops of the following solutions:

1. saturated uranyl acetate (8% w/v) in dH_2O, 15 min
2. dH_2O, 6 X 1 min
3. 40 mM lead nitrate and 60 mM sodium citrate in dH_2O, 3 min
4. dH_2O, 6 X 1 min

5. air dry for 1 h

The labeling of the samples were viewed under a JEOL 1200EX electron microscope.

In other pre-embedding labeling studies, freshly dissected bovine retina tissue was fixed in 100 mM cocadylate-HCl buffer, pH 7.2, containing 1% glutaraldehyde and 0.2% sucrose for 1 h at 4°C. After rinsing the tissue in the same buffer in the absence of glutaraldehyde, the sample was blocked with 1% glycine and 2% bovine serum albumin in PBS and then labeled with the MAb PMe 2D9 conjugated to gold-dextran particles 10 nm for 4 h. The samples were then prepared and viewed as described for the ROS.

2.11 Enzymatic Deglycosylation:

For O-linked carbohydrate studies, 2.1 mg of ROS in 50 mM sodium acetate buffer, pH 5.3, containing 20% sucrose were first treated with 10 mU of *Arthrobacter Ureafaciens* (Boehringer Mannheim) for 1 h on ice. The ROS membranes were obtained by hypotonic lysis in 10 mM Hepes buffer, pH 7.4, as described before (section 2.2) and solubilized in 1.0 ml of 10 mM Hepes-KOH buffer, pH 7.4, containing 18 mM CHAPS, 150 mM KCl and 2 mM $CaCl_2$. After incubating the solubilized ROS membranes with 50 µl of PMe 2A11-Sepharose 2B beads (section 2.4.1) for 1 h, the matrix was washed 6 times with 1.0 ml of the same solubilization buffer indicated above. The bound exchanger was treated with 0.5 mU of *Diplococcus Pneumoniae* O-glycosidase (Boehringer Mannheim) in 20 mM sodium cocadylate-maleate buffer, pH 6.0, for 1 h at 28°C and eluted with 50 µl of 3% SDS in dH_2O.

For N-linked carbohydrate studies, untreated ROS, neuraminidase treated ROS or the neuraminidase followed by O-glycosidase treated exchanger were solubilized in 50 mM sodium phosphate buffer, pH 7.5, containing 1% SDS, 1% NP-40 and 0.5% βME and incubated with

1000 units of *Flavobacterium Meningosepticum* PNGase F (New England Biolabs) for 1 h at 28°C.

2.12 Limited Proteolysis:

Intact ROS (2 mg protein) were digested with 2 μg/ml tosyl-phenylalanine chloromethyl ketone treated trypsin (Sigma) in 2 ml of 10 mM Hepes-KOH buffer, pH 7.4, containing 20% sucrose, 2 mM KCl and 2 mM $CaCl_2$ at 25°C. The ROS were washed with 10 ml of the same buffer containing 10 μg/ml soybean trypsin inhibitor (SBTI) three times and collected by centrifugation at 4000g for 5 min after each wash. In other studies, ROS membranes (1 mg/ml protein) in 3 ml of 10 mM Hepes-KOH buffer, pH 7.4, containing 2 mM $CaCl_2$ and 1 mM DTT were digested with 2 ml of 5 units/ml of porcine pancreatic kallikrein (Sigma) for 20 min at 25°C. After digestion, the membranes were washed three times with 3.5 ml of ice cold 10 mM Hepes-KOH buffer, pH 7.4, containing 1 mM DTT, 100 μg/ml phenylmethylsulfonyl fluoride and 0.1 mg/ml Pefabloc® (Boehringer Mannheim). The ROS membranes were solubilized in CHAPS for either Western blot analysis or functional reconstitution.

In other studies, one ml of ROS membrane proteins reconstituted into lipid vesicles (section 2.12) were treated with 5 μg/ml of trypsin in 5 mM Hepes-KOH buffer, pH 7.4, containing 100 mM KCl and 2 mM $CaCl_2$ for 30 min at room temperature. After stopping the digestion with 15 μl of SBTI (1 mg/ml), the trypsin treated vesicles were dialyzed in 5 mM Hepes-KOH buffer, pH 7.4, containing 100 mM KCl for 1 h and then passed through a Chelex-100 column (Biorad) equilibrated with the same buffer. The trypsin treated vesicles were analyzed by Western blotting or by Ca^{2+} efflux assays. In all the proteolytic studies, the untreated control samples were handled identical to the protease treated samples.

2.13 Functional Reconstitution of the Exchanger:

2.13.1 Ca^{2+} Efflux Assays:

The CHAPS solubilized exchanger was reconstituted into Ca^{2+} loaded lipid vesicles by dialysis (Cook and Kaupp, 1988). The solubilized ROS membranes (1 mg/ml) were combined with an equal volume of a soybean L-α-phosphotidylcholine (Sigma type IV) solution to give a final mixture of 10 mg/ml of lipid, 10 mM CHAPS, 100 mM KCl, 2 mM $CaCl_2$ and 1 mM DTT in 10 mM Hepes-KOH buffer, pH 7.4. The mixture was dialyzed for 18 h in reconstitution buffer (5 mM Hepes-KOH buffer, pH 7.4, 100 mM KCl and 2 mM $CaCl_2$) with 3 changes of 1 l each. The transmembrane Ca^{2+} gradient was established by first dialyzing the liposomes for 2 h against 1 l of reconstitution buffer without $CaCl_2$ and then passing the vesicles through a Chelex-100 (Biorad) ion exchange column equilibrated in the same buffer.

Calcium efflux assays were carried out by adding 0.3 ml of liposomes to 1.7 ml Ca^{2+} free reconstitution buffer containing 75 μM Arsenazo III. Calcium release from the vesicles was initiated by adding the indicated concentrations of NaCl at 25°C in the presence of 2 μM FCCP, 2 μM valinomycin and 100 mM symmetrical KCl. The activity of the exchanger was monitored spectrophotometrically using a SLM Aminco DW2000 spectrophotometer in the dual wavelength mode (650-730nm).

The initial rates were obtained by taking the tangent of the absorbance curve, which represents the release of calcium from the vesicles, immediately following the addition of NaCl. The absorbance values were converted to nmol Ca^{2+} by calibration with 1 nmol $CaCl_2$ ($A_{650\text{-}730}$ = 0.0085). Plots of the calcium efflux assays were obtained by transferring the data from the DW2000 files to Sigma Plot (Jandel Scientific).

2.13.2 Potassium Dependent Efflux Assays:

For K^+ dependent Ca^{2+} efflux assays, Tris-HCl was used to titrate the Hepes buffer to pH 7.4 and the KCl was replaced with 100 mM choline chloride in the solubilization and reconstitution buffers. Calcium efflux assays were performed essentially as described in section 2.12.1, but KCl was added to the assay for a final concentration of 2.5 mM in the presence of 2 μM valinomycin and allowed to equilibrate for 2 min before the addition of 50 mM NaCl.

Alternatively, the solubilized exchanger was incorporated into lipid vesicles by dialyzing in reconstitution buffer containing 50 mM KCl instead of 100 mM KCl. The vesicles (0.3 ml) were diluted with 1.7 ml of reconstitution buffer containing 75 μM Arsenazo III to give the indicated extravesicular potassium concentrations (Friedel *et al.* 1991).

2.13.3 Ca^{2+} Efflux Assays from ROS:

Trypsin treated or untreated, intact Ca^{2+} loaded ROS (section 2.10) were washed 3 times with 10 ml of 10 mM Hepes buffer, pH 7.4, containing 20% sucrose and 2.5 mM KCl. The ROS were resuspended with the wash buffer containing 110 μM Arsenazo III at a protein concentration of 0.25 mg/ml. For Ca^{2+} efflux assays, 2.0 ml of the resuspended ROS were used.

2.14 $^{45}Ca^{2+}$ Binding to the Cytoplasmic Loop:

Ca^{2+} binding studies were carried out using the method described by Maruyama *et al.* (1984). The cardiac cytoplasmic domain β-galactosidase fusion protein, p240-679, (kindly provided by Dr. Kenneth Philipson, UCLA) and the rod exchanger GST fusion proteins were expressed in *Escherichia coli* (XL-1 Blue) as described in section 2.7.2. After transferring the fusion proteins onto nitrocellulose, the membranes were washed four times for 15 min each in 10 mM imidazole-HCl buffer, pH 7.2, containing 60 mM KCl and 5 mM $MgCl_2$. The membranes

were incubated in the same buffer containing 2 μCi/ml of $^{45}Ca^{2+}$ for 10 min and washed twice for 5 min each in deionized water containing 40% methanol. All the incubations and washes were carried out at 25°C. The membranes were air dried for 1 h and exposed to X-ray film overnight.

2.15 Cross-linking:

Typically, 45 μg of ROS membranes (section 2.2) were resuspended with 995 μl of 10 mM Hepes-KOH buffer, pH 6.5, containing 1 mM EDTA and 150 mM KCl and chemically cross-linked by adding 5 μl of 1.8 mM N,N-para-phenylene-dimaleimide prepared fresh in DMF. After 30 min at 25°C, the reaction was stopped by the addition of 90 μl of 1 M DTT. The membranes were washed 4 times with 3.5 ml each of 10 mM Hepes-KOH buffer, pH 7.4, containing 1 mM DTT. The membranes were collected by centrifugation at 4°C for 10 min at 40,000 RPM in a Beckman TLA 100.4 rotor following each wash. The chemically modified membranes were solubilized as described before (section 2.2) for Western blot analysis or velocity sedimentation.

2.16 Hydrodynamic Studies:

The hydrodynamic properties of the detergent solubilized exchanger from ROS membranes was obtained by velocity sedimentation and size exclusion chromatography using the modified protocol of Clarke (1975) and described by Goldberg et al. (1995). Untreated, neuraminidase treated (section 2.10) and pPDM cross-linked (section 2.13) ROS membranes were solubilized at a final protein concentration of 1.0 mg/ml in Buffer A (10 mM Hepes buffer, pH 7.4, 150 mM KCl, 2 mM $CaCl_2$, 1 mM DTT) containing either 1.0% TX-100 or 16 mM CHAPS.

2.16.1 Size Exclusion Chromatography:

The Stoke's radius of the detergent solubilized exchanger was determined by the method of Laurent and Killander (1964). Samples of 150 µl containing 3% glycerol were chromatographed at 4°C on a 33 X 0.7 cm Sepharose CL-4B (Sigma) or Sepharose CL-6B (Sigma) column equilibrated in Buffer A containing 0.2% TX-100 or 12 mM CHAPS. Fractions of ~125 µl were collected at a flow rate of ~60 µl/min. The elution of the exchanger was monitored by Western blot analysis and quantitated by laser densitometry. The column was calibrated with marker proteins (aldolase, catalase, ferritin and thyroglobulin) with known Stoke's radius and assayed as described below. Blue dextran and vitamin B_{12} were used to determine the void (V_o) and total (V_t) volumes of the column, respectively. The protein elution volumes were standardized to the distribution coefficient (K_{av}) of the column

(1) $K_{av} = (V_e - V_o)/(V_t - V_o)$

where V_e is the elution volume at the peak concentration of the protein. A calibration curve was constructed by plotting $(-\log K_{av})^{1/2}$ versus Stoke's radius.

2.16.2 Velocity Sedimentation:

Linear gradients of 5%-20% sucrose (w/v) in H_2O or 98.5% D_2O (Sigma) were prepared by sequentially adding 1.2 ml of 20%, 15%, 10% and 5% sucrose in Buffer A containing either 0.2% TX-100 or 12 mM CHAPS to Ultraclear centrifuge tubes (Beckman). The step gradients were allowed to diffuse at 25°C for 3.5 h and then chilled on ice for 30 min. A sample volume of 100 µl containing the marker enzymes (catalase, aldolase and malate dehydrogenase) were layered on top of the gradients and centrifuged at 49 000 rpm in a Beckman SW 50.1 rotor at 4°C for 6.5 h (H_2O) and 16 h (D_2O). After centrifugation, the bottom of the centrifuge tubes was punctured, and the gradients were collected in 8 drop fractions. Sedimentation profiles of the

exchanger were determined by Western blot analysis followed by laser densitometry. The sedimentation of the marker proteins was monitored as described below.

The density of the 5% and 20% stock sucrose solutions were measured gravitometrically by weighing a fixed volume of the solution. Since density has a linear relationship with the concentration of sucrose, the intermediate fractions were assumed to be linear with its radial position. The refractive index of each fraction was measured to ensure the linearity of the gradients.

2.16.3 Detection of Marker Proteins:

The marker proteins, aldolase, catalase and malate dehydrogenase, were detected by using the assays described in the Worthington Enzyme Manual. Thyroglobulin and ferritin were monitored by SDS-PAGE followed by Coomassie Blue staining and then quantitated by laser densitometry. The physical properties of the marker enzymes are listed in Table 2 (Sober, 1968; De Haen, 1987).

Table 2: Hydrodynamic properties of the marker enzymes

Marker Enzyme	Stoke's Radius	Sedimentation Coefficient $S_{20,w}$	Partial Specific Volume
aldolase	4.6 nm	7.70 S	0.742 ml/g
catalase	5.2 nm	11.3 S	0.730 ml/g
malate dehydrogenase		4.32 S	0.734 ml/g
thyroglobulin	8.5 nm		
ferritin	6.7 nm		

2.17 Calculation of the Hydrodynamic Parameters of the Exchanger:

The molecular mass of the exchanger was calculated using a program created in Microsoft Excel. The program calculates the molecular mass by using a number of formulas described by Clarke (1975).

The sedimentation coefficient ($S_{T,m}$) at a given temperature T in solvent m is given by the equation

(2) $S_{T,m} = [(r_f - r_o)/t]/\omega^2 r_{avg}$

where r_f is the distance of the protein at time t from the center of the axis of rotation, r_o is the initial radial position, ω is the angular velocity of the rotor and r_{avg} is the average radial position defined by $r_{avg} = (r_o+r_f)/2$. The sedimentation coefficient is corrected to the standard state condition at 20°C in water ($S_{20,w}$) by using the following equation

(3) $S_{20,w} = S_{T,m}(\eta_{T,m}/\eta_{20,w})[(1-\nu_c\rho_{20,w})/(1-\nu_c\rho_{T,m})]$

where η is the viscosity, ρ is the density and ν_c is the partial specific volume of the protein-detergent complex. Since density has a linear relationship with sucrose concentration, the density ($\rho_{T,m}$) at r_{avg} is calculated by linear regression. The viscosity of the solvent ($\eta_{T,m}$) at r_{avg} is determined by calculating the viscosity experienced by the marker proteins using the equation

(4) $\eta_{T,m}/\eta_{20,w} = (S_{20,w}/ S_{T,m})[(1-\nu\rho_{T,m})/(1-\rho_{20,w})]$

where $S_{20,w}$ and ν are the sedimentation coefficient and partial specific volume, respectively, of the marker proteins from the literature. The viscosity at r_{avg} for the unknown protein is extrapolated from a plot of η_{avg} versus r_{avg} for the marker proteins.

The partial specific volume of the protein-detergent complex (ν_c) is determined by velocity sedimentation analysis in H_2O ($_{Havg}$) and D_2O ($_{Davg}$) based sucrose gradients and then calculated using the equation

(5) $\nu_c = [(S_{Davg}\eta_{Davg}/S_H\eta_{Havg}) - 1]/[\rho_{Havg}(S_D\eta_{Davg}/S_H\eta_{Havg}) - \rho_{Davg}]$

After experimentally determining the $S_{20,w}$, ν, and a for the protein-detergent complex, the molecular mass of the complex is calculated using the Svedberg equation as described by Siegel and Monty (1966):

(6) $MM_{complex} = (6\pi N\eta_{20,w}S_{20,w}\, a)/[(1-\nu\rho_{20,w})]$

where N is Avogadro's number, $\eta_{20,w}$ is the viscosity of water at 20°C, $\rho_{20,w}$ is the density of water at 20°C, ν is the partial specific volume of the complex and a is the Stoke's radius.

The molecular mass of the protein portion of the complex is calculated by taking into consideration the amount of detergent bound to the protein using the equation:

(7) $MM_{protein} = (MM_{complex})/[1+(\nu_c - \nu_p)/(\nu_d - \nu_c)]$

where ν_c, ν_p, and ν_d are the partial specific volumes of the protein-detergent complex, protein and detergent, respectively. The partial specific volumes used in the calculation are 0.908 ml/g for TX-100 (Tanford et al., 1974), 0.81 ml/g for CHAPS (Hjelmeland et al., 1983) and 0.714 ml/g for exchanger [calculated from the amino acid composition (Zamyatnin, 1984)].

A number of assumptions are made with this study:

- The amount of detergent bound in D_2O and H_2O is the same.
- The temperature of the entire sucrose gradient remains at 4°C for the duration of the centrifugation.
- The contribution of the carbohydrates to the partial specific of the exchanger is negligible.
- The additivity principle for calculating the partial specific volume is valid.

RESULTS

3.0 Specificity of the Monoclonal Antibodies:

3.0.1 Western blot Analysis of the Purified Exchanger:

Eight MAbs were generated against the bovine rod photoreceptor Na/Ca-K exchanger to characterize the molecular properties of this ion transporter. The specificity of these MAbs was determined by Western blot analysis of ROS and the exchanger purified by the method of Cook and Kaupp (1988). As shown in Fig. 14 for antibodies PMe 2D9 and PMe 2A11, all eight antibodies specifically labeled the 230 kDa exchanger in both the ROS and purified exchanger. In addition, the antibodies also labeled several lower molecular weight proteins. Antibodies PMe 4G1, PMe 3D12, PMe 7A5 and PMe 6E2 had a similar immunoreactivity as PMe 2D9 and weakly labeled a 190 kDa protein. On the other hand, antibodies PMe 1B3 and PMe 4G7 had a similar immunoreactivity as PMe 2A11 and labeled 150 kDa and 75 kDa proteins. The lower molecular weight proteins are generally believed to be degradation products, since they were present in variable amounts in different ROS preparations.

3.0.2 Heterologous Expression of the Exchanger in COS-1 Cells:

The specificity of the antibodies was also demonstrated by Western blot analysis of the heterologously expressed bovine rod Na/Ca-K exchanger in COS-1 cells (Fig. 15). Both MAbs PMe 2A11 and PMe 2D9 weakly labeled a 225 kDa protein in extracts of COS-1 cells transfected with the exchanger cDNA. MAb PMe 2A11 also strongly labeled a 180 kDa protein and weakly labeled a 100 kDa protein. These polypeptides most likely represent degradation products of the exchanger that do not contain the epitope for the PMe 2D9 antibody. No labeling was observed in extracts of COS-1 cells transfected with the vector alone. The faster mobility of

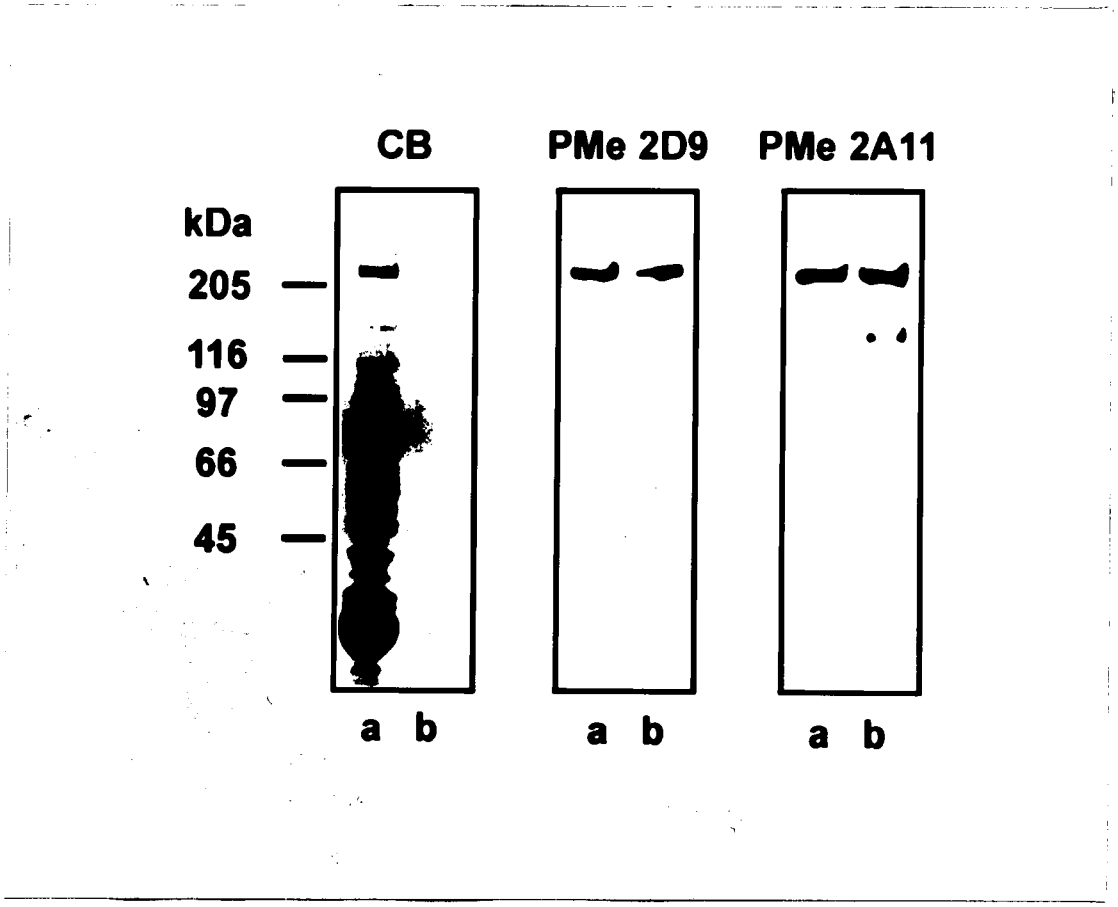

Fig. 14: Westerns blots of ROS and the purified Na/Ca-K exchanger labeled with monoclonal antibodies.

Bovine ROS (lane a) and the Na/Ca-K exchanger purified by DEAE followed by red dye chromatography (lane b) were subjected to SDS-PAGE (8% gels) and either stained with Coomassie Blue (CB) or transferred to Immobilon membranes for labeling with the PMe 2D9 and PMe 2A11 monoclonal antibodies. Approximately, 40 μg of ROS and 0.7 μg of the exchanger were applied to the gel for Coomassie Blue staining and 28 μg of ROS and 0.14 μg of exchanger were applied to the gel for Western blotting.

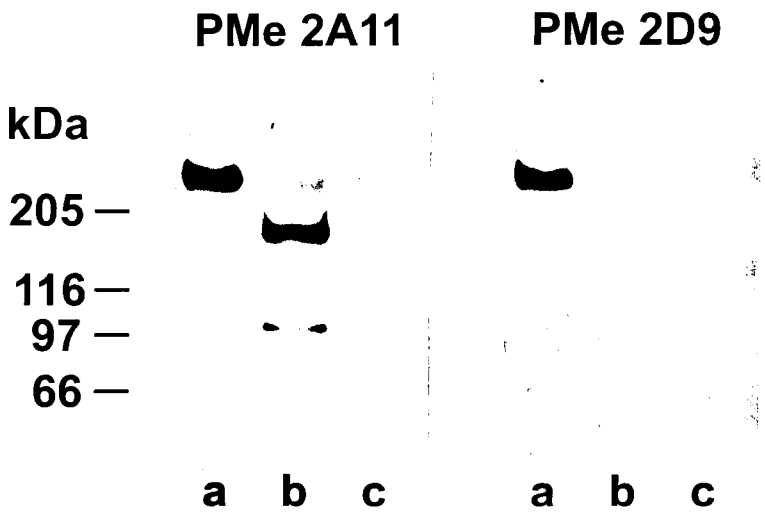

Fig. 15: Western blots of heterologously expressed exchanger in COS-1 cells.
Bovine ROS membranes (lane a) and CHAPS extracts of COS-1 cells transfected with either the bovine Na/Ca-K exchanger cDNA (lane b) or vector alone (lane c) were separated by SDS-PAGE (8% gels) and transferred onto Immobilon membranes for labeling with MAbs PMe 2A11 and PMe 2D9.

the 225 kDa expressed exchanger relative to the 230 kDa ROS exchanger is most likely due to the differences in glycosylation between COS-1 cells and rod photoreceptor cells.

Western blot analysis of ROS and extracts of COS-1 cells transfected with the exchanger cDNA indicates that the MAbs are specific to the exchanger and proteolytic fragments present in these preparations.

3.1 Epitope Mapping:

Epitopes of the anti-exchanger MAbs were mapped by expressing glutathione S-transferase (GST) fusion proteins containing selected regions of the exchanger in *E. coli* (Fig. 16A). The MAb PMe 2D9 labeled both fusion proteins EX1 and EX2 as shown in Fig. 16B. Since EX1 and EX2 have an overlapping sequence, PMe 2D9 must bind to an epitope between residues 83 and 148. The MAb PMe 2A11 labeled fusion proteins EX6 and EX7, but did not label the other fusion proteins (Fig. 16B). The sequences of fusion proteins EX6 and EX7 do not overlap; however, both fusion proteins contain a repeat sequence which is present in the large hydrophilic region between the putative transmembrane segments H5 and H6 (Reiländer *et al.*, 1992)(see Fig. 19). The PMe 2A11 epitope was further defined to the nine amino acid sequence DEDEGEIQA by analyzing MAb PMe 2A11 immunoreactivity to a number of overlapping synthetic peptides spanning the EX7 fusion protein sequence (Fig. 17). Similar studies were carried out with the other MAbs to map their epitopes. The results are shown in Table 3.

3.2 Identification of the Intracellular and Extracellular Regions of the Exchanger:

The intracellular and extracellular regions of the exchanger were identified using anti-exchanger MAbs in conjunction with pre-embedding immunogold labeling methods.

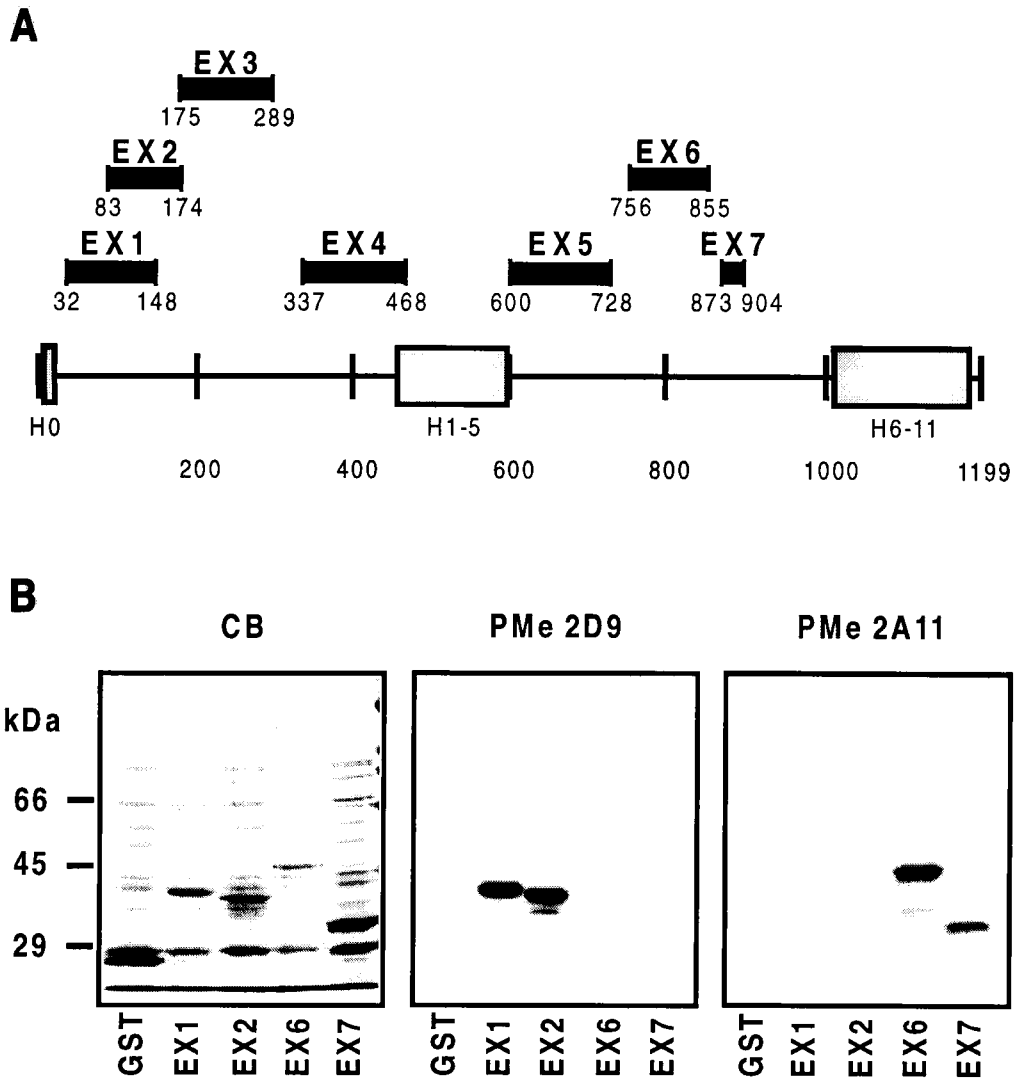

Fig. 16. Mapping the epitopes of the anti-exchanger MAbs using GST-fusion proteins.
A) The GST-fusion protein constructs (EX1-EX7) containing various segments of the exchanger are shown in relation to the linear primary sequence. The shaded boxes indicate the putative transmembrane segments (H0-H11) and the numbers refer to the amino acid sequence of the bovine Na/Ca-K exchanger (Reiländer *et al.*, 1992). B) After expressing GST or GST-fusion proteins in *E. coli*, the cell extracts were separated by SDS-PAGE (8% gels) and either stained with Coomassie blue (CB) or electrophoretically transferred onto Immobilon-P membranes. Western blots were labeled with PMe 2D9 and PMe 2A11 antibodies.

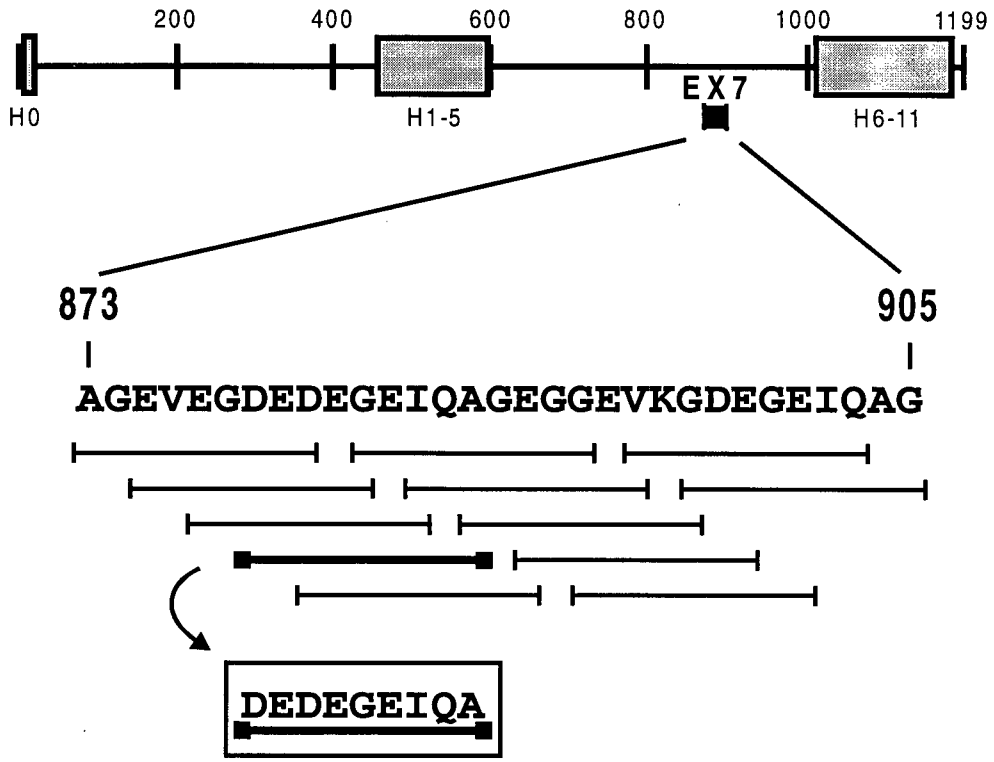

Fig. 17: Localization of the PMe 2A11 epitope using synthetic peptides.
Nine amino acid peptides (represented by lines) overlapping by seven residues were synthesized spanning the entire sequence of fusion protein EX7. Enzyme-linked immunosorbent assays were used to localize the PMe 2A11 epitope to the nine amino acid sequence DEDEGEIQA (box). The numbers represent the primary sequence of the bovine Na/Ca-K exchanger (Reiländer *et al.*, 1992).

Immunocytochemical studies were carried out on either intact or hypotonically lysed ROS. When ROS are lysed, the plasma membrane forms inside-out vesicles with the disks attached to the cytoplasmic surface as shown in Fig. 18A. When lysed ROS were labeled with PMe 2A11, the majority of the immunogold particles were distributed on the cytoplasmic side of the inverted plasma membrane (Fig. 18A). This labeling pattern is similar to that previously reported for the PMe 1B3 antibody (Reid *et al.*, 1990). In contrast, the MAbs PMe 2D9 (Fig. 18B), PMe 3D12

(Fig. 18C) and PMe 6E2 (Fig. 18D) labeled the extracellular side of the plasma membrane, ie. the side of the membrane which does not have attached disks. No labeling was observed with the MAb PMe 4G7, most likely because of the inaccessibility of the epitope. Labeling was not observed to any significant degree on disk membranes by any of the anti-exchanger antibodies.

Results of the electron microscopy studies performed with the other MAbs are shown in Table 3. Together with the epitope mapping studies, these results indicate that the N-terminal domain containing the epitopes of the MAbs PMe 4G1, PMe 2D9, PMe 7A5, PMe 3D12, and PMe 6E2 is located on the extracellular surface of the ROS plasma membrane, whereas the hydrophilic region containing the PMe 2A11, PMe 1B3 and PMe 4G7 epitopes is found on the cytoplasmic side (Fig. 19).

Table 3: Epitopes of various anti-exchanger MAbs and their localization

MAb	Fusion Protein(s) labeled	Deduced Epitope residues/sequence	Electron Microscopy localization
PMe 4G1	EX1	66-74 DLSNKEMMM	extracellular
PMe 2D9	EX1 & EX2	83-148	extracellular
PMe 7A5	EX1 & EX2	83-148	extracellular
PMe 3D12	EX3	175-289	extracellular
PMe 6E2	EX4	342-350 AWKVRNPLP	extracellular
PMe 4G7	EX5	600-728	—
PMe 1B3	EX6	756-856	cytoplasmic
PMe 2A11	EX6 & EX7	repeat DEDEGEIQA	cytoplasmic

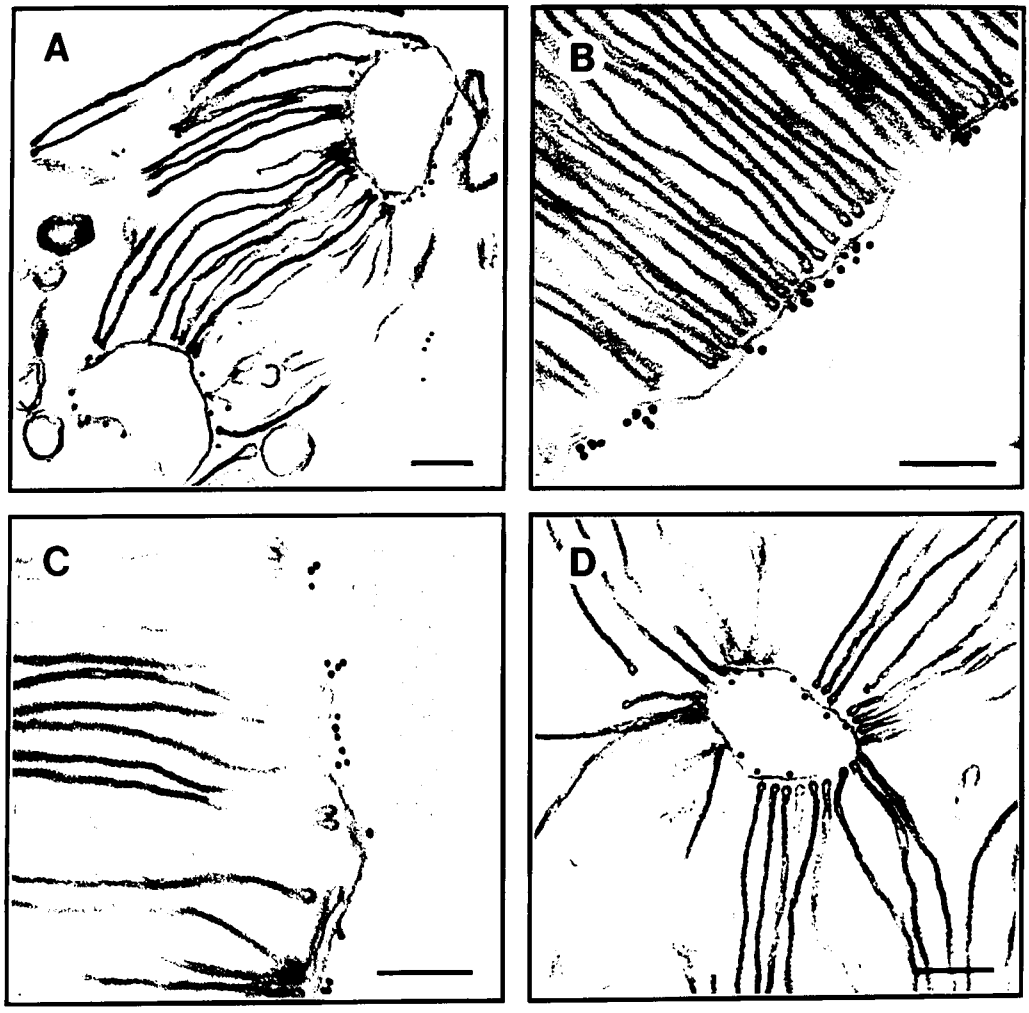

Fig. 18: Immunogold localization of the anti-exchanger MAb binding sites to the intracellular or extracellular surface of the ROS plasma membrane.
Electron micrographs of hypotonically lysed ROS membranes (A and D) or intact ROS (B and C) labeled with the PMe 2A11 (A), PMe 2D9 (B), PMe 3D12 (C) or PMe 6E2 (D) antibodies followed by goat anti-mouse-gold particles (10 nm diameter) prior to processing for electron microscopy. Bar = 100 nm.

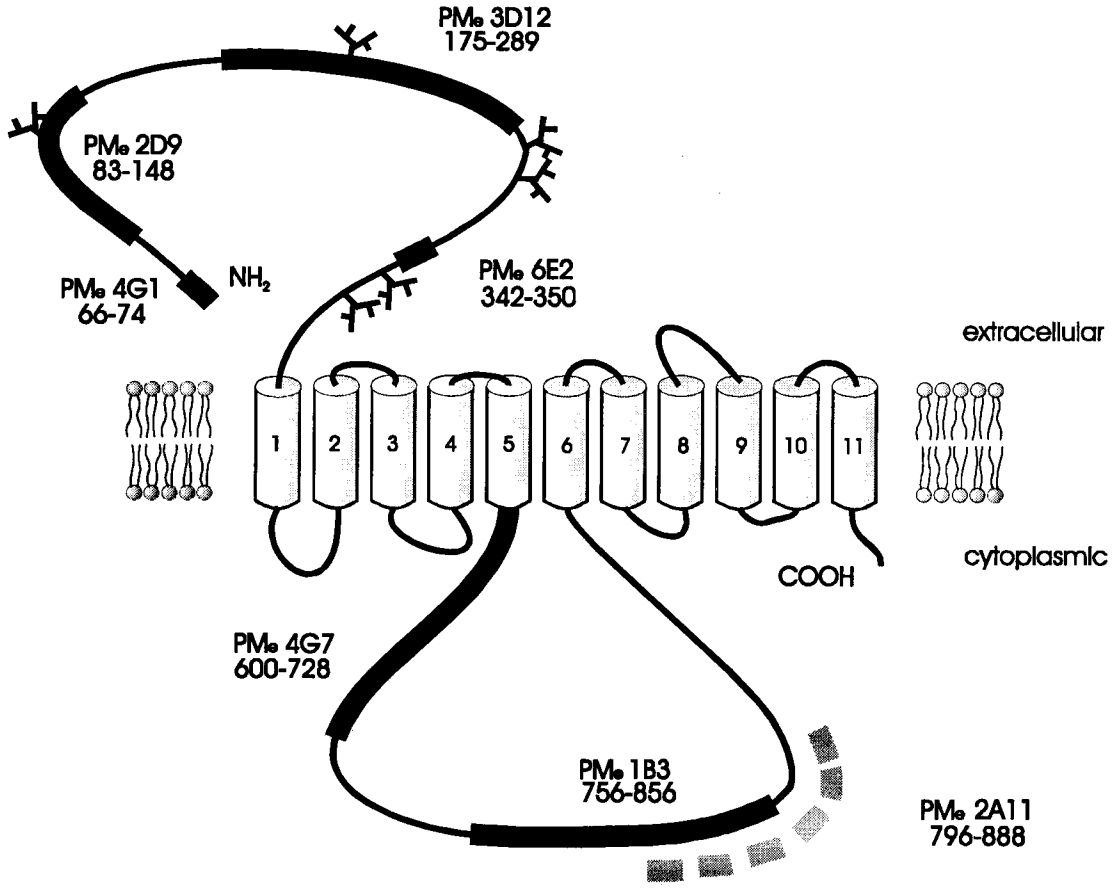

Fig. 19: Topological model for the rod Na/Ca-K exchanger.
The model of the exchanger is based on both the hydrophobicity profiles and the localization of the monoclonal antibody epitopes. The antibodies PMe 4G1, PMe 2D9, PMe 3D12 and PMe 6E2 bound to the extracellular side while the antibodies PMe 4G7, PMe 1B3 and PMe 2A11 bound to the intracellular side of the ROS plasma membrane. Shaded boxes indicate the repeat regions containing the PMe 2A11 epitope. The six, putative N-linked glycosylation sites for the exchanger in the extracellular domain are indicated by the branched structures. N-terminal sequencing indicated that the first residue was Asp 66 and the numbers represent the amino acid sequence reported by Reiländer *et al.* (1992).

3.3 Localization of the Na/Ca-K exchanger in the retina:

The distribution of the exchanger within the bovine retina tissue was examined using immunofluorescence microscopy. Retinal cryosections were first labeled with the MAb PMe 2A11 and followed by goat anti-mouse conjugated to the fluorescent dye Cy3. As shown in Fig. 20A, the rod photoreceptor outer segment layer was intensely labeled. Weak labeling of the inner segment layer was observed after prolonged exposure, but no labeling was seen in other neuronal cells of the retina nor in the cone outer segments, which are sparsely distributed just below the rod outer segment layer. Antibody labeling was specific since no fluorescence was observed when labeling was carried out in the presence of the 2A11 peptide (Fig. 20C). A similar pattern of labeling was observed with the other anti-exchanger MAbs (Table 3).

The distribution of the exchanger within the photoreceptor cells was determined by immunogold labeling methods for electron microscopy (performed by Delyth M. Reid). When retinal tissue was labeled with the MAb PMe 2D9 conjugated to gold-dextran, gold particles were distributed on the extracellular surface of the ROS plasma membrane (Fig. 21). The base of the ROS, where the plasma membrane evaginates to form the disk, was also labeled, although at a lower density. No significant labeling was observed on the connecting cilium, calycal process, rod inner segment or cone outer segment (Fig. 21 B & C).

3.4 Immunoaffinity purification of the exchanger:

Purification of the exchanger using a PMe 2A11-Sepharose 2B matrix was compared to purification by DEAE followed by Red dye chromatography. As shown in Fig. 22A, the fraction obtained after DEAE followed by Red dye chromatography (lane c) had a number of Coomassie

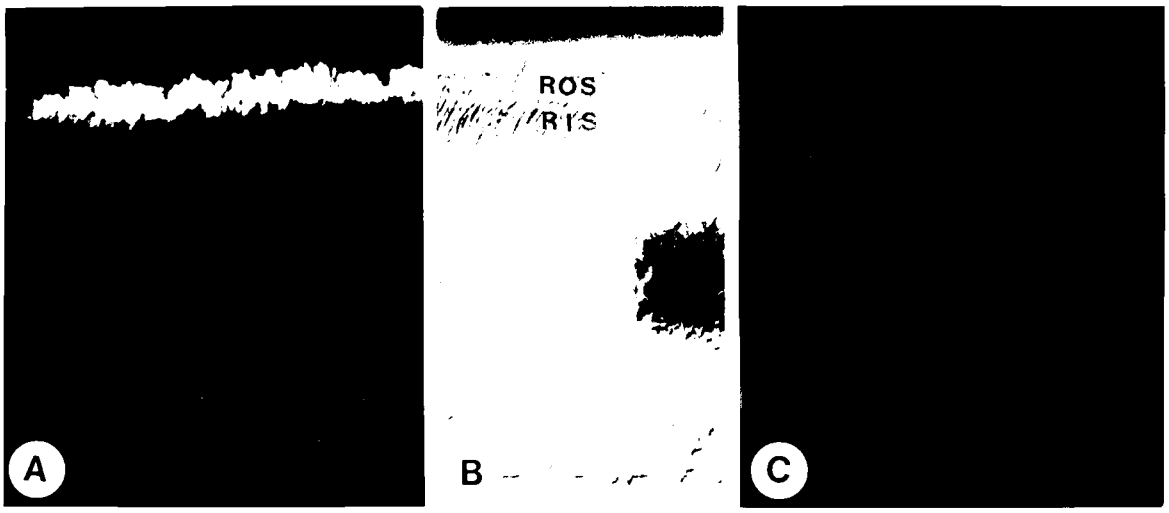

Fig. 20: Immunofluorescence localization of the Na/Ca-K exchanger in retina tissue. Cryosections of bovine retina were labeled with the PMe 2A11 antibody in the absence (A) or presence (C) of competing peptide. The rod outer segment (ROS), rod inner segment (RIS) and nuclear layers are shown in the differential interference contrast micrograph (B). The MAb PMe 2A11 specifically labels the ROS but not other neuronal cells of the retina.

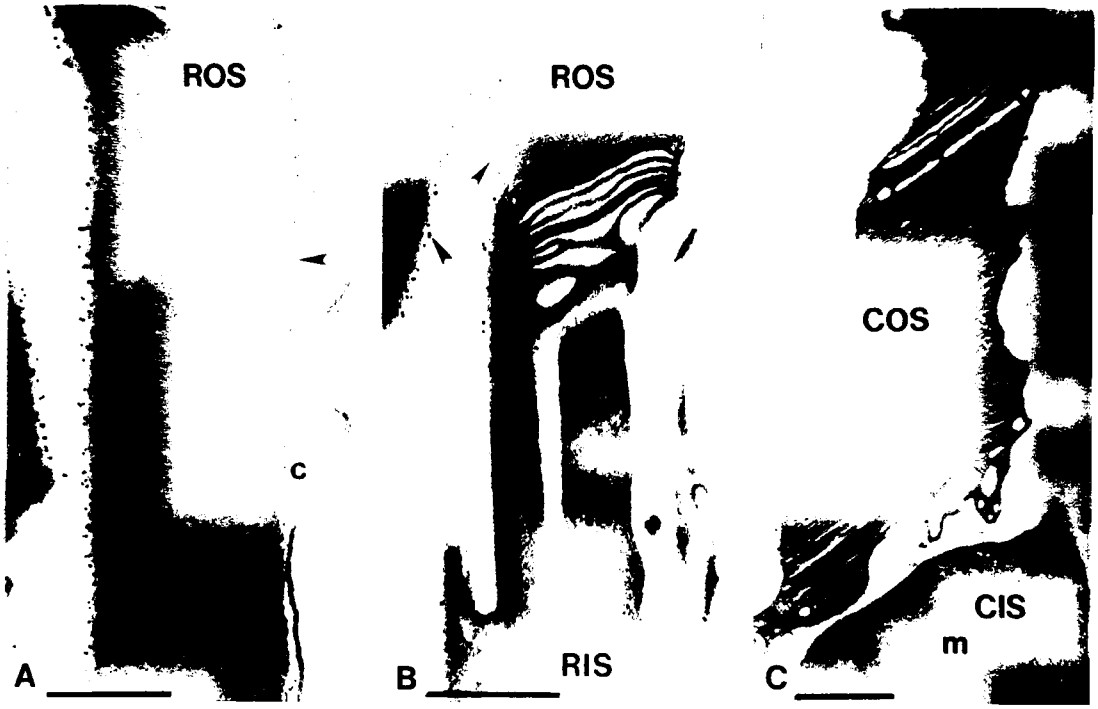

Fig. 21: Immunoelectron microscopic localization of the Na/Ca-K exchanger in photoreceptors of retina.

Bovine retina tissue was labeled with the PMe 2D9 antibody conjugated to 10 nm gold-dextran particles, and subsequently fixed and embedded in resin. Electron micrographs of rod photoreceptor cells (A and B) and a cone photoreceptor cell (C). The ROS plasma membrane including the basal region are labeled with gold particles (arrow), whereas the calycal process (c), cilium (cc), the cone outer segment (COS) and cone inner segment (CIS) are not labeled. An occasional gold particle is seen along the plasma membrane of the rod inner segment (RIS). Mitochondria (m) within the inner segment of rods and cones are indicated. Bar = 500 nm. (Performed by Delyth M. Reid.)

Blue stained bands that were not present in the immunoaffinity-purified fraction (lane b). Besides the 230 kDa exchanger, no other significant bands were observed in the immunoaffinity-purified fraction by SDS-PAGE followed by Coomassie Blue staining.

Functional assays have suggested that the exchanger and the cGMP-gated channel are associated (Bauer and Dreschler, 1992). The channel, however, was not observed in the immunoaffinity purified preparation by Western blot analysis using the anti-channel MAb PMc 1D1 (Fig. 22A). Similarly, no cGMP-dependent Ca^{2+} efflux activity was observed after reconstituting the immunoaffinity-purified fraction into lipid vesicles (data not shown).

The immunoaffinity-purified exchanger was further characterized by Western blot analysis and functional reconstitution. Both MAbs PMe 2D9 and PMe 2A11 labeled the 230 kDa exchanger and their respective proteolytic fragments (Fig. 22A). The activity of the immunoafffinity-purified exchanger was determined by measuring Na^{+}-dependent Ca^{2+} efflux activity after reconstituting the exchanger into lipid vesicles. As shown in Fig. 22B, ion transport activity was measured in the immunoaffinity purified fraction. Low activity was observed in the unbound fraction of the PMe 2A11-Sepharose column, indicating that the affinity matrix absorbed most of the exchanger. These results show that the exchanger can be purified in a functionally active state on the MAb PMe 2A11-Sepharose column. A 68 fold purification was obtained with an 18% recovery (Table 4).

Table 4: Immunoaffinity Purification of the Na/Ca-K Exchanger

	Volume (ml)	Protein (mg/ml)	Units[a]/ml	Total Units	Yield	Units/mg	Purification fold
ROS	12.5	0.98	43.1	539	100%	44.0	1
purified exchanger	2.4	0.014	40.8	97.9	18%	2978	68

[a] One unit is defined as 1 nmole Ca^{2+} released per minute at 50 mM NaCl

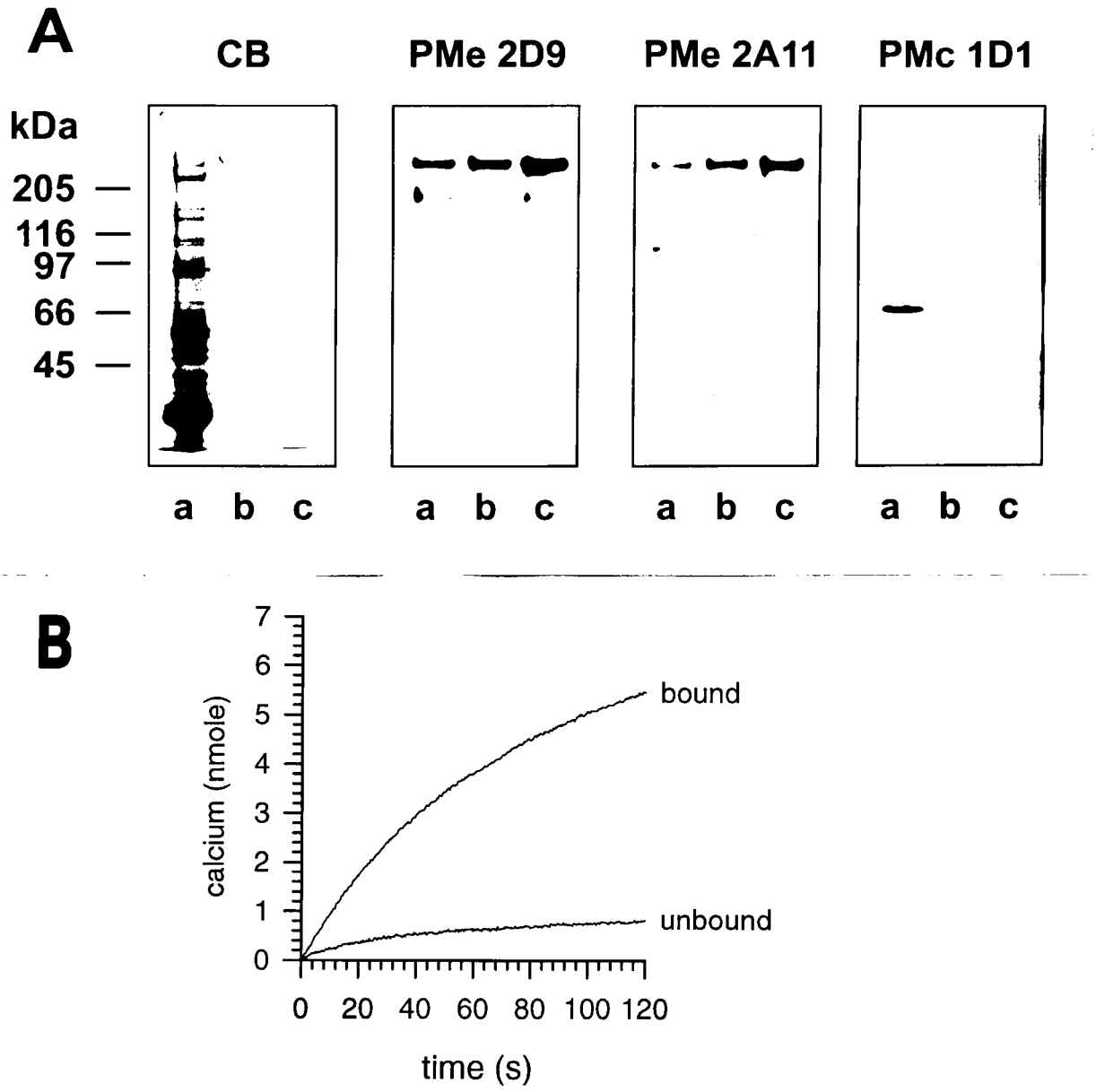

Fig. 22: Immunoaffinity purification of the Na/Ca-K exchanger.
The exchanger was purified from the CHAPS solubilized ROS membranes on an antibody column (PMe 2A11 conjugated to Sepharose 2B beads) and eluted with the 2A11 peptide. (A) Bovine ROS membranes (a), immunoaffinity purified exchanger (b) and DEAE followed by red dye chromatography purified exchanger (c) were separated by 8% SDS PAGE for either Coomassie Blue staining (CB) or Western blotting with PMe 2D9, PMe 2A11 and PMc 1D1. (B) The PMe 2A11 bound and unbound fractions were reconstituted into Ca^{2+} loaded vesicles for Na^{+} dependent Ca^{2+} efflux assays. At time zero 50 mM NaCl was added to the assay.

3.5 Deglycosylation:

Previous biochemical studies have indicated that the exchanger is a heavily glycosylated membrane protein (Cook and Kaupp, 1988; Reid *et al.*, 1990). In this study, the type of glycosylation, N-linked or O-linked, was investigated by sequential enzymatic deglycosylation with neuraminidase and O-glycosidase or PNGase F. Removal of sialic acid residues with neuraminidase decreased the molecular mass of the exchanger from 230 kDa to 205 kDa by SDS-PAGE (Fig. 23, lane b). Treatment of the neuraminidase treated exchanger with O-glycosidase further decreased the molecular mass to 180 kDa (Fig. 23, lane c). When the untreated, neuraminidase treated or O-glycosidase treated exchanger was subjected to PNGase F, no significant shift in mobility of the exchanger was observed (data not shown). These results suggest that the exchanger contains extensive O-linked and little or no N-linked carbohydrates.

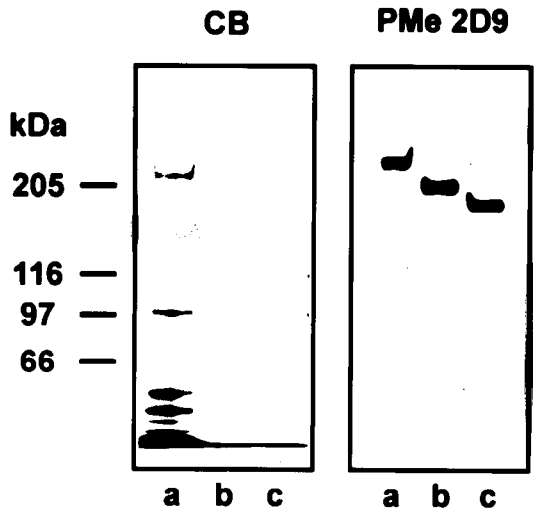

Fig. 23: Deglycosylation of the Na/Ca-K exchanger.
ROS membranes were treated with neuraminidase and solubilized in CHAPS detergent. The exchanger was then immobilized on PMe 2A11-Sepharose, treated with endo-O-glycosidase and eluted with 3% SDS for analysis by Coomassie Blue staining (CB) and Western blotting with PMe 2D9. Lane a: ROS; lane b: exchanger treated with neuraminidase; lane c: exchanger treated with neuraminidase and endo-O-glycosidase.

3.6 Structure-Function Studies:

Structure-function relationships of the exchanger were examined using the anti-exchanger MAbs as probes to monitor the sensitivity of the exchanger to proteolysis. The effect of proteolysis on exchange activity was studied by reconstituting the exchanger into lipid vesicles for functional assays.

3.6.1 Effect of Proteolysis on the Structure of the Exchanger:

The panel of MAbs was used to identify regions of the exchanger that are sensitive to degradation by specific proteases. Intact ROS were incubated with trypsin, and membrane bound fragments were analyzed for immunoreactivity by Western blot analysis. As shown in Fig 24A, MAb PMe 2D9 labeling was removed following trypsin digestion. A similar result was observed for the other MAbs that bound to the extracellular surface (see Fig. 19). In contrast, MAb PMe 2A11 labeled proteolytic fragments of 150 kDa, 135 kDa and 75 kDa. Extended proteolysis decreased the amount of the 150 kDa fragment but increased the amount of the 75 kDa fragment. MAbs PMe 4G7 and PMe 1B3 produced the same labeling pattern as that of PMe 2A11. These results indicate that a considerable part of the N-terminal domain of the exchanger extending up to and perhaps beyond the PMe 6E2 epitope (residue 350) is preferentially removed when intact ROS are digested with trypsin (Fig. 24B).

Proteolysis of the exchanger with porcine pancreatic kallikrein was carried out using hypotonically lysed ROS. As shown in Fig. 25A, the MAb PMe 2D9 labeled a 180 kDa membrane bound proteolytic fragment, whereas the MAb PMe 2A11 epitope was degraded. The other MAbs localized to the extracellular side labeled the 180 kDa proteolytic fragment, while no labeling was observed with the MAbs localized to the cytoplasmic side in the kallikrein treated

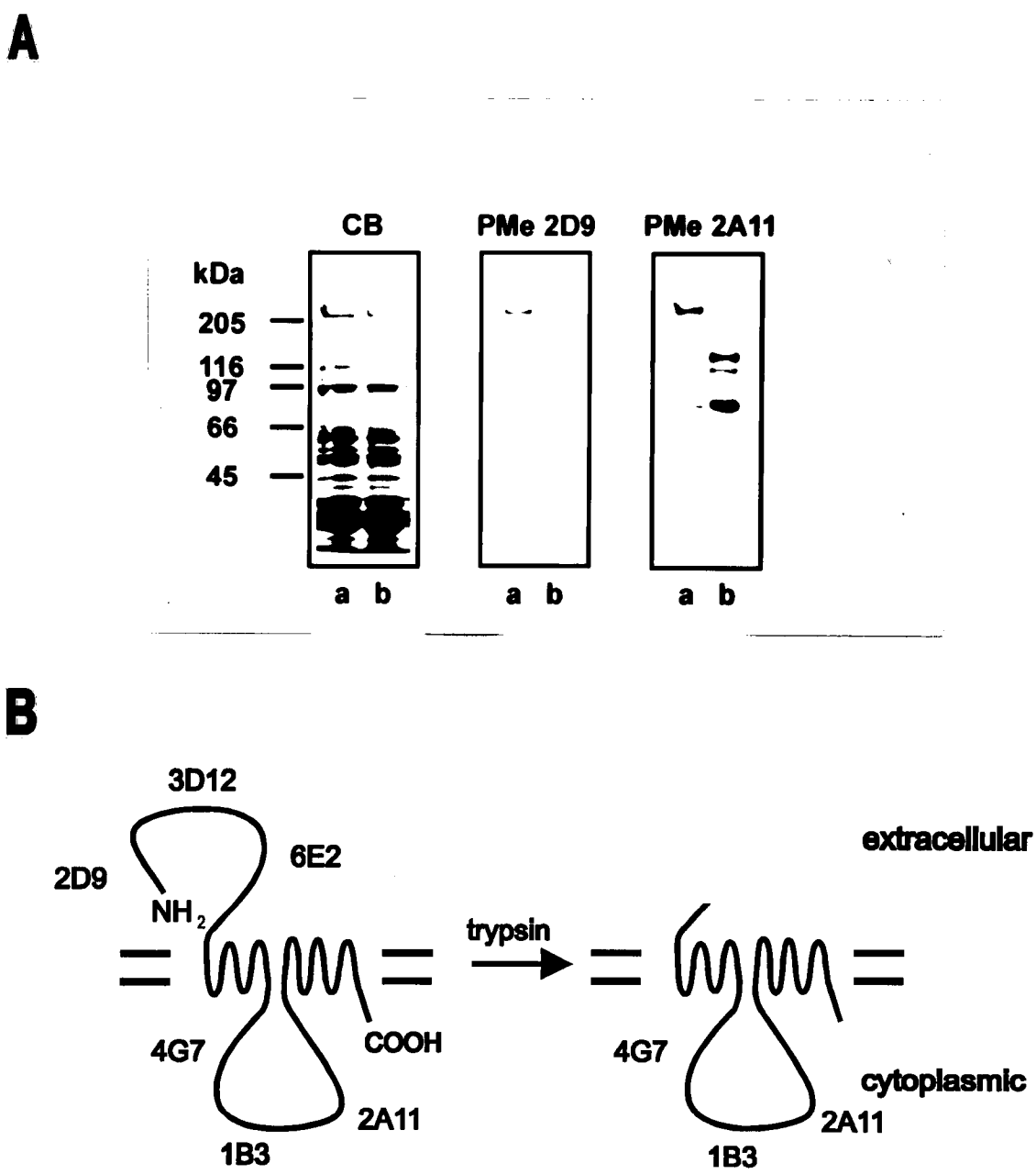

Fig. 24: Proteolysis of the extracellular hydrophilic domain of the Na/Ca-K exchanger. (A) Intact ROS were treated with trypsin and then washed in the presence of SBTI before solubilizing in CHAPS. The untreated (a) and trypsin treated (b) ROS were separated on SDS polyacrylamide gels for either staining with Coomassie Blue (CB) or Western blotting with PMe 2D9 or PMe 2A11 antibody. (B) Diagram illustrating the preferential removal of a large part of the extracellular loop based on the immunoreactivity of the anti-exchanger antibodies against the trypsin treated exchanger.

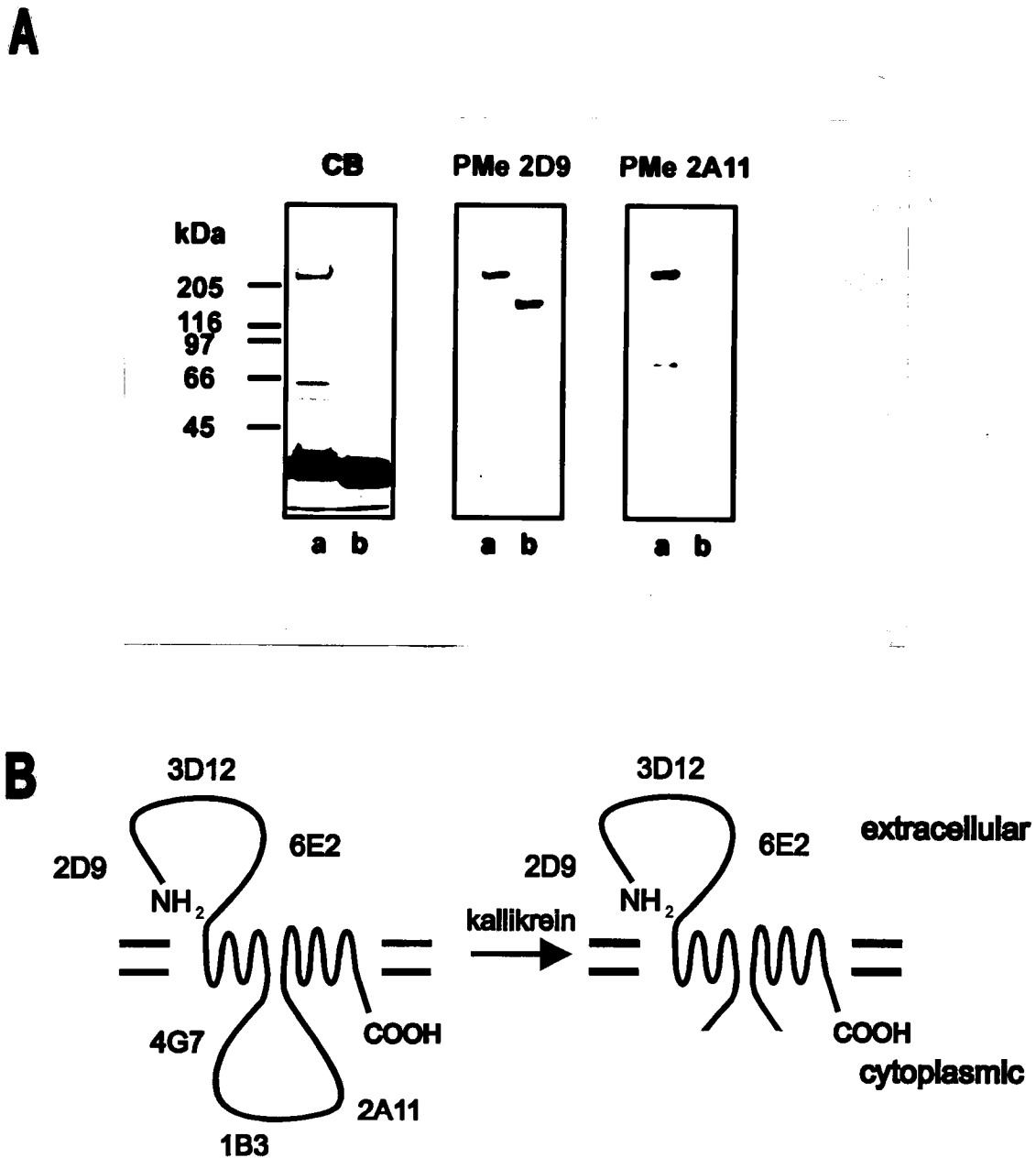

Fig. 25: Proteolysis of the intracellular hydrophilic domain of the Na/Ca-K exchanger. (A) Hypotonically lysed ROS membranes were treated with kallikrein and then washed in the presence of Pefabloc before solubilizing in CHAPS. The untreated (a) and kallikrein treated (b) ROS membranes were separated on SDS polyacrylamide gels for either staining with Coomassie Blue (CB) or Western blotting with PMe 2D9 or PMe 2A11 antibody. (B) Diagram illustrating the preferential removal of a large part of the cytoplasmic loop based on the immunoreactivity of the antibodies against the kallikrein treated exchanger.

samples. In summary, a large part of the cytoplasmic loop connecting transmembrane segments 5 and 6 is selectively removed when lysed ROS are treated with kallikrein (Fig. 25B).

3.6.2 Effect of Proteolysis on Na^+-Dependent Ca^{2+} Efflux Activity:

The effect of limited protease treatment on exchange activity was determined by reconstituting the protease treated exchangers into lipid vesicles for Ca^{2+} efflux assays. Both the kallikrein (data not shown) and trypsin treated exchangers displayed Na^+-dependent Ca^{2+} efflux activities similar to that of the untreated exchanger (Fig. 26 A & B). The trypsin treated and kallikrein treated exchanger had Km values for Na^+ of 54±4 mM and 41±7 mM, respectively, while the untreated exchanger had a Km for Na^+ of 46±4 mM (Fig. 27). Both protease treated exchangers maintained cooperativity for Na^+ as indicated by the sigmoidal curve. The trypsin and kallikrein treated exchangers had a Hill coefficient of 2.9±0.2 and 2.7±0.2 (three experiments), respectively, while the untreated exchanger had a Hill coefficient of 2.9±0.6 (six experiments). These results suggest that most of the large extracellular and cytoplasmic domains are unlikely to play a significant role in Na^+ or Ca^{2+} transport.

The Vmax for both protease treated exchangers, however, increased ~2 fold (Fig. 26). A similar increase in Na^+-dependent Ca^{2+} exchange activity was observed when intact ROS were treated with trypsin and then assayed for Ca^{2+} efflux activity from the ROS (data not shown). Furthermore, a 2 fold faster ion transport rate was observed when the exchanger was first reconstituted into lipid vesicles and then treated with trypsin (Fig. 28 A & B). The increase in activity was not due to the leakiness of the trypsin treated vesicles because an equivalent amount of calcium was released from the untreated and trypsin treated vesicles by A23187 (Fig. 28A). The increase in activity following proteolysis was therefore due to the removal of a specific

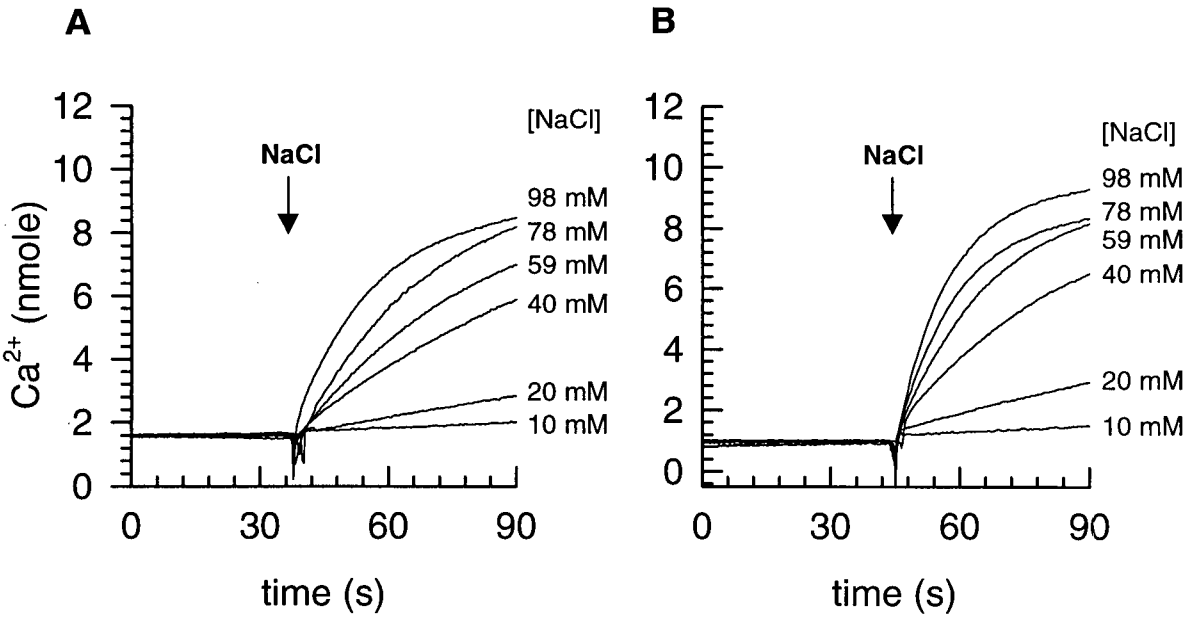

Fig. 26: Effect of trypsin on the Na^+-dependent Ca^{2+} efflux activity of the Na/Ca-K exchanger.

Untreated (A) and trypsin (B) digested ROS membranes were solubilized in CHAPS and reconstituted into Ca^{2+} containing vesicles for Na^+-dependent Ca^{2+} efflux assays. The arrow indicates the addition of the indicated concentrations of NaCl. The release of Ca^{2+} was monitored on a dual wavelength spectrophotometer at 650 and 730 nm using the Ca^{2+} indicating dye Arsenazo III.

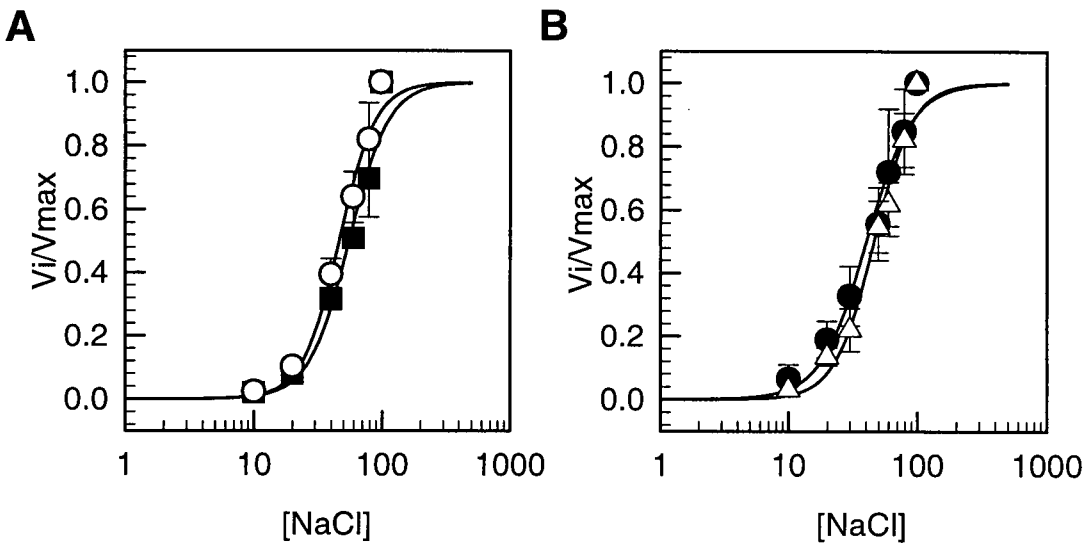

Fig. 27: Characterization of the Na^+-dependent transport properties of the protease treated Na/Ca-K exchangers.

Untreated and trypsin digested ROS (A) and untreated and kallikrein digested ROS membranes (B) were solubilized in CHAPS and reconstituted into Ca^{2+} containing lipid vesicles for Na^+-dependent Ca^{2+} efflux assays. The initial velocities (Vi) were normalized to the velocity (Vmax) at 100 mM NaCl and the data representing the mean from three experiments was fitted to the Hill equation $V/Vmax=[Na+]^n/([Na+]^n+Km^n)$ where Km and n are the Michaelis constant and Hill coefficient, respectively. (A) The untreated exchanger (O) had a Km=46 mM and n=3.1 and the trypsin treated exchanger (■) had a Km=54 mM and n=3.1. (B) The untreated exchanger (Δ) had a Km=46 mM and n=2.9 and the kallikrein treated exchanger (●) had a Km=40 mM and n=2.5.

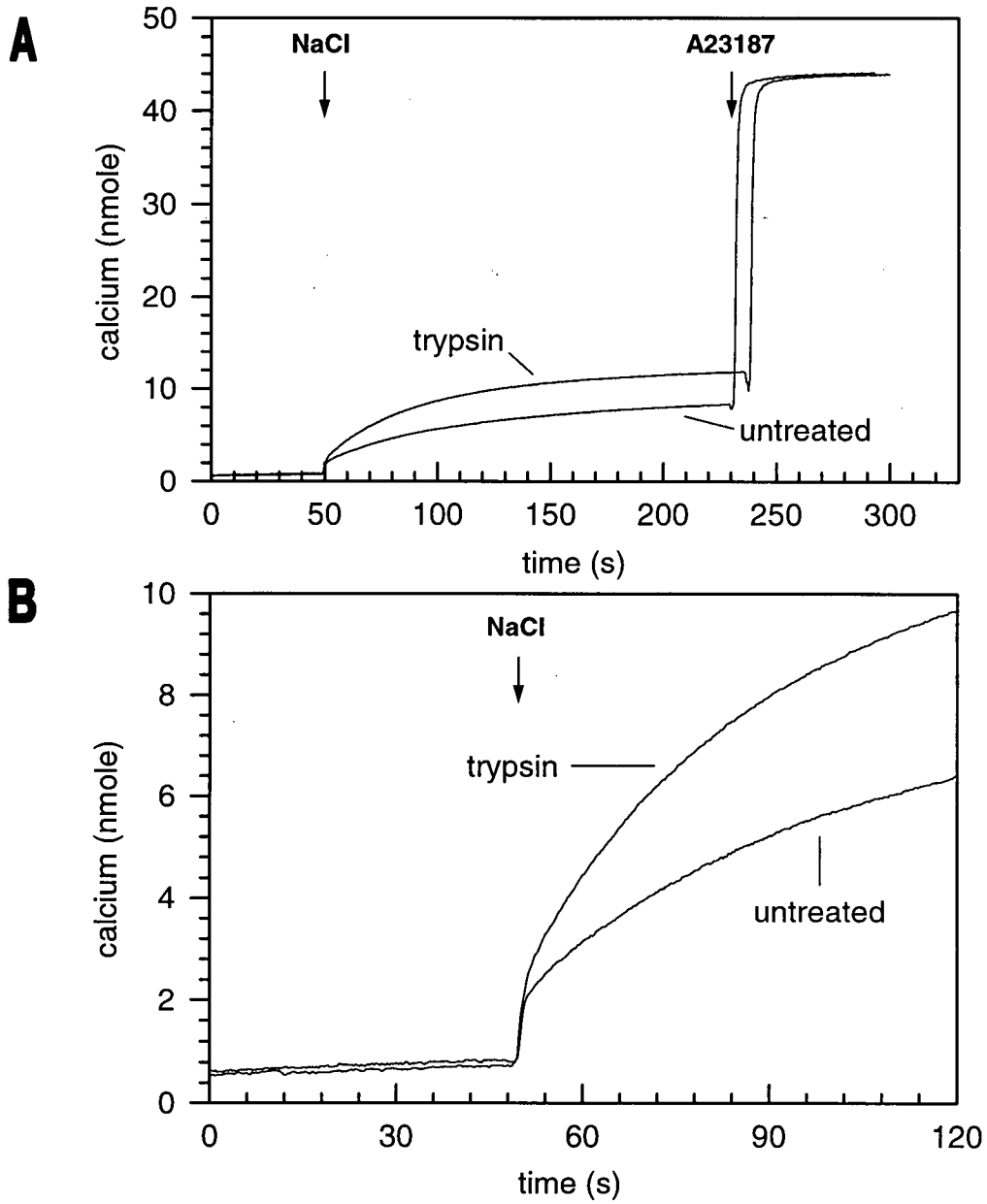

Fig. 28: Increased activity of the exchanger reconstituted into vesicles and then treated with trypsin.

After the ROS membranes were solubilized in CHAPS and reconstituted into lipid vesicles, one ml of the vesicle solution was treated with 5 μg/ml of trypsin. The digestion was stopped with 15 μg/ml SBTI and then dialyzed for 1 h before passing through a Chelex-100 column. The untreated and trypsin treated vesicles were assayed for Na-dependent Ca^{2+} efflux activity. In panel A, the first arrow indicates the addition of 50 mM NaCl and the second arrow indicates the addition of A23187 (calcium ionphore). Panel B shows the same assay as in panel A but with a shorter time-scale.

region of the exchanger and not to any enhanced detergent extraction or a more efficient reconstitution of the protease treated exchanger.

On the other hand, more extensive proteolysis using a higher enzyme concentration or prolonging the digestion time decreased the exchange activity and eventually inactivated the exchanger.

The reconstituted exchanger was treated with trypsin and analyzed by Western blot analysis to determine if the exchanger has a preferred orientation within the lipid vesicles. As shown in Fig. 29, both MAbs PMe 2D9 and PMe 2A11 labeled the proteolytically degraded exchanger suggesting that the exchanger is randomly oriented in the vesicles, in agreement with Ca^{2+} efflux studies by Huppertz and Bauer (1994).

3.6.3 Effect of Kallikrein Treatment on K^+-Dependent Ca^{2+} Efflux Activity:

The kallikrein treated exchanger was reconstituted into lipid vesicles for Ca^{2+} efflux assays in the presence or absence of K^+ in order to determine whether the cytoplasmic domain plays a role in K^+-dependent Na^+/Ca^{2+} exchange activity of the rod exchanger. As shown in Fig. 30, the activity of both the untreated and kallikein treated exchangers was faster in the presence of K^+ than in its absence, suggesting that the kallikrein treated exchanger maintained both K^+-dependent and independent Ca^{2+} efflux activity similar to that of the untreated exchanger. Consistent with the previous studies, the activity of the kallikrein treated exchanger was found to be ~2 fold faster than that of the untreated exchanger.

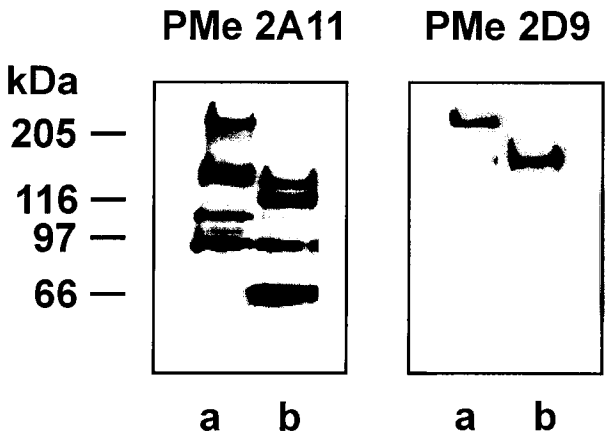

Fig. 29: Western blots of the exchanger reconstituted into vesicles and then treated with trypsin. Vesicles were prepared and treated as described in the legend of Fig. 15. The untreated (lane a) and trypsin treated (lane b) vesicles were subjected to SDS-PAGE (8% gels) and electrophoretically transferred onto Immobilon membranes for labeling with MAbs PMe 2A11 and PMe 2D9.

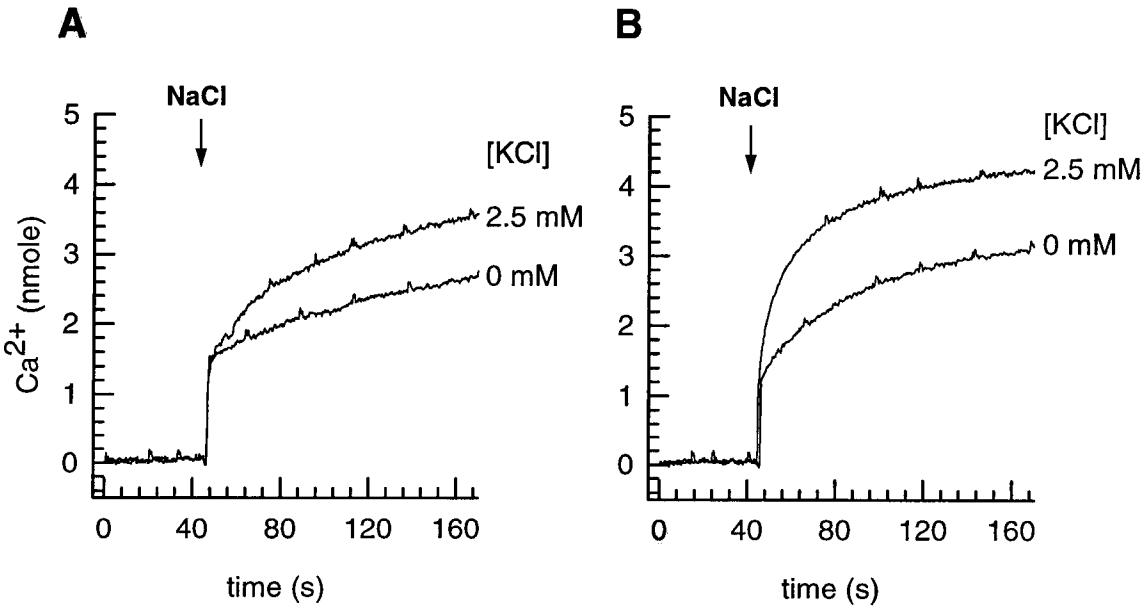

Fig. 30: Effect of proteolysis on the K^+-dependent Na/Ca exchange activity.
Untreated (A) and kallikrein digested (B) ROS were solubilized in CHAPS and reconstituted into Ca^{2+} containing lipid vesicles in 100 mM choline chloride for activity assays in the absence or presence of 2.5 mM symmetrical KCl. Ca^{2+} release was initiated with 50 mM NaCl.

3.7 Ca^{2+} Binding to the Intracellular Domain:

$^{45}Ca^{2+}$ binding studies were performed to determine if the large intracellular domain has a Ca^{2+} binding site, which is independent of the Ca^{2+} transport site. Expression of the fusion proteins containing various regions of the cytoplasmic domain of the rod and cardiac exchanger was detected by Coomassie Blue staining and Western blot analysis. As shown in Fig. 31, PMe 4G7 antibody labeled the rod exchanger-GST fusion proteins (lanes b, c and d), while C2C12 antibody specifically labeled the cardiac exchanger-β galactosidase fusion protein and most likely its proteolytic fragments (lane a). The cardiac exchanger fusion protein bound $^{45}Ca^{2+}$, as previously shown by Levitsky *et al.*, (1994); however, no $^{45}Ca^{2+}$ binding was observed for the rod exchanger fusion proteins (Fig. 31). These results indicate that the rod exchanger either does not have a Ca^{2+} binding site in the large cytoplasmic domain or the Ca^{2+} binding site could not be detected with the current experimental procedure.

3.8 Hydrodynamic Properties of the Exchanger:

Determining the molecular mass of a membrane protein in a non-denatured state is not a straightforward procedure because of the uncertainty in measuring the amount of detergent bound to the protein upon solubilization. Thus, the hydrodynamic properties of the detergent solubilized exchanger were determined by size exclusion chromatography and velocity sedimentation according to Clarke (1975). In this study, the molecular mass for the exchanger was estimated and its oligomeric nature was determined.

The Stoke's radius of the Triton X-100 (TX-100) solubilized exchanger was determined by size exclusion chromatography on a Sepharose CL-4B column calibrated with well characterized marker proteins (Fig. 32 inset). The exchanger-detergent complex eluted from the column as a single broad peak with a Stoke's radius of 10 ± 0.2 nm (Fig. 32).

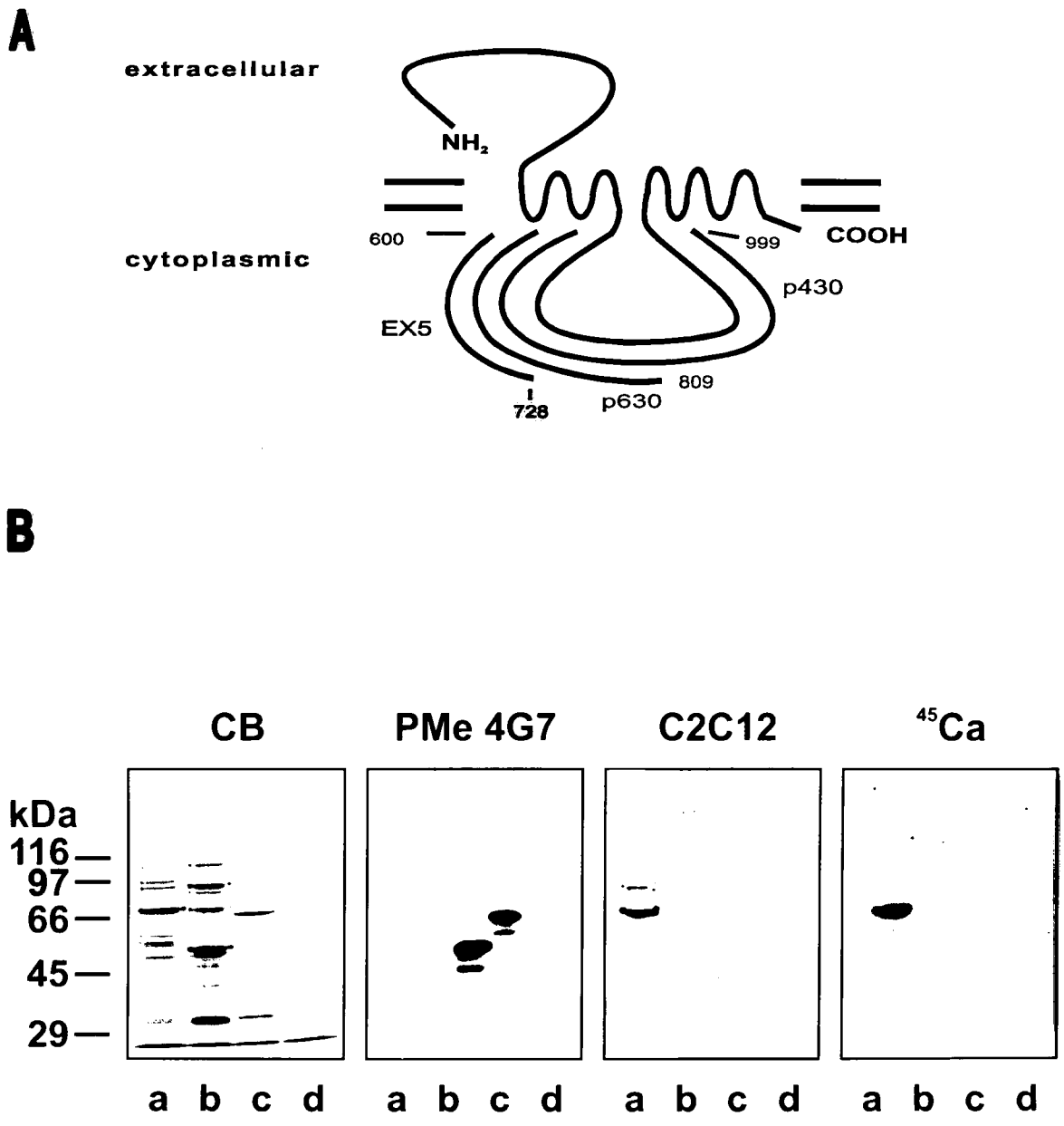

Fig. 31: $^{45}Ca^{2+}$ Binding to the intracellular domain.
A) Fusion protein constructs (EX5, p630 and p430) of the rod exchanger containing the indicated regions of the cytoplasmic domain are shown in relation to the proposed topological model. B) After the cardiac (p240-679, lane a) and rod (EX5, lane b; p630, lane c; and p430, lane d) fusion proteins were expressed in *E. coli*, the cell extracts were separated by SDS-PAGE (8% gels) and either stained with Coomassie Blue or transferred onto nitrocellulose. Western blots were labeled with $^{45}Ca^{2+}$ or MAbs C2C12 and PMe 4G7.

The sedimentation coefficient and partial specific volume of the TX-100 solubilized exchanger were determined by velocity sedimentation through a 5%-20% sucrose gradient. The exchanger-detergent complex sedimented as a single species with a sedimentation coefficient of $S_H = 3.27 \pm 0.21$ S (n = 7) and $S_D = 1.65 \pm 0.10$ S (n = 4) in H_2O and D_2O based sucrose gradients, respectively (Fig. 33). The lack of a shift in the sedimentation of the exchanger relative to the marker enzymes in H_2O versus D_2O suggested that the exchanger bound only a small amount of detergent. From the sedimentation analysis, the exchanger-detergent complex had a calculated partial specific volume (ν) of 0.739 ml/g. A value of 0.148 g of TX-100 bound per g of protein (Table 5) was calculated from the partial specific volume of the exchanger-detergent complex.

A molecular mass of 236 kDa was obtained for the exchanger-TX-100 complex from the sedimentation coefficient at standard state conditions ($S_{20,w} = 5.42$ S), partial specific volume (ν = 0.739 ml/g) and Stoke's radius (a = 10 nm). After correcting for the amount of bound detergent, a molecular mass of 205 kDa was obtained for the exchanger.

Hydrodynamic properties of the CHAPS solubilized exchanger were obtained using the same methods. The CHAPS solubilized exchanger had a molecular mass of 214 kDa (Table 5).

The large carbohydrate moiety on the exchanger was not taken into account in the above molecular mass calculations. When the sialic acid sugars were removed with neuraminidase, the partial specific volume of the exchanger-detergent complex increased to 0.754 ml/g, resulting in an increase in TX-100 bound to the protein (0.265 g of TX-100 per g of protein, Table 5). The neuraminidase treated exchanger had a calculated molecular mass of 174 kDa (Table 5), indicating that the exchanger contains a significant amount of carbohydrate.

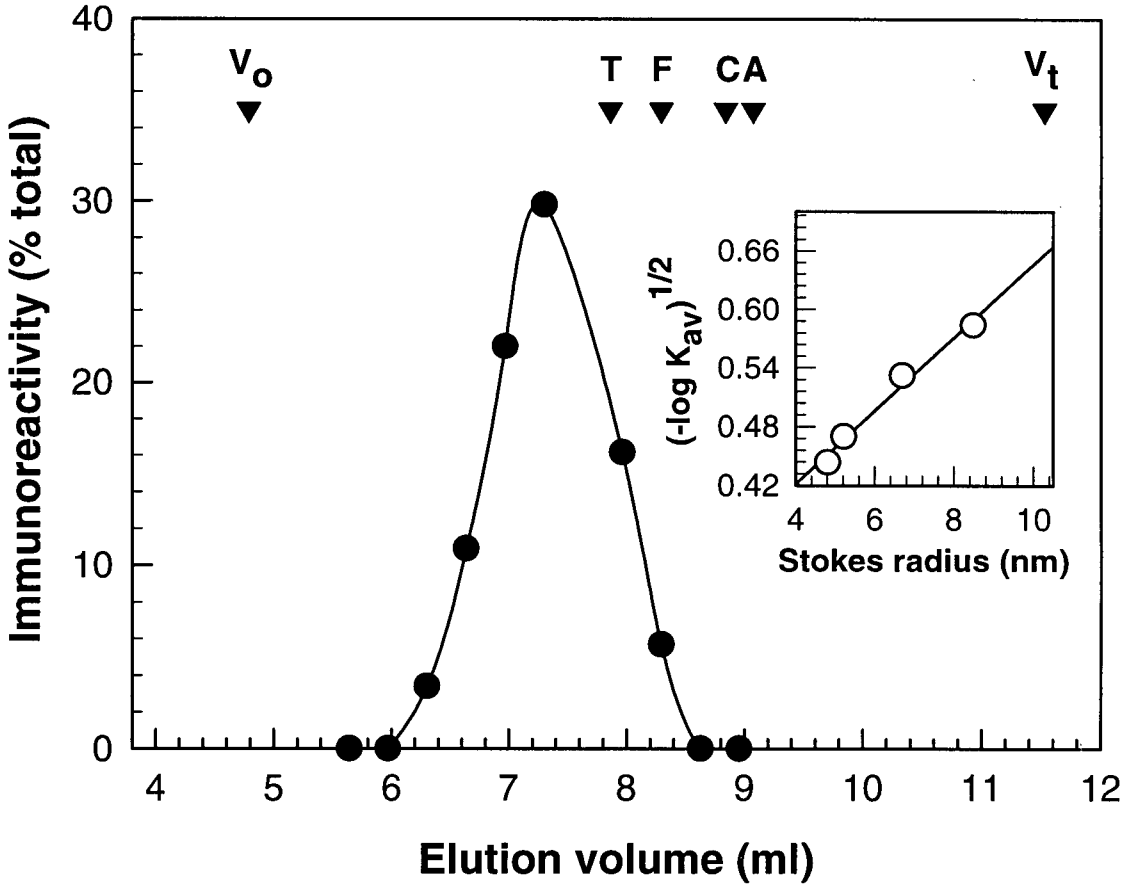

Fig. 32: Gel filtration chromatography of the Triton X-100 solubilized Na/Ca-K exchanger. ROS membranes (150 μg) solubilized in 1% Triton X-100 were applied to a Sepharose CL-4B column and fractions were assayed for the presence of the exchanger on Western blots labeled with the PMe 2D9 antibody and quantified by laser densitometry. Positions of the void volume (Vo), total volume (Vt) and marker proteins, thyroglobulin (T), ferritin (F), catalase (C), and aldolase (A) are indicated. The inset illustrates the calibration plot for marker proteins of known Stokes radii.

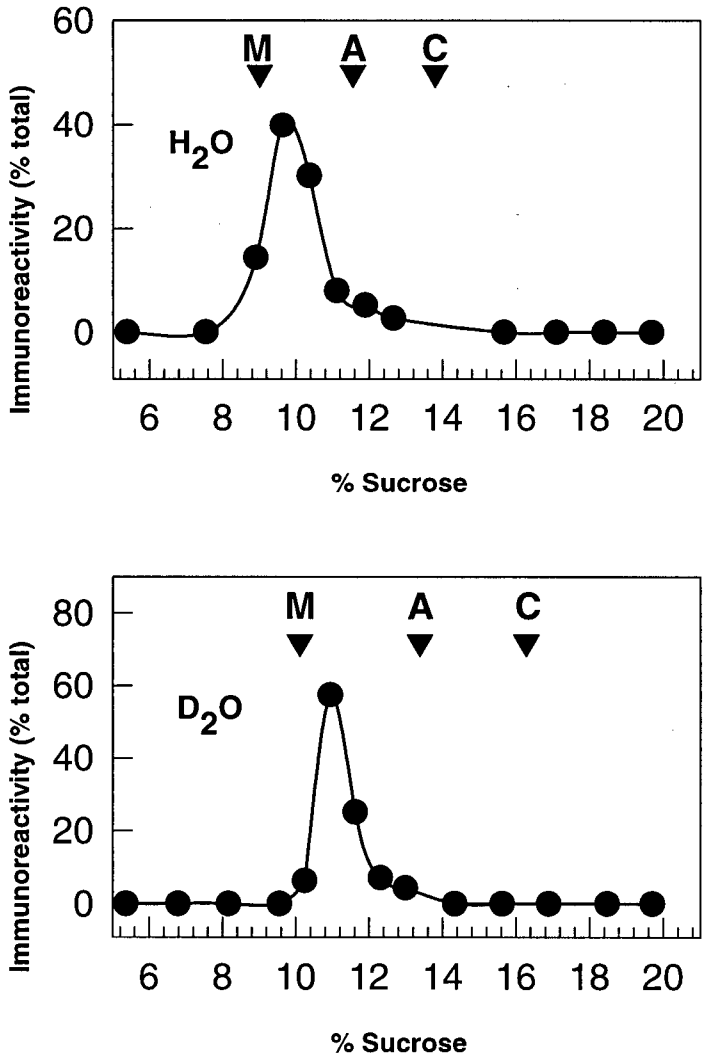

Fig. 33: Velocity sedimentation of the Triton X-100 solubilized Na/Ca-K exchanger.
ROS membranes, solubilized in 1% Triton X-100, were sedimented through a 5-20% sucrose gradient prepared in H_2O (upper panel) or D_2O (lower panel) together with marker enzymes. Fractions were assayed for exchanger on Western blots labeled with the PMe 2D9 antibody and quantified by laser densitometry. Marker enzymes, malate dehydrogenase (M), aldolase (A) and catalase (C) sedimented at the indicated positions.

Table 5: Hydrodynamic Properties of the Bovine Rod Photoreceptor Na/Ca-K Exchanger and the Neuraminidase-Treated Exchanger[a]

Parameter	Triton X-100[b]	CHAPS[c]
sedimentation coefficient ($S_{20,w}$)	5.42 ± 0.32 S (4.95 S)	5.87 S
partial specific volume (ν)	0.739 ± 0.025 ml/g (0.754 ml/g)	0.720 ml/g
Stoke's radius (a)	10.0 ± 0.2 nm (9.6 ± 0.2 nm)	9.4 ± 0.2 nm
molecular mass of exchanger-detergent complex (kDa)	236 ± 27 (219)	229
detergent binding (g/g of protein)[d]	0.148 ± 0.008 (0.264)	0.067
molecular mass of exchanger (kDa)[free of detergent]	205 ± 33 (174)	214

[a] The numbers represent the mean value and when indicated ± standard deviation calculated at the 90 % probability level. [b] Calculated from velocity sedimentation experiments in H_2O (n = 5) and D_2O (n = 4) sucrose gradients and three trials of Sepharose CL-4B chromatography. [c] Calculated from velocity sedimentation experiments in H_2O (n = 2) and D_2O (n = 2) sucrose gradients and three trials of CL-4B chromatography. [d] Calculated using ν = 0.714 ml/g for the exchanger protein, ν = 0.908 ml/g for Triton X-100 and ν = 0.81 ml/g for CHAPS. The values in parentheses represent the hydrodynamic properties of the neuraminidase treated exchanger from velocity sedimentation experiments in H_2O (n = 2) and D_2O (n = 2) sucrose gradients and three trials of CL-4B chromatography.

Assuming that 1) the amount of detergent bound to the exchanger in D_2O and H_2O are the same, 2) changes in viscosity due to fluctuations in temperature during centrifugation are negligible, and 3) the partial specific volume for the exchanger and the exchanger-detergent complex is additive (section 2.15 equation 7), the above results suggest that the Triton X-100 or CHAPS solubilized exchanger exists primarily as a monomer.

3.0 Oligomeric Nature of the Exchanger:

3.9.0 Chemical Cross-linking:

The oligomeric nature of the exchanger in the ROS membrane was examined by chemical cross-linking. ROS membranes were treated with the thiol-specific cross-linking reagent phenylene dimaleimide (pPDM), and the effect of the chemical modification on the exchanger was examined by Western blot analysis. As shown in Fig. 34, MAb PMe 2D9 labeled a high molecular mass cross-linked exchanger in pPDM treated membranes in addition to the 230 kDa uncross-linked exchanger. Quantitation by laser densitometry indicated that ~50% of the exchanger forms a cross-linked product.

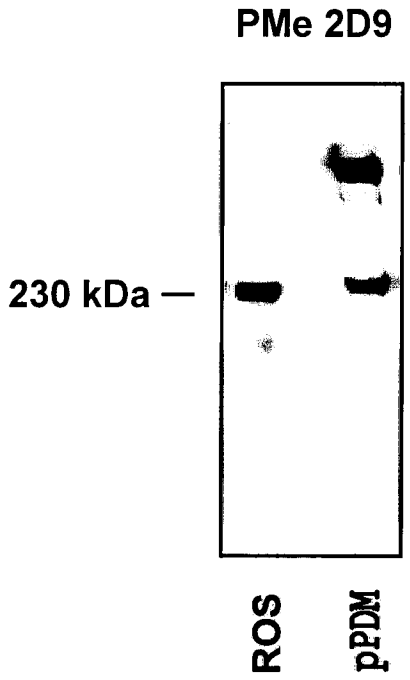

Fig. 34: Chemical cross-linking of the exchanger using a thiol specific reagent.
ROS membranes were treated with the non-reducible thiol specific reagent pPDM. Untreated and pPDM treated ROS membranes were solubilized in Triton X-100 and separated by SDS-PAGE (3.5% to 7.0% linear gradient) and then transferred onto an Immobilon membrane for labeling with the PMe 2D9 antibody.

The inefficient cross-linking observed with the homo-bifunctional reagent may be due to one or two reasons. First, the cysteine residues that form covalent bonds with the cross-linker may have been oxidized. Second, the two adjacent cysteines may have reacted with two separate cross-linkers and prevented the formation of cross-linked products.

The possibility that the exchanger forms cross-links with another high molecular mass protein and not to itself has been extensively investigated. Evidence suggesting that the exchanger cross-links into a homodimer, and not a heterodimer, has been provided by Schwarzer et al. (1997).

3.9.1 Sedimentation Analysis of the Cross-linked Exchanger:

The sedimentation behavior of the cross-linked exchanger relative to the uncross-linked exchanger was analyzed by centrifugation through a H_2O based sucrose gradient. MAb 2D9 labeled two distinct immunoreactive species with different sedimentation rates (Fig. 35A). The slower of the two species, with a molecular mass of 230 kDa by SDS-PAGE, sedimented at the same rate as the uncross-linked exchanger in TX-100 extracts of untreated ROS membranes (Fig. 35B & Fig. 33). The cross-linked exchanger migrated further into the gradient relative to the uncross-linked exchanger, in agreement with its increased mass.

In some experiments, larger oligomeric species were found to sediment further into the gradient for both the cross-linked and the uncross-linked exchanger. Since no labeling was observed with PMe 2D9 higher than the 490 kDa cross-linked exchanger, the larger oligomeric species may be caused by the aggregation of the pPDM treated exchanger that can be disrupted by SDS but not DTT.

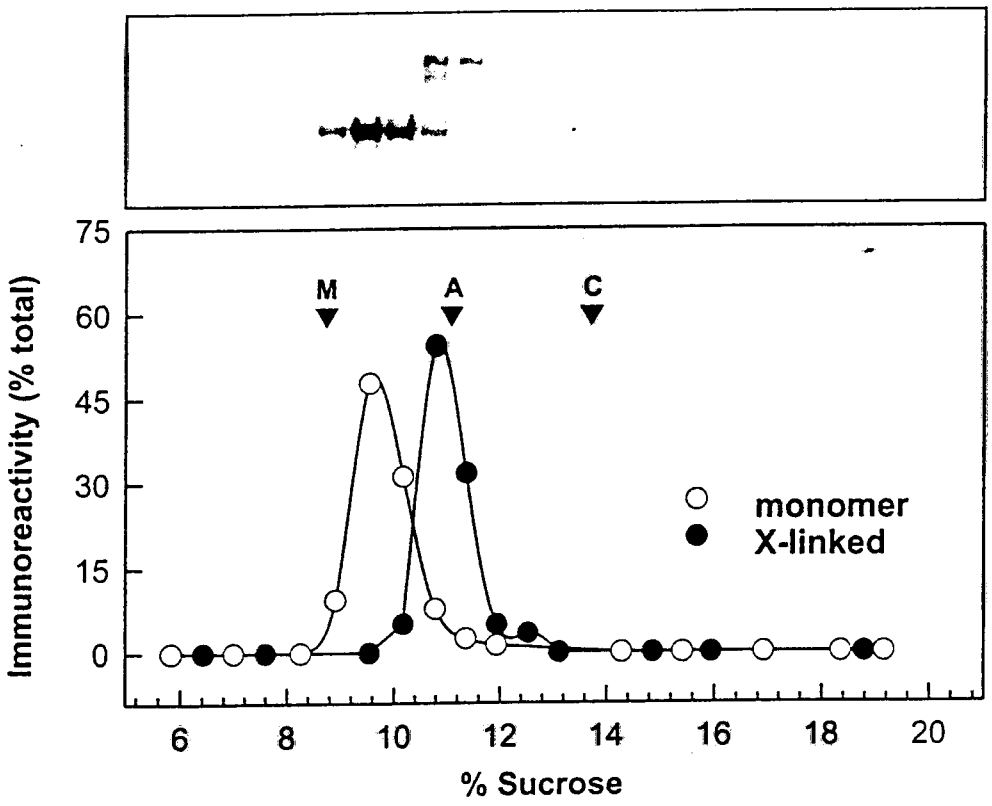

Fig. 35: Velocity sedimentation of the pPDM crosslinked Na/Ca-K exchanger.
ROS membranes were cross-linked with pPDM, solubilized in Triton X-100 and sedimented through a 5-20% sucrose gradient prepared in H_2O. Fractions were assayed for the noncrosslinked (-O-) exchanger (apparent Mr ~ 250 K by SDS-PAGE) and the crosslinked (-●-) exchanger (Mr ~ 490 K by SDS-PAGE) on Western blots labeled with the PMe 2D9 antibody (panel A) and quantified by laser densitometry (panel B). Positions of the marker enzymes, malate dehydrogenase (M), aldolase (A) and catalase (C) are indicated.

DISCUSSION

The bovine rod photoreceptor Na/Ca-K exchanger has been cloned (Reiländer *et al.*, 1992), but structure-function analysis of this protein has been limited due to the inability to express a functional exchanger in heterologous expression systems. In this study eight monoclonal antibodies have been generated against two immunodominant regions of the exchanger and used as probes to examine the structural and functional properties of exchanger and its distribution in the retina.

4.1 Topological Organization:

Recently, cysteine or N-glycosylation scanning mutagenesis studies have shown that the topology of some transporters deviate from its model based on hydropathy plots. These include the glucose (Turk *et al.*, 1996), GABA (Bennett and Kanner, 1996) and glycine transporters (Olivares *et al.*, 1997).

In this study, the topological model of the rod exchanger based on hydropathy plots (Reiländer *et al.*, 1992) has been examined using anti-exchanger antibodies as probes. Immunoelectron microscopy studies show that the large, hydrophilic N-terminal domain is on the extracellular surface of the plasma membrane, while the hydrophilic segment connecting the two putative transmembrane domains is on the cytoplasmic side. These studies provide experimental evidence confirming the membrane topology of the exchanger purposed by Reiländer *et al.*, (1992). In this model a large extracellular N-terminal hydrophilic domain precedes a membrane domain consisting of 5 transmembrane segments. A large intracellular hydrophilic domain connects the first membrane domain to a second hydrophobic domain consisting of 6 transmembrane segments (Fig. 36). The binding sites of the antibodies in context

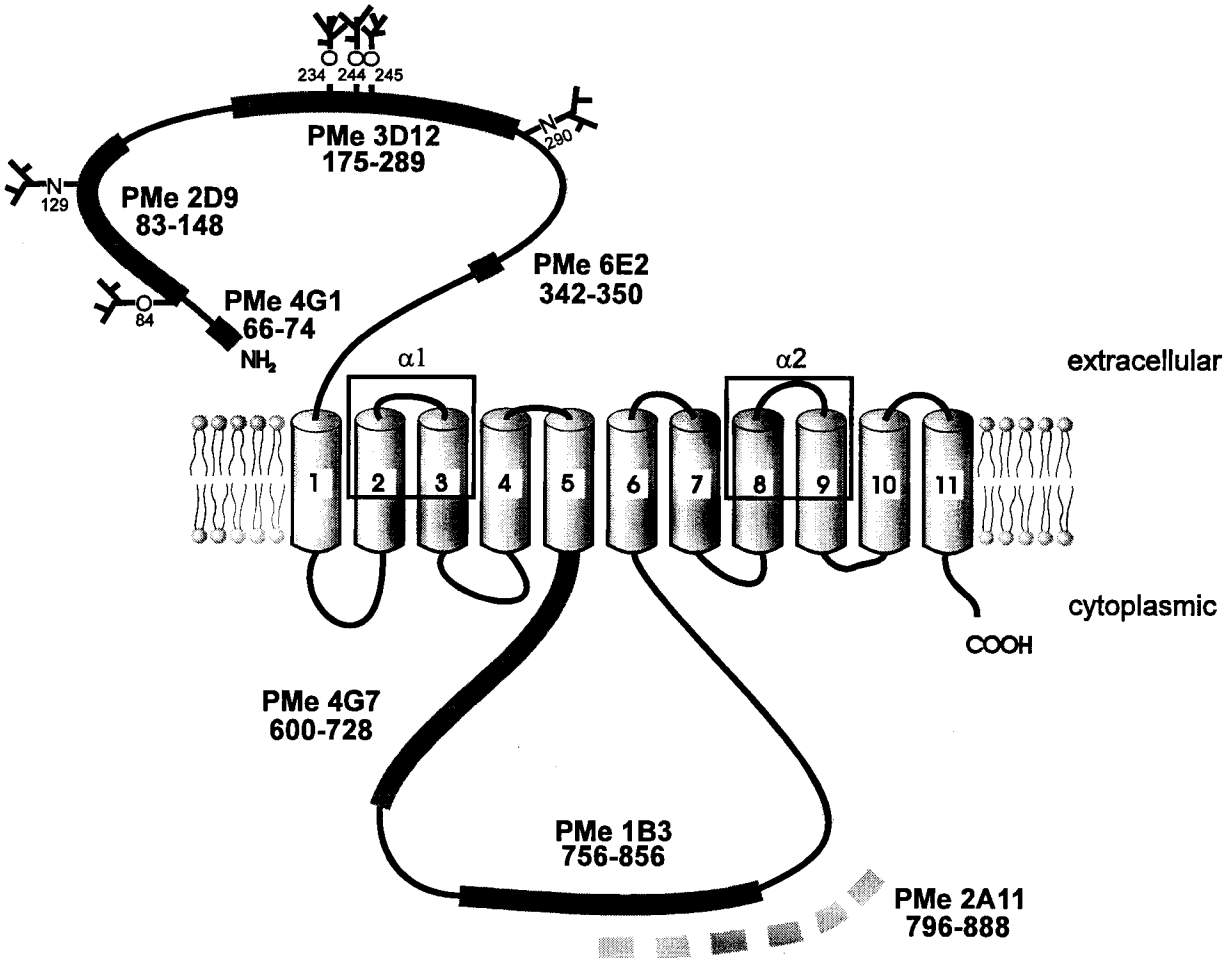

Fig. 36: Topological model for the rod Na/Ca-K exchanger.
The model is based on hydrophobicity profiles and localization of the epitopes for antibodies PMe 4G1, PMe 2D9, PMe 3D12 and PMe 6E2 to the extracellular side and the epitopes for antibodies PMe 4G7, PMe 1B3 and PMe 2A11 to the intracellular side of the ROS plasma membrane. Several possible sites for O-linked glycosylation and conserved consensus sites for N-linked glycosylation are shown. The repeat regions that contain the epitope for PMe 2A11 are shown with shaded bars. The model also indicates the two α repeat regions. The numbers indicate the amino acid positions in the primary structure of the bovine exchanger as reported by Reiländer *et al.*(1992).

to the topological model of the rod exchanger are shown in Fig. 36. Further studies are required to elucidate the detailed organization of the transmembrane segments of the rod exchanger and its proximal regions.

Hydropathy analysis of the Na/Ca-K exchanger (NCK2) from the rat brain (Tsoi *et al.*, 1998) and the cardiac-type Na/Ca exchanger (NCX) isoforms (Nicoll *et al.*, 1996a) also predict a similar membrane topology as the rod exchanger. NCK2 and NCX isoforms, however, lack the large N-terminal hydrophilic domain.

4.2 Glycosylation:

Previous biochemical studies have shown that the exchanger is heavily glycosylated (Cook and Kaupp, 1988; Reid *et al.*, 1990), but the type of glycosylation is unknown. Studies with neuraminidase and O-glycosidase indicate that the exchanger contains extensive O-linked oligosaccarides. Removal of the O-linked carbohydrates decreases the apparent molecular mass of the exchanger by SDS-PAGE from 230 kDa to 180 kDa.

The sites of O-linked glycosylation are unknown. The inability to detect Ser 84, Thr 234, Thr 244 and Thr 245 during peptide sequencing (Reiländer *et al.*, 1992), however, suggests that these residues are covalently modified. Furthermore, these four residues are within a cluster of other serines and threonines juxtaposed to a proline. This distribution of amino acids has been proposed to be a characteristic consensus sequence of O-linked glycosylation (Jentoft 1990) and has been found in other O-linked glycoproteins such as glycophorin (Pisano *et al.*, 1993). Sequence alignment of the bovine exchanger with the recently cloned human orthologue indicates that these four residues are conserved even though the surrounding sequences lack identity (Fig. 37).

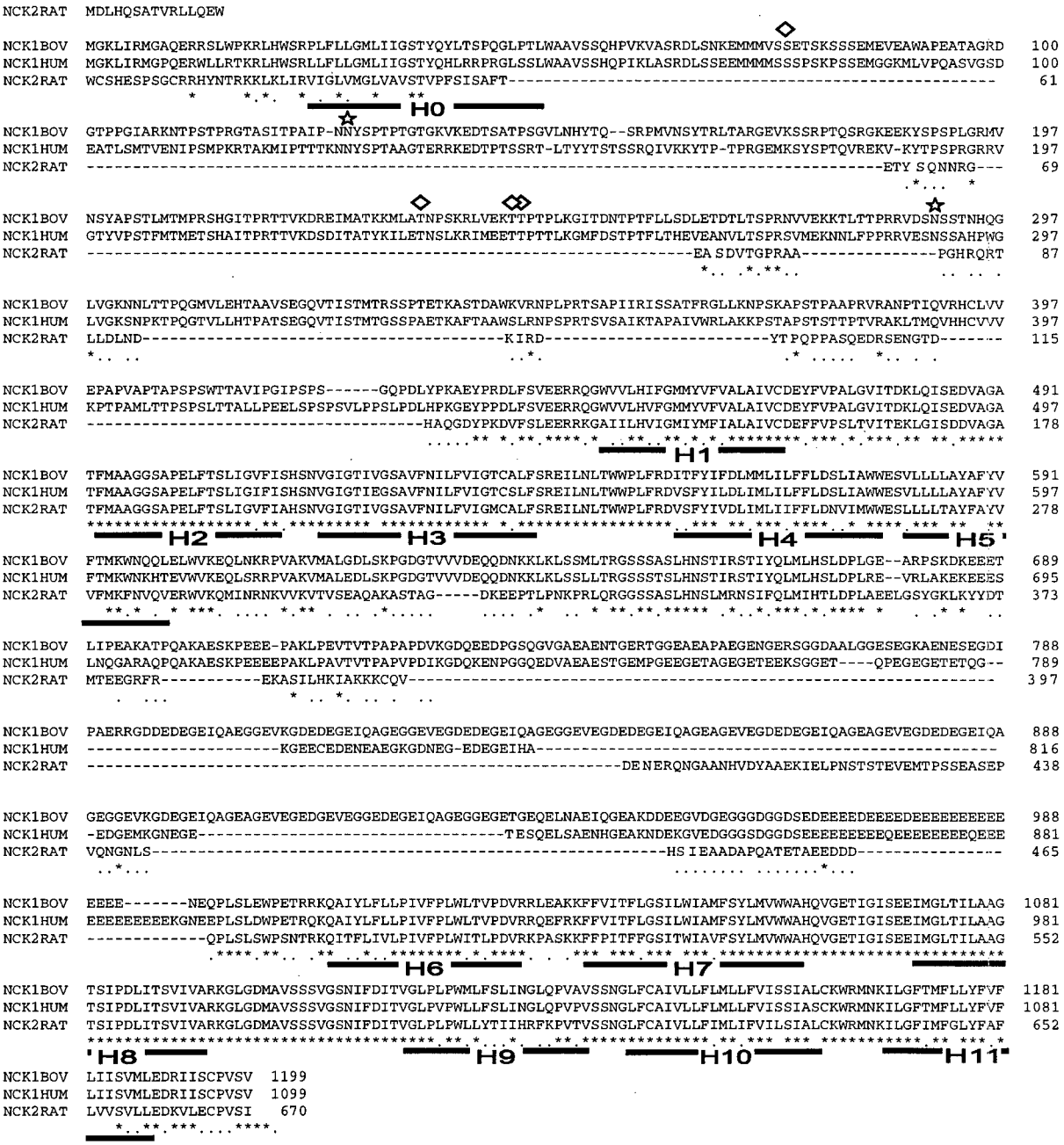

Fig. 37: Protein sequence alignment of the Na/Ca-K exchangers. The bovine (NCK1BOV) (Reiländer *et al.*, 1992) and human (NCK1HUM) (Tucker *et al.*, 1998) rod photoreceptor exchangers and the rat (NCK2RAT) brain exchanger (Tsoi *et al.*, 1998) amino acid sequences were aligned with the Clustal program (PC gene, Intelligenetics), and the first transmembrane segment (HO) for the rat sequence was further optimized manually. Identical residues are indicated by an *asterisk* and similar residues are indicated by a *dot*. The putative membrane spanning helices (H0-H11) are *underlined* and the alignment gaps are indicated by *dashes*. Potential O-linked (S84, T234, T244 and T245) and N-linked (N129 and N290) glycosylation sites on the rod photoreceptor exchangers are indicated by *diamonds* and *stars*, respectively.

Studies with PNGase F suggest that the exchanger is not extensively N-glycosylated. Sequence alignment of the bovine and human exchangers indicate two conserved consensus N-linked sequences (Fig. 37). If the exchanger has a small amount of N-linked oligosaccharides, the putative glycosylation site(s) may be Asn 129 and 290 (Fig. 36).

4.3 Distribution of the Exchanger:

Immunofluorescent and immunogold labeling studies have provided evidence for the cellular and subcellular distribution of the exchanger in the retina. The Na/Ca-K exchanger is expressed in the outer segments of rod photoreceptor cells but not in the other neuronal cells of the retina. Within the ROS, the exchanger is exclusively localized in the ROS plasma membrane. Similar results have been reported by Haase *et al.*, (1990) and Reid *et al.* (1990).

The anti-exchanger MAbs do not label cone photoreceptors. Electrophysiological studies, however, have shown that cone photoreceptors contain a Na^+-dependent Ca^{2+} exchanger (Nakatani and Yau, 1989). Therefore, the lack of cone labeling with the rod exchanger MAbs suggests that two distinct genes encode for the rod and cone exchangers. Other proteins with similar functions in rod and cone photoreceptors have been shown to be encoded by separate genes. These proteins include the opsins (Chiu *et al.*, 1994), transducin (Lerea *et al.*, 1986), phosphodiesterase (Hurwitz *et al.*, 1985), and the cGMP-gated channel (Bönigk *et al.*, 1993; Pittler *et al.*, 1992).

4.4 Immunoaffinity Purification:

Purification methods by Cook and Kaupp (1988) or Nicoll and Applebury (1989) require several different affinity matrices, whereas the immunoaffinity purification described here

utilizes a single step isolation procedure. The exchanger can be efficiently purified on a PMe 2A11-Sepharose column, and subsequently eluted with the corresponding peptide in a functionally active state. No other proteins are observed in the immunoaffinity-purified fraction by SDS-PAGE followed by Coomassie Blue staining. These results suggest that the detergent solubilized exchanger does not appear to interact with other ROS membrane proteins. Due to the limitations of immunoaffinity purification and CB stained gels, in vivo interactions of the exchanger with other proteins may be disrupted or may not be detected.

Ca^{2+} efflux assays have suggested that the exchanger and the cGMP-gated channel are associated in the ROS membranes (Bauer and Drechsler, 1992). However, the channel was not detected in the purified fraction of the exchanger by either western blotting or Ca^{2+} efflux assays. Similarly, immunoaffinity purification of the channel complex by Hsu and Molday (1993) has also indicated a lack of association between the exchanger and the channel. In contrast, immunoaffinity purification studies by Molday and Molday (1998) have shown that manipulating the solubilization conditions can result in the co-purification of the channel and exchanger. Taken together the above results suggest that the channel and exchanger may be associated in ROS membranes and that this interaction can be disrupted or maintained depending on the detergent solubilization conditions. Further studies are required to ascertain whether the exchanger and the channel are indeed associated.

4.5 Effect of Proteolysis on Exchange Activity:

The difference in stoichiometry for Na^+ and K^+ dependence between the rod exchanger and the NCX isoforms may reside in the extracellular and/or the intracellular domains. The functional role of the large extracellular and intracellular domains in exchange activity of the rod

exchanger has been examined by limited proteolysis followed by functional reconstitution. When a large part of the N-terminal domain, at least the first 350 residues, is removed with trypsin, the Na^+-dependent Ca^{2+} exchange activity remains essentially unaffected with respect to the cooperativity and affinity for Na^+. Likewise, when a significant part of the large cytoplasmic loop is degraded with kallikrein, the exchanger exhibits not only Na^+-dependent Ca^{2+} transport with a similar Km and Hill coefficient as the native exchanger but also K^+-dependent Ca^{2+} transport. These results indicate that the large hydrophilic domains do not play a significant role in ion transport.

Studies of other ion transporters have also shown that the cytoplasmic domain is not required for transport activity. The Na-H exchanger (Wakabayashi *et al.*, 1992), cardiac NCX (Matsuoka *et al.*, 1993) and erythrocyte anion transporter (Grinstein *et al.*, 1978; Linsey *et al.*, 1990) retain ion transport activity following the removal of the cytoplasmic domain.

Instead, the transmembrane domains and possibly the proximal hydrophilic regions mediate ion binding and transport. The high sequence identity within the membrane spanning regions between the bovine rod photoreceptor exchanger (Reiländer *et al.*, 1992) and the recently cloned human rod photoreceptor (Tucker *et al.*, 1998) and rat brain (Tsoi *et al.*, 1998) Na/Ca-K exchangers support the importance of these domains in the ion transport function of these proteins (Fig. 37).

Interestingly, removal of either the extracellular or intracellular domain increased the Vmax of the rod exchanger transport activity by ~2 fold relative to the untreated exchanger. A similar increase in activity of the rod exchanger has been observed following chymotrypsin treatment (Nicoll *et al.*, 1991). The bulky hydrophilic domains may sterically hinder the conformational change that facilitative ion transporters undergo as part of the transport

mechanism (Niggli and Lederer, 1991; Stein 1990). Thus, removing these bulky hydrophilic domains may permit the exchanger to undergo more rapidly a conformational change required for the translocation of ions across the membrane bilayer.

A similar increase in activity of other exchangers has also been observed following mild protease treatment. Limited proteolysis of the cardiac NCX (Nicoll *et al.*, 1991; Philipson and Nishimoto, 1982) and Na-H exchanger (Weinman *et al.*, 1992) stimulated their exchange activity. In these studies, however, degradation of the protein was not monitored and the ion transport properties were not characterized thoroughly. The increase in transport activity was suggested to be due to the removal of an inhibitory domain.

Other modifications have also been shown to stimulate the transport activity of the cardiac NCX in vesicles. The activity of the cardiac NCX is potentiated when vesicles are treated with phospholipase (Philipson and Nishimoto, 1984) or if the exchanger is reconstituted into vesicles with a higher cholesterol (Vermuri and Philipson, 1988) or unsaturated fatty acid content (Philipson and Ward, 1985). All of these procedures increase the fluidity of the membrane. This may facilitate a conformational change of the cardiac NCX required for ion transport.

4.6 Functional Significance of the Large Hydrophilic Domains:

4.6.1 Extracellular Domain:

The functional role of the extracellular domain of the rod exchanger is unknown. The carbohydrates on the N-terminal domain do not appear to be necessary for function, since no significant effect is observed on the transport activity of the exchanger after the removal of the extracellular domain. Likewise, the cardiac NCX (Hrysko *et al.*, 1993), Na-H exchanger

(Counillon *et al.*, 1994), anion (Groves and Tanner, 1994), glucose (Wheeler and Hinkel, 1981), glutamate (Conradt *et al.*, 1995), norepinephrine (Melikian *et al.*, 1994) and glycine (Nunez and Aragon, 1994) transporters are also glycosylated; the oligosaccharide chains on these proteins are not required for functional activity. On the other hand, removal of sialic acid residues from the rat brain dopamine transporter has been shown to decrease its transport activity (Zaleska and Erecinska, 1987).

Perhaps glycosylation plays a role in the proper folding and targeting of the rod exchanger. Heterologous expression studies have shown that the deglycosylated glucose (Asano *et al.*, 1993), erythrocyte anion (Groves and Tanner, 1994), glycine (Olivares *et al.*, 1995), norepinephrine (Melikian *et al.*, 1994) and serotonin (Tate and Blakely, 1994) transporters are not properly folded and targeted to the plasma membrane.

Another possible function for the carbohydrates on the extracellular surface of the rod exchanger may be to anchor the interphotoreceptor matrix to the ROS or to mediate cell-cell interactions between the ROS and the adjacent retinal pigment epithelium (RPE). The rod and cone outer segments are continually phagocytosed by the retinal pigment epithelium. The protein(s) involved in this process has yet to be determined. Since the rod exchanger is the only plasma membrane protein found to date that has a large, glycosylated extracellular domain, it may serve as the candidate cell surface protein that binds to receptors on the RPE cells. Recently a mannose receptor has been shown to be present in RPE cells (Lutz *et al.*, 1995). Since the rod exchanger binds to Concanavalin A (Cook and Kaupp, 1988), a lectin that has an affinity for α-mannose and α-glucose, the exchanger may be the ligand for the mannose receptor.

The carbohydrates on the exchanger may also interact with a member of the selectin or sialoadhesion family of receptors. The role of the selectin family of receptors is to initiate the

interaction of leukocytes with the endothelial cells required for the movement of the leukocytes from the bloodstream into tissue (Lasky 1992). The biological role of the sialoadhesion receptors is broad yet these receptors share a common function in cell-cell interaction. The defining characteristic of the selectin ligands is the local high density of O-linked sialo-oligosaccharides (Lasky *et al.*,1992; Baumhueter *et al.*, 1993; Berg *et al.*, 1993; Sako *et al.*, 1993); the sialoadhesion receptors have a high specificity for sialic acid residues (Kelm *et al.*, 1996). Although neither family of lectin-like receptors have been shown to be present in RPE cells, the extensive O-linked sialoglycosylation of the exchanger suggests that it may be a ligand for an existing or a novel member of the lectin-type of receptors yet to be found in RPE cells.

The dense array of sialic acid residues on the exchanger may have two opposing functional implications. The extended configuration of the oligosaccharides from the protein backbone may allow the exchanger to present itself to a receptor, and yet the negative charge imparted by the sialic acid residues may provide the rod outer segment with a negative charge that prevents non-specific cell-cell interactions. A bifunctional role for the cell surface carbohydrates has also been suggested for the selectin ligands (Shimizu and Shaw, 1993) and leukosialin (Fukuda, 1991). Glycophorin, another highly O-glycosylated plasma membrane protein, has been suggested to prevent the aggregation of erythrocytes (Fukuda, 1993).

Another possible role for the carbohydrates may be to protect the exchanger from proteolytic attack. The variable amount of proteolytic fragments present in the different ROS preparations suggests that the exchanger is highly sensitive to degradation.

4.6.2 Cytoplasmic Domain:

The functional role of the intracellular domain also remains to be determined. The bovine rod exchanger and its human orthologue share limited sequence similarity within the cytoplasmic domain except in the N-terminal region of the cytoplasmic loop (Fig. 37). This region of the exchanger may contain a regulatory Ca^{2+} binding site similar to the one present in the cardiac exchanger (Matsuoka *et al.*, 1995). The cytoplasmic domain of the rod exchanger, however, did not bind $^{45}Ca^{2+}$ under the same conditions that the cardiac exchanger bound $^{45}Ca^{2+}$. These results suggest that either the rod exchanger has a unique Ca^{2+} binding motif or does not have a regulatory Ca^{2+} site in the cytoplasmic domain.

Studies on salamander and bovine ROS have shown that the intracellular Ca^{2+} level reaches a minimum of 50-100 nM (Gray-Keller and Detwiller, 1994; Schnetkamp *et al.*, 1991a). In the absence of Ca^{2+} influx, however, an exchange stoichiometry of 4 Na^+/ 1Ca^{2+}, 1 K^+ indicates that thermodynamically, the exchanger should be able to lower the intracellular Ca^{2+} concentration even further based on the equation:

$$(1) \qquad [Ca^{2+}]_i/[Ca^{2+}]_o = ([Na^+]_i/[Na^+]_o)^4([K^+]_o/[K^+]_i) \exp(V_m zF/RT)$$

where subscripts i and o refer to intracellular and extracellular concentrations, respectively, V_m is the membrane potential, z is the net charge transported after each transport cycle, F is the Faraday's constant, R is the Gas constant, and T is the temperature. The inactivation of the Na^+-dependent Ca^{2+} efflux mode of the rod exchanger has been suggested to prevent the intracellular Ca^{2+} concentration from reaching detrimentally low levels (Schnetkamp *et al.*, 1991a; Schnetkamp 1995). The conserved N-terminal region of the cytoplasmic loop may somehow serve as a Ca^{2+} sensor and regulate the inactivation of the exchanger.

Another possible role for the intracellular domain may be to interact with other proteins. As previously mentioned (section 4.3), the channel and the exchanger are suggested to be associated. The juxaposition of the channel and the exchanger may play a significant role in regulating the intracellular calcium levels, perhaps by a positive or negative feedback mechanism. Alternatively, the cytoplasmic loop may be involved in the interaction with cytoskeletal elements. The cardiac exchanger (Li *et al.*, 1993) and band 3 (Low, 1986) have been shown to interact with ankyrin. Perhaps, the cytoplasmic loop interacts with the filamentous-like structures that connect the disks to the plasma membrane (Usukura and Yamada, 1981).

4.7 Oligomeric Nature of the Exchanger:

The oligomeric state of the bovine rod Na/Ca, K exchanger has been deduced from the hydrodynamic properties of the detergent solubilized exchanger. Solubilizing the exchanger in CHAPS appears to maintain the native conformation, since the exchanger can be reconstituted into lipid vesicles for functional assays. Thus, the hydrodynamic measurements reflect that of the native conformation. From these measurements, a molecular mass of 205 kDa for the Triton X-100 or 214 kDa for the CHAPS solubilized exchanger is determined. These values are considerably higher than 130 kDa for a monomer and lower than 260 kDa for a dimer, calculated from its amino acid sequence.

Since the large carbohydrate moiety on the exchanger has not been taken into consideration in these molecular mass calculations, the measured value most likely represents the mass of a monomer. The difference between the estimated and the predicted molecular mass of the monomer would be smaller, if the carbohydrates were accounted for in the calculation of the

predicted molecular mass of 130 kDa and the partial specific volume of 0.714 ml/g for the exchanger (see section 2.15). The low partial specific volume of carbohydrates would decrease the overall partial specific volume of the exchanger (ν_p), thereby increasing the amount of detergent bound and decreasing the molecular mass of the exchanger ($MM_{protein}$) according to the equation

(7) $MM_{protein} = (MM_{complex})/[1+(\nu_c - \nu_p)/(\nu_d - \nu_c)]$ (section 2.16)

Furthermore, the low partial specific volume of the carbohydrates may have counterbalanced the effect of the high partial specific volume of the detergent bound to the exchanger during velocity sedimentation. Thus the carbohydrates may have caused the lack of a shift in the sedimentation rate between the D_2O versus H_2O based sucrose gradient, leading to an underestimate of the partial specific volume of detergent-exchanger complex (0.714 ml/g) and an overestimate of the $MM_{protein}$ (205 kDa). Indeed, removal of the sialic acid residues increased the partial specific volume to 0.754 ml/g for the exchanger-detergent complex and decreased the molecular mass to 175 kDa, a value closer to the predicted value of 130 kDa. Taken together, the above results support the view that the exchanger solubilized in Triton X-100 or CHAPS exists as a monomer.

4.8 Cross-linking:

The oligomeric state of the rod exchanger has also been studied by chemical cross-linking and velocity sedimentation analysis. Chemical cross-linking studies of the exchanger within the plasma membrane have shown that the exchanger forms homodimers (Schwarzer *et al.*, 1997). Due to the inefficient cross-linking of sulfydryl specific cross-linker, only 50% of the exchanger formed cross-linked products. When the cross-linked exchanger was analyzed by

velocity sedimentation, the cross-linked exchanger migrated farther into the gradient than the uncross-linked exchanger, which sedimented at the same rate as the monomeric exchanger (Fig. 35). The difference in sedimentation rate between cross-linked and uncross-linked exchanger suggests that the exchanger is associated as a dimer within the plasma membrane but dissociates into a monomer in the absence of cross-linking upon detergent solubilization.

The oligomeric state of other members of the 12 transmembrane family of transporters has also been studied. The Na-H exchanger (Fafournoux *et al.*, 1994), Na-glucose transporter (Pessino *et al.*, 1991) and band 3, the erythrocyte anion transporter, (Casey and Reithmeier, 1991, 1993; Steck, 1972) have been shown to be homodimers. On the other hand, hydrodynamic measurements have indicated that the Na^+ and Cl^- coupled glycine transporter exists as a monomer in CHAPS (López-Corcuera *et al.*, 1993). Whether the glycine transporter is a dimer in the plasma membrane requires further investigation.

4.9 Function:

What is the functional subunit stoichiometry of the exchanger? The near complete oxidation of the exchanger in the membrane into a homodimer along with the activity measurements of the exchanger in intact ROS by electrophysiological or biochemical methods indicate that the exchanger functions as a dimer. On the other hand, the reconstituted exchanger was inefficiently cross-linked but still displayed exchange activity. Whether the transport activity of the reconstituted exchanger is due to the monomeric or dimeric species remains to be investigated in detail.

Although other transport proteins form dimers and sometimes higher oligomers, the functional significance of oligomerization remains uncertain. Both the monomeric and dimeric

forms of the Na-glucose transporter (Burant and Bell, 1992; Pessino *et al.*, 1991) and the anion exchanger (Lindenthal and Schubert, 1991) have been shown to be functional.

4.10 Conclusion:

The experiments described in this thesis provide insight into the structure-function relationships and the topological organization of the bovine rod photoreceptor Na/Ca-K exchanger. The heavily O-linked sialoglycosylated rod exchanger is exclusively localized in the plasma membrane of the ROS. The rod exchanger has a large N-terminal extracellular domain followed by a membrane domain consisting of 5 membrane spanning segments. The first membrane domain is connected to a second membrane domain consisting of 6 membrane spanning segments by a large intracellular domain. Removal of the large hydrophilic domains has been shown to have no significant affect on the Na^+ or K^+-dependent Ca^{2+} transport activity of the rod exchanger. Thus, the transmembrane domains or regions proximal to the hydrophobic domains of the exchanger appear to mediate ion binding and translocation across the bilayer. The transport of ions, however, are stimulated by the removal of the large hydrophilic domains, perhaps by permitting a faster conformational change. Finally, the rod exchanger appears to be a homodimer in the membrane but dissociates into a monomer upon solubilization in detergent.

4.11 Future Directions:

Although the three dimensional structure of a few membrane proteins has been successfully determined by X-ray crystallography, in general determining the structure of membrane spanning proteins by either X-ray crystallography or NMR has been futile. Until the technical problems in determining the structure of membrane proteins by crystallography and

NMR are overcome, the topological model of the rod exchanger can be refined by alternative approaches. Structures of the large hydrophilic extracellular and intracellular domains of the rod exchanger could be determined by separately expressing these domains in bacterial or insect cells for crystallography and/or NMR studies. The organization of the membrane spanning segments and the regions proximal to the hydrophobic regions of the rod exchanger can be determined by cysteine or N-glycosylation mutagenesis studies.

While the present study indicates that the rod exchanger exists as a dimer in the plasma membrane, the cysteine residues involved in the cross-linking have not been defined. Site-directed mutagenesis studies may identify the residues responsible for the cross-linking and thereby indicate the regions of the exchanger that are proximal to each other. The functional unit of the exchanger appears to be uncertain. Functional reconstitution of the cross-linked and uncross-linked exchanger following velocity sedimentation would indicate whether the ion transport properties of the monomer and dimer are different.

An intriguing question raised in this study concerns the molecular mechanism of ion transport. Structural information of the rod exchanger may help to determine the different conformational states of the exchanger during ion transport and the enhanced turnover rate following the removal of the large hydrophilic domains. Does the protease treated exchanger undergo the same conformational change as the untreated exchanger?

The cardiac NCX and the rod photoreceptor exchanger share little sequence similarity but both proteins exhibit Na^+-dependent Ca^{2+} exchange activity. Site-directed mutagenesis studies of the rod exchanger, rat brain NCK2 and the cardiac NCX1 may identify the residues responsible for the binding and transport of Na^+, Ca^{2+} and K^+. The results from these studies may also clarify whether the rod exchanger exhibits K^+ independent exchange activity.

Studying protein-protein interactions with the yeast two-hybrid system could provide some insight into the function of the large extracellular and intracellular domains. The large hydrophilic domains could be used as bait to screen the yeast two-hybrid bovine retinal library to identify potential proteins that interact with the exchanger. The extracellular domain may interact with a receptor in the retinal pigment epithelial cells or a protein in the inter-photoreceptor matrix. The intracellular domain may interact with a modulator of the exchanger or a cytoskeletal element.

Phosphorylation studies could determine whether the rod exchanger is regulated by a kinase/phosphatase mechanism.

Several ROS proteins have been identified as the cause for retinal degeneration, a hereditary group of diseases that is characterized by the degeneration of the rod and/or cone photoreceptors and the eventual loss of peripheral or central vision. The recent cloning of the human orthologue has indicated that it is most likely not linked to a disease causing retinal degeneration. To determine whether mutations resulting in a non-functional exchanger are lethal, cause blindness or have no affect on vision, a transgenic mouse with the corresponding mutation(s) in the rod exchanger would provide insight into the functional importance of the exchanger.

REFERENCES

Asano, T., Takata, K., Katagiri, H., Ishihara, H., Inukai, K., Anal, M., Hirano, H., Yazaki, Y., and Oka, Y. (1993) The role of N-glycosylation in the targeting and stability of GLUT1 glucose transporter. *FEBS Lett.* **324**, 258-261

Antonny, B., Otto-Bruc, A., Chabre, M. and Vuong, T.M. (1993) GTP hydrolysis by purified α-subunit of transducin and its complex with the cyclic GMP phosphodiesterase inhibitor. *Biochemistry* **32**, 8646-8653.

Angleson, J.K. and Wensel, T.G. (1993) A GTPase-accelerating factor for transducin, distinct from its effector cGMP phophodiesterase, in rod outer segment membranes. *Neuron* **11**, 939-949

Andrews, P. (1965) Estimation of the molecular weights of proteins by sephadex gel filtration. *Biochem. J.* **91**, 222-233

Altschul, S.F., Boguski, M.S., Gish, W. and Wootton, J.C. (1994) Issues in searching molecular sequence databases. *Nat. Genet.* **6**, 119-129

Bascom, R.A., Manara, S., Collins, L., Molday, R.S., Kalnins, V.I., and McInnes, R.R. (1992) Cloning of the cDNA for a novel photoreceptor membrane protein (rom-1) identifies a disk rim protein family implicated in human retinopathies. *Neuron* **8**, 1171-1184

Bauer, P.J. (1988) Evidence for two functionally different membrane fractions in bovine retinal rod outer segments. *J. Physiol.* **401**, 309-327

Bauer, P.J. and Dreschsler, M. (1992) Association of cyclic GMP-gated channels and Na^+-Ca^{2+}-K^+ exchangers in bovine retinal rod outer segment plasma membranes. *J. of Physiol.* **451**, 109-131

Baumhueter, S., Singer, M.S., Henzel, W., Hemmerich, S., Renz, M., Rosen, S.D. and Lasky, L.A. (1993) Binding of L-selectin to the vascular sialomucin CD34 *Science* **262**, 436-438

Baylor, D.A., Lamb, T.D., and Yau, K.-W. (1979a) The membrane current of single rod outer segments. *J. Physiol.* **242**, 685-727

Baylor, D.A., Lamb, T.D., and Yau, K.-W. (1979b) Responses of retinal rods to single photons. *J. Physiol.* **288**, 613-634.

Beech, D.J., and Barnes, S. (1989) Characterization of a voltage-gated K^+ channel that accelerates the rod response to dim light. *Neuron* **3**, 573-581

Bennett, E.R., and Kanner, B.I. (1997) The membrane topology of GAT-1, a (Na^+ + Cl^-)-coupled γ-aminobutyric acid transporter from the rat brain. *J. Biol. Chem.* **272**, 1203-1210

Berg, E.L., McEvoy, L.M., Berlin, C., Bargatze, R.F., and Butcher, E.C. (1993) L-selectin-mediated lymphocyte rolling on MAdCAM-1. *Nature* **366**, 695-698 selectin O-link

Boesze-Battaglia, K. and Albert, A.D. (1989) Fatty acid composition of bovine rod outer segment plasma membrane. *Exp. Eye. Res.* **49**, 699-701

Bok, D. (1989) Retinal photoreceptor disc shedding and pigment epithelium phagocytosis. In: Retina. Ryan, S.J., Odgen, T.E., and Schachat, A.P. (eds), St. Louis, Missouri: The C.V. Mosby Company, 69-81

Bönigk, W., Altenhofen, W., Müller, F., et al., (1993) Rod and cone photoreceptor cells express distinct genes for cGMP-gated channels. *Neuron* **10**, 865-877

Bridge, J.H., Smolley, J.R. and Spitzer, K.W. (1990) The relationship between charge movements associated with ICa and INa-Ca in cardiac myocytes. *Science* **248**, 376-378

Burant, C.F., and Bell, G.I. (1992) Mammalian facilitative glucose transporters: evidence for similar substrate recognition sites in functionally monomeric proteins. *Bioc.* **31**, 10414-10420

Casey, J.R., and Reithemeier, R.A.F. (1991) Analysis of the oligomeric state of band 3, the anion transport protein of the human erythrocyte membrane, by size exclusion high performance liquid chromatography. *J. Biol. Chem.* **266**, 15726-15737

Casey, J.R., and Reithemeier, R.A.F. (1993) Detergent interaction with band 3, a model polytopic membrane protein. *Bioc.* **32**, 1172-1179

Carafoli, E. (1987) Intracellular calcium homeostasis. *Annu. Rev. Biochem.* **56**, 395-433.

Cervetto, L., Lagnado, L., Perry, R.J., Robinson, D.W., and McNaughton, P.A. (1989) Extrusion of calcium from rod outer segments is driven by both sodium and potassium gradients. *Nature* **337**, 740-743

Chen, C. and Okayama, H. (1987) High-efficiency transformation of mammalian cells by plasmid DNA. *Mol. Cell. Biol.* **7**, 2745-2752

Chen, C.K., Inglese, J., Lefkowitz, R.J. and Hurley, J.B. (1995) Ca(2+)-dependent interaction of recoverin with rhodopsin kinase. *J. Biol. Chem.* **270**, 18060-18066

Chen, C.K., Wieland, T., and Simon, M.I. (1996) RGS-r, a retinal specific RGS protein, binds an intermediate conformation of transducin and enhances recycling. *Proc. Natl. Acad. Sci. USA.* **93**, 12885-12889

Cheon, J., and Reeves, J.P. (1988) Site density of the sodium-calcium exchange carrier in reconstituted vesicles form bovine cardiac sarcolemma. *J. Biol. Chem.* **263**, 2309-2315

Chiu, M.I., Zack, D.J., Wang, Y. and Nathans, J. (1994) Murine and bovine blue cone pigment genes: cloning and characterization of two new members of the S family of visual pigments. *Genomics.* **21,** 440-3

Clarke, S. (1975) The size and detergent binding of membrane proteins. *J.Biol. Chem.* **250**, 5459-5469

Cobbs, W.H. and Pugh, E.N. (1986) Two components of outer segment membrane current in salamander rods and cones. *Biophys. J.* **49,** 280a

Conradt, M., Storck, T., and Stoffel, W. (1995) Localization of N-glycosylation sites and functional role of the carbohydrate units of GLAST-1, a cloned rat brain L-glutamate/L-aspartate transporter. Eur. J. Biochem. 229, 682-687

Cook, J.J., Molday, L.L., Reid, D., Kaupp, U.B., and Molday, R.S. (1989) The cGMP-gated channel of bovine rod photoreceptors is localized exclusively in the plasma membrane. *J. Biol. Chem.* **264**, 6996-6999

Cook, N.J. and Kaupp, U.B.(1988) Solubilization, purification and functional reconstitution of the sodium-calcium exchanger from bovine rod outer segments. *J. Biol. Chem.* **263**, 11382-11388

Copenhagen, D.R., and Jahr, C.E. (1989) Release of endogenous excitatory amino acids from turtle photoreceptors. *Nature* **341**, 356-359

Counillon, L., Pouyssegur, J. and Reithmeier, R.A. (1994) The Na^+/H^+ exchanger NHE-1 possesses N- and O-linked glycosylation restricted to the first N-terminal extracellular domain. *Biochemistry* **33**, 10463-9

Crespo, L.M., Grantham, C.J. and Cannell, M.B. (1990) Kinetics, stoichiometry and role of the Na-Ca exchange mechanism in isolated cardiac myocytes. *Nature* **339**, 476-478

Cuatrecasas, P. (1970) Protein purification by affinity chromatography. Derivatizations of agarose and polyacrylamide beads. *J. Biol. Chem.* **245**, 3059-3065

Dahan, D., Spanier, R. and Rahamimoff, H. (1991) The modulation of rat brain Na^+-Ca^{2+} exchange by K^+. *J. Biol. Chem.* **266**, 2067-75

De Haën, C., (1987) Molecular weight standards for calibration of gel filtration and sodium dodecyl sulfate-polyacrylamide gel electrophoresis: ferritin and apoferritin. *Anal. Biochem.* **166**, 235-245.

Dizhoor, A.M., Olshevskaya, E.V., Henzel, W.J., Wong, S.C., Stults, J.T., Ankoudinova, I., and Hurley, J.B. (1995) Cloning, sequencing, and expression of a 24 kDa Ca^{2+} binding protein activating photoreceptor guanylyl cyclase. *J. Biol. Chem.* **270**, 25200-25206

Doering, A.E. and Lederer, W.J. (1994) The action of Na^+ as a cofactor in the inhibiton by cytoplasmic protons of the cardiac Na^+-Ca^{2+} exchanger in the guinea-pig. *J. Physiol.* **480**, 9-20

Dosé, A. (1995) Molecular characterization of the cyclic nucleotide-gated cation channel of bovine rod outer segments. Ph. D. Thesis. University of British Columbia

Durkin, J.T., Ahrens, D.C., Pan, Y.-C.E. and Reeves, J.P. (1991) Purification and amino-terminal sequence of the bovine cardiac sodium-calcium exchanger: evidence for the presence of a signal sequence. *Arch. Biochem. Biophys.* **290**, 369-375

Eisner, D.A. and Lederer, W.J. (1985) Na-Ca exchange: Stoichiometry and elecrogenicity. *Am. J. Physiol.* **248**, C189-C202

Fafournoux, P., Noel, J., and Pouyssegur, J. (1994) Evidence that Na^+/H^+ exchanger isoforms NHE1 and NHE3 exists a stable dimers in membranes with a high degree of specificity for homodimers. *J. Biol. Chem.* **269**, 2589-2596

Faurobert, E., and Hurley, J.B. (1997) The core domain of a new retina specific RGS protein stimulates the GTPase activity of transducin *in vitro*. *Proc. Natl. Acd. Sci. USA.* **94**, 2945-2950

Fesenko, E.E., Kolesnikov, S.S., and Lyubarsky, A.L. (1985) Induction by cyclic GMP of cationic conductance in plasma membrane of retinal rod outer segment. *Nature* **313**, 310-313

Friedel, U., Wolbring, G., Wohlfart, P. and Cook, N.J. (1991) The sodium-calcium exchanger of bovine rod photoreceptors: K^+ dependence of the purified and reconstituted protein. *Biochim. Biophys. Acta* **1061**, 247-252

Fukuda, M. (1991) Leukosilain, a major O-glycan-containing sialoglycoprotein defining leukocyte differentiation and maligancy. *Glycobiology* **1**, 347-356

Fukuda, M. (1993) Molecular genetics of the glycophorin A gene cluster. *Semin. Hematol.* **30**, 138-151

Goding, J.W.ed. (1986) Monoclonal Antibodies. Principals and Practice. 2nd ed. Academic Press, London

Goldberg, A.F., Moritz, O.L. and Molday, R.S. (1995) Heterologous expression of photoreceptor peripherin/rds and Rom-1 in COS-1 cells: assembly, interactions, and localization of multisubunit complexes. *Biochemistry* **34**, 14213-9

Gray-Keller, M.P. and Detwiler, P.B. (1994) The calcium feedback signal in the phototransduction cascade of vertebrate rods. *Neuron* **13**, 849-861

Gray-Keller, M.P., Biernbaum, M.S., and Bownds, M.D. (1990) Transducin activation in electropermeabilized frog rod outer segments is highly amplified, and a portion equivalent to phosphodiesterase remains membrane-bound. *J. Biol. Chem.* **265**, 15323-15332

Gray-Keller, M.P., Polans, A.S., Palczewski, K., and Detwiler, P.B. (1993) The effect of recoverin-like calcium-binding proteins on the photoresponse of retinal rods. *Neuron* **10**, 523-531

Grinstein, S., Ship, S. and Rothstein, A. (1978) Anion transport in relation to proteolytic dissection of band 3 protein. *Biochim. Biophys. Acta.* **507**, 294-304

Groves, J. D., and Tanner, M. J. (1994) Role of N-glycosylation in the expression of human band 3- mediated anion transport. *Mol. Membr. Biol.* **11**, 31-38

Gurevich, V.V. and Benovic, J.L. (1992) Cell-free expression of visual arrestin. Truncation mutagenesis identifies multiple domains involved in rhodopsin interaction. *J. Biol. Chem.* **267**, 21919-21923

Haase, W., Friese, W., Gordon, R.D., Muller, H. and Cook, N.J. (1990) Immunological characterization and localization of the Na+/Ca2(+)-exchanger in bovine retina. *J. Neuroscience.* **10**, 1486-94

He, Z., Doering, A., Lu, L., and Philipson, K.D. (1996) Cloning of a squid Na^+-Ca^{2+} exchanger: NCX-SQ1. *Biophys. J.* **70**, A201

Heimer, G.V. and Taylor, C.E. (1974) Improved mountant for immunofluorescence preparations. *J. Clin. Pathol.* **27,** 254-256

Hestrin, S. and Korenbrot, J.I. (1990) Activation kinetics of retinal cones and rods: Response to intense flashes of light. *J. Neurosci.* **10**, 1967-1973

Hilgemann, D.W. and Ball, R. (1996) Regulation of cardiac Na^+-Ca^{2+} exchange and K_{ATP} potassium channels by PIP_2. *Science* **273**, 956-959

Hilgemann, D.W., Nicoll, D.A., and Philipson, K.D. (1991) Charge movement during Na^+ translocation by native and cloned cardiac Na^+/Ca^{2+} exchanger. *Nature* **352**, 715-718

Hjelmeland, L.M., Nebert, D.W. and Osborne, J.C. (1983) Sulfobetaine derivatives of bile acids: non-denaturing surfactants for membrane biochemistry. *Anal. Bioc.* **130**, 72-82

Hryshko, L.V., Nicoll, D.A., Weiss, J.N. and Philipson, K.D. (1993) Biosynthesis and initial processing of the cardiac sarcolemmal Na^+-Ca^{2+} exchanger. *Biochim. Biophys. Acta* **1151**, 35-42

Hsu, S.-C., and Molday, R.S. (1991) Glycolytic enzymes and a GLUT-1 glucose transporter in the outer segments of rod and cone photoreceptor cells. *J. Biol. Chem.* **266**, 21745-21752

Hsu, Y.-T. and Molday, R.S. (1993) Modulation of the cGMP-gated channel of rod photoreceptor cells by calmodulin. *Nature* **361**, 76-79

Hsu, Y.T., Wong, S.Y., Connell, G.J., and Molday, R.S. (1993) Structural and functional properties of rhodopsin form rod outer segment disk and plasma membrane. *Biochim. Biophys. Acta* **1145**, 85-92.

Huppertz, B. and Bauer, P.J. (1994) Na^+-Ca^{2+}-K^+ exchanger in bovine retinal rod outer segments: quantitative characterization of normal and reversed mode. *Biochim. Biophys. Acta* **1189**, 119-126

Hurley, J.B. and Stryer, L. (1982) Purification and characterization of the gamma regulatory subunit of the cyclic GMP phosphodiesterase from retinal rod outer segments. *J. Biol. Chem.* **257**, 11094-11099

Hurwitz, R.L., Bunt-Milam, A.H., Chang, M.L. and Beavo, J.A. (1985) cGMP phosphodiesterase in rod and cone outer segments of the retina. *J. Biol. Chem.* **260**, 568-73

Illing, M., Molday, L.L., and Molday, R.S. (1997) The 220-kDa rim protein of retinal rod outer segments is a member of the ABC transporter superfamily. *J. Biol. Chem.* **272**, 10303-10310

Iwamoto, T., Pan, Y. Wakabayashi, S., Imagawa, T., Yamanaka, H.I. and Shigekawa, M. (1996) Phosphorylation-dependent regulation of cardiac Na^+/Ca^{2+} exchanger via protein kinase C. *J. Biol. Chem.* **271**, 13609-13615

Jan, L.Y. and Revel, J.P. (1974) Ultrastructural localization of rhodopsin in the vertebrate retina. *J. Cell. Biol.* **62**, 257-273

Jentoft, N. (1990) Why are proteins O-glycosylated? *Trends Bioc Sciences.* **15**, 291-4

Khananshvili, D. (1991) Voltage-dependent modulation of ion binding and translocation in the cardiac Na-Ca exchange system. *J. Biol. Chem.* **266**, 13764-13769

Kawamura, S. (1993) Rhodopsin phosphorylation as a mechanism of cyclic GMP phosphodiestersase regulation by S-modulin. *Nature* **362**, 355-357

Kelm, S., Schauer, R., and Crocker, P.R. (1996) The sialo adhesins- A family of sialic acid dependent cellular recognition molecules within the immunoglobulin superfamily. *Glycoconjugate J.* **11**, 913-926.

Kimura, M., Aviv, A., and Reeves, J.P. (1993) K^+-dependent Na^+/Ca^{2+} exchange in human platelets. *J. Biol. Chem.* **268**, 6874-6877

Kimura, J., Miyamae, S. and Noma, A. (1987) Identification of sodium-calcium exchange current in single ventricular cells of guinea-pig. *J. Physiol.* **384**, 199-222

Kimura, J., Noma, A. and Irisawa, H. (1986) Na-Ca exchange current in mammalian heart cells. *Nature* **319**, 596-597

Klenchin, V.A., Calvert, P.D. and Bownds, M.D. (1995) *J. Biol. Chem.* **270**, 18060-18066

Koch, K.W. (1995) Control of photoreceptor proteins by Ca^{2+}. *Cell Calcium* **18**, 314-321

Kraev, A., and Carafoli, E. (1998) A gene family, coding for sodium-calcium exchangers in C. elegans. unpublished gi |2826837|

Kraev, A.S., Bertaggia, D. and Carafoli, E. (1998) Two distinct gene families code for Na/Ca and Na/Ca, K exchangers. unpublished gi |3096956|

Laemmli, U.K. (1970) Cleavage of structural proteins during the assembly of the head of bacteriophage T4. *Nature* **227**, 680-5

Lagnado, L., Cervetto, L. and McNaughton, P.A. (1988) Ion transport by the Na-Ca exchange in isolated rod outer segments. *Proc. Natl. Acad. Sci. USA* **85**, 4548-4552

Lagnado, L., Cervetto, L. and McNaughton, P.A. (1992) Calcium homeostasis in the outer segments of retinal rods from the tiger salamander. *J. Physiol.* **455**, 111-142

Lagnado, L. and McNaughton, P.A. (1990) Electrogenic Properties of the Na/Ca exchange. *J. Membrane Biol.* **113**, 177-191

Lamola, A.A., Yamane, T. and Zipp, A. (1974) Effects of detergents and high pressures upon the metarhodopsin I--metarhodopsin II equilibrium. *Biochemistry* **13**, 738-45

Lasky, L.A. (1992) Slectins: interpreters of cell-specific carbohydrate information during inflammation. *Science* **258**, 964-969

Lasky, L.A., Singer, M.S., Dowbenko, D., Imai, Y., Henzel, W.J., Grimley, C., et al. (1992) An endothelial ligand for L-selectin in a novel mucin-like molecule. *Cell* **69**, 927-938

Laurent, T.C. and Killander, J. (1964) A theory of gel filtration and its experimental verification. *J. Chromatogr.* **14**, 317-330

Lerea, C.L., Somers, D.E., Hurley, J.B., Klock, I.B. and Bunt-Milam, A.H. (1986) Isolation of specific transducin α-subunits in retinal rod and cone photoreceptors. *Science* **234**, 77-80

Levitsky, D.O., Nicoll, D.A. and Philipson, K.D. (1994) Identification of the high affinity Ca(2+)-binding domain of the cardiac Na(+)-Ca2+ exchanger. *J. Biol. Chem.* **269**, 22847-52

Li, Z., Burke, E.P., Frank, J.S., Bennett, V., and Philipson, K.D. (1993) The cardiac Na^+-Ca^{2+} exchanger binds to the cytoskeletal protein ankyrin. *J. Biol. Chem.* **268**, 11489-11491.

Li, Z., Matsuoka, S., Hryshko, L.V., Nicoll, D.A., Bersohn, M.M., Burke, E.P., Lifton, R.P. and Philipson, K.D. (1994) Cloning of the NCX2 isoform of the plasma membrane Na^+-Ca^{2+} exchanger. *J. Biol. Chem.* **269**, 17434-17439

Li, Z., Nicoll, D.A., Collins, A., Hilgemann, D.W., Filoteo, A.G., Penniston, J.T., Weiss, J.N., Tomich, J.M. and Philipson, K.D. (1991) Identification of a peptide inhibitor of the cardiac sarcolemmal Na(+)-Ca2+ exchanger. *J. Biol. Chem.* **266**, 1014-20

Lindenthal, S., and Schubert, D., (1991) Monomeric erythrocyte band 3 protein transports anions. Proc. Natl. Acad. Sci. U.S.A. **88**, 6540-6544

Lindsey, A.E., Schneider, K., Simmons, D.M., Baron, R., Lee, B.S. and Kopito, R.R. (1990) Functional expression and subcellular localization of an anion exchanger cloned from choroid plexus. *Proc. Natl.Acad. Sci. U.S.A.* **87**, 5278-82

López-Corcuera, B., Alcántara, R., Vázquez, J., and Aragón, C. (1993) Hydrodynamic properties and immunological identification of the sodium- and chloride- coupled glycine transporter. **266**, 2239-2243

Low, P.S. (1986) Structure and function of the cytoplasmic domain of band 3: center of erythrocyte membrane-peripheral protein interactions. *Biochim. Biophys. Acta* **864**, 145-167

Low, W., Kasir, J., and Rahaminoff (1993) Cloning of the rat heart Na^+-Ca^{2+} exchanger and its functional expression in HeLa cells. *FEBS Letter* **316**, 63-67

Lowe, D.G., Dizhoor, A.M., Liu, K., Gu, Q., Spencer, M., Laura, R., Lu, L., and Hurley, J.B. (1995) Cloning and expression of a second photoreceptor-specific membrane retina guanylyl cyclase (RetGC), RetGC-2. *Proc. Natl. Acad. Sci. USA* **92**, 5535-5539

Lutz, D.A., Guo, Y., and McLaughlin, B.J. (1995) Natural, high-mannose glycoproteins inhibit ROS binding and ingestion by RPE cell cultures. *Exp. Eye Res.* **61**, 487-493

Mackenzie, D. and Molday, R.S. (1982) Organization of rhodopsin and a high molecular weight glycoprotein in rod photoreceptor disc membranes using monoclonal antibodies. *J. Biol. Chem.* **257**, 7100-7105

Maruyama, K., Mikawa, T., and Ebashi, S. (1984) Detection of calcium binding proteins by $^{45}Ca^{2+}$ autoradiography on nitrocellulose membrane after sodium dodecyl sulfate gel electrophoresis. *J. Biochem.* **95**, 511-519

Matsuoka, S. and Hilgemann, D.W. (1992) Steady-state and dynamic properties of cardiac sodium-calcium exchange: Ion and voltage dependencies of the transport cycle. *J. Gen. Physiol.* **100**, 963-1001

Matsuoka, S., Nicoll, D.A., He, Z. and Philipson, K.D. (1997) Regulation of the cardiac Na^+-Ca^{2+} exchanger by the endogenous XIP region. *J. Gen. Physiol.* **109**, 273-286

Matsuoka, S., Nicoll, D.A., Hryshko, L.V., Levitsky, D.O., Weiss, J.N. and Philipson, K.D. (1995) Regulation of the cardiac Na^+-Ca^{2+} exchanger by Ca^{2+}: mutational analysis of the Ca^{2+} binding domain. *J. Gen. Physiol.* **105**, 403-420

Matsuoka, S., Nicoll, D.A., Reilly, R.F., Hilgemann, D.W. and Philipson, K.D. (1993) Initial localization of regulatory regions of the cardiac sarcolemmal Na^+-Ca^{2+} exchanger. *Proc. Natl. Acad. Sci.U.S.A.* **90**, 3870-4

Matthews, H.R., Murphy, R.L.W., Fain, G.L. and Lamb, T.D. (1988) Photoreceptor light adaptation is mediated by cytoplasmic calcium concentration. *Nature* **334**, 67-69

Melikian, H.E., McDonald, J.K., Gu, H., Rudnick, G., Moore, K.R., and Blakely, R.D. (1994) Human norepinephrine transporter; biosynthetic studies using a site-directed polyclonal antibody. *J. Biol. Chem.* **269**, 12290-12297

Miura, Y. and Kimura, J. (1989) Sodium-calcium exchange current: Dependence on internal Ca and Na and competitive binding of external Na and Ca. *J. Gen. Physiol.* **93**, 1129-1145

Molday, L.L. and Molday, R.S. (1987) Glycoproteins specific for the retinal rod outer segment plasma membrane. *Biochim. Biophy. Acta* **897**, 335-40

Molday, R.S. and Molday, L.L. (1998) Molecular properties of the cGMP-gated channel of rod photoreceptors. *Vision Res.* **38**, 1315-1323

Molday, R.S., Hicks, D., and Molday, L. (1987) Peripherin. A rim-specific membrane protein of rod outer segment discs. *Inves. Ophth. Vis. Sci.* **28**, 50-61

Morgans, C.W., Far, O.E., Berntson, A., Wässle, H., and Taylor, W.R. (1998) Calcium extrusion from mammalian photoreceptor terminals. *J. Neurosci.* **18**, 2467-2474

Moritz, O.L. and Molday, R.S. (1996) Molecular cloning, membrane topology, and localization of bovine rom-1 in rod and cone photoreceptor cells. *Invest. Opthalmol. Vis. Sci.* **37**, 352-362

Nakatani, K. and Yau, K.-W. (1989) Sodium-dependent calcium extrusion and sensitivity regulation in retinal cones of the salamander. *J. of Physiol.* **409**, 525-548

Nakatani, K. and Yau, K.-W. (1988) Calcium and magnesium fluxes across the plasma membrane of the toad rod outer segment. *J. Physiol. (Camb.)* **395**, 695-729

Nakatani, K. and Yau, K.-W. (1988b) Calcium and light adaptation in retinal rods and cones. *Nature* **334**, 69-71

Nicoll, D.A. and Applebury, M.L. (1989) Purification of the bovine rod outer segment Na^+/ Ca^{2+} exchanger. *J. Biol. Chem.* **264**, 16207-162113

Nicoll, D.A., Barrios, B.R. and Philipson, K.D. (1991) Na^+-Ca^{2+} exchangers from the rod outer segments and cardiac sarcolemma: comparison of properties. *Am. J. Physiol.* **260** (*Cell Physiol.* **29**) C1212-C1216

Nicoll, D.A., Longoni, S. and Philipson, K.D. (1990) Molecular cloning and functional expression of the cardiac sarcolemmal Na^+-Ca^{2+} exchanger. *Science* **250**, 562-565

Nicoll, D.A., Quednau, B.D., Qui, Z., Xia, Y.-R., Lusis, A.J. and Philipson (1996a) Cloning of a third mammalian Na^+-Ca^{2+} exchanger, NCX3. *J. Biol. Chem.* **271**, 24914-24921

Nicoll, D.A., Hryshko, L.V., Matsuoka, S., Frank, J.S. and Philipson, K.D. (1996b) Mutation of amino acid residues in the putative transmembrane segments of the cardiac sarcolemmal Na-Ca exchanger. *J. Biol. Chem.* **271**, 13385-13391

Niggli, E., and Lederer, W.J. (1991) Molecular operations of the sodium-calcium exchanger revealed by conformation currents. *Nature* **349**, 621-624

Nir, I., Cohen, D. and Papermaster, D.S. (1984) Immunocytochemical localization of opsin in the cell membrane of developing rat retinal photoreceptors. *J. Cell Biology* **98,** 1788-95

Nunez, E. and Aragon, C. (1994) Structural analysis and functional role of the carbohydrate component of glycine transporter. *J. Biol. Chem.* **269**, 16920-16924

Olivares, L., Aragon, C., Gimenez, C., and Zafra, F. (1995) The role of N-glycosylation in the targeting and activity of the GLYT1 glycine transporter. *J. Biol. Chem.* **270**, 9437-9442

Olivares, L., Aragón, C., Giménez, C., and Zafra, F. (1997) Analysis of the transmembrane topology of the glycine transporter GLYT1. *J. Biol. Chem.* **272**, 1211-1217

Osterberg, G. (1935) Topography of the layer of rods and cones in the human retina. *Act. Ophthalmol.* (Copenh.) **6**, 1-102

Palczewski, K., Buczylko, J., Imami, N.R., McDowell, J.H. and Hargrave, P.A. (1991) Role of the carboxyl-terminal region of arrestin in binding to phosphorylated rhodopsin. *J.Biol. Chem.* **266**, 15334-15339

Palczewski, K. (1994) Is vertebrate phototransduction solved? New insights into the molecular mechanism of phototransduction. *Invest. Ophth. Vis. Sci.* **35**, 3577-3581

Palczewski, K., Subbaraya, I., Gorczyca, W.A., Helekar, B.S., Ruiz, C.C., Ohguro, H., Huang, J., Zhao, X., Crabb, J.W., and Johnson, R.S. (1994) Molecular cloning and characterization of retinal photoreceptor guanylyl cyclase-activating protein. *Neuron* **13**, 395-404

Papermaster, D.S. and Dreyer, W.J. (1974) Rhodopsin content in the outer segment membranes of bovine and frog retinal rods. *Biochemistry* **13,** 2438-44

Papermaster, D.S., Schneider, B.G., Zorn, M.A., and Kraehenbuhl, J.P. (1978) Immunocytochemical localization of a large intrinsic membrane protein to the incisures and margins of frog rod outer segment disks. *J. Cell Biol.* **78**, 415-425

Perry, R.J. and McNaughton, P.A. (1993) The mechanism of ion transport by the Na^+-Ca^{2+}, K^+ exchange in rods isolated form the salamander retina. *J. Physiol.* **466**, 443-480

Pessino, A., Hebert, J.M., Woon, C.W., Harrison, S.A., Clancy, B.M., Buxton, J.M., Carruthers, A., and Czech, M.P. (1991) Evidence that functional erythrocyte-type glucose transporters are oligomers. *J. Biol. Chem.* **266**, 20213-20217

Philipson, K.D. (1990) The cardiac Na^+-Ca^{2+} exchanger. In: Calcium and the heart. Langer, G.A. (ed), New York: Raven, 85-107

Philipson, K.D. and Nicoll, D.A. (1993) Molecular and kinetic aspects of sodium-calcium exchange. *Intern. Rev. Cytol.* **137C**, 199-227

Philipson, K.D. and Nishimoto, A.Y. (1981) Efflux of Ca^{2+} from cardiac sarcolemmal vesicles. Influence of external Ca^{2+} and Na^+. *J. Biol. Chem.* **256**, 3698-3702

Philipson, K.D. and Nishimoto, A.Y. (1982) Stimulation of Na^+-Ca^{2+} exchange in cardiac sarcolemmal vesicles by proteinase pretreatment. *Am. J. Physiol.*, **243**, C191-C195

Philipson, K.D. and Nishimoto, A.Y. (1984) Stimulation of Na-Ca exchange in cardiac sarcolemmal vesicles by phospholipase D. *J. Biol. Chem.* **259**, 16-19

Philipson, K.D., Longoni, S., and Ward, R. (1988) Purification of the cardiac Na-Ca exchange protein. *Biochim. Biophys. Acta* **945**, 298-306

Philipson, K.D. and Ward, R. (1985) Effect of fatty acids on Na-Ca exchange and Ca^{2+} permeability of cardiac sarcolemmal vesicles. *J. Biol. Chem.* **260**, 9666-9671

Piriev, N.I., Voczian, A.S., Ye, J., Kerner, B., Korneberg, J.R., and Farber, D.B. (1995) Gene structure and amino acid sequence of the human cone photoreceptor cGMP-phosphodiesterase alpha-subunit (PDEA2) and its chromosomal localization to 10q24. *Genomics* **28**, 429-435

Pisano, A., Redmond, J.W., Williams, K.L., and Gooley, A.A. (1993) Glycosylation sites identified by solid-phase Edman degradation: O-linked glycosylation motifs on human glycophorin A. *Glycobiology.* **3,** 429-35

Pittler, S.J., Lee, A.K., Altherr, M.R., Howard, T.A., Seldin, M.F., Hurwitz, R.L., Wasmuth, J.J. and Baehr, W. (1992) Primary structure and chromosomal localization of human and mouse rod photoreceptor cGMP-gated cation channel. *J. Biol. Chem.* **267**, 6257-62

Polans, A., Baehr, W., and Palczewski, K. (1996) Turned on by Ca^{2+}! The physiology and pathology of Ca^{2+}-binding proteins in the retina. *Trends Neurosci.* **19**, 547-554

Powell, T., Noma, A., Shioya, T. and Kozlowski, R.Z. (1993) Turnover rate of the cardiac Na^+-Ca^{2+} exchanger in guinea-pig ventricular myocytes. *J. of Physiol.* **472**, 45-53

Read, S.M. and Northcote, D.H. (1981) Minimization of variation in the response to different proteins of the Coomassie blue G dye-binding assay for protein *Anal. Biochem.* **116**, 53-64

Reeves, J.P. (1990) Sodium-calcium exchange. In: Intracellular calcium regulation. Bonner, F. (ed), New York: Alan, R. Liss, 305-347

Reeves, J.P. and Hale, C.C. (1984) The stoichiometry of the cardiac sodium-calcium exchange system. *J. Biol. Chem.* **259** 7733-7739

Reeves, J.P. and Sutko, J.L. (1979) Na-Na exchange in cardiac membrane vesicles. *Fed. Proc. Fed. Am. Soc. Exp. Biol.* **38**, 1199

Reid, D.M., Friedel, U., Molday, R.S., and Cook, N.J. (1990) Identification of the sodium-calcium exchanger as the major ricin-binding glycoprotein of bovine rod outer segments and its localization to the plasma membrane. *Biochemistry* **29**, 1601-1607

Reiländer, H., Achilles, A., Friedel, U., Maul, G., Lottspeich, F., and Cook, N.J. (1992) Primary structure and functional expression of the Na/Ca, K exchanger from bovine rod photoreceptors. *EMBO J.* **11**, 1689-1695

Roof, D. and Heuser, J.E. (1982) Surfaces of rod photoreceptor disk membranes: Intergral membrane components. *J. Cell Biol.* **95**, 487-500

Ruknudin, A., Valdivia, C., Kofuji, P., Lederer, W.J. and Schulze, D.H. (1997) Na^+/Ca^{2+} exchanger in Drosophila: cloning, expression, and transport differences. *Am. J. Physiol.* **273**, C257-C265

Sako, D., Chang, X.J., Barone, K.M., Vachino, G., White, H.M., Shaw, G., Veldman, G.M., Bean, K.M., Ahern, T.J., Furie, B., et al. (1993) *Cell* Expression cloning of a functional glycoprotein ligand for P-selectin. **75**, 1179-1186

Schnafp, J.L. and McBurney, R.N. (1980) Light-induced changes in membrane current in cone outer segments of tiger salamander and turtle. *Nature* **287**, 239-241

Schnetkamp, P.P.M. (1980) Ion selectivity of the cation transport system of isolated cattle rod outer segments: evidence of a direct communication between the rod plasma membrane and the rod disk membranes. *Biochim. Biophys. Acta* **598**, 66-90

Schnetkamp, P.P.M. (1989) Na/ Ca or Na/ Ca-K exchange in the outer segments of vertebrate rod photoreceptors. *Prog. Biophys. Mol. Biol.* **54**, 1-29

Schnetkamp, P.P.M. (1991) Optical measurement of Na-Ca-K exchange currents in intact outer segments isolated form bovine retinal rods. *J. Gen. Physiol.* **98**, 555-573

Schnetkamp, P.P.M. (1995) Chelating properties of the Ca^{2+} transport site of the retinal rod Na-Ca+K exchanger: evidence for a common Ca^{2+} and Na^+ binding site. *Biochemistry* **34**, 7282-7287

Schnetkamp, P.P.M. and Bownds, M.D. (1987) Sodium and cGMP-induced Ca^{2+} fluxes in frog rod photoreceptors. *J. Gen. Physiol.* **89**, 481-500

Schnetkamp, P.P.M. and Szerencsei, R.T. (1991) Effect of potassium ions and membrane potential on the Na-Ca-K exchanger in isolated intact bovine rod outer segments. *J. Biol. Chem.* **266**, 189-197

Schnetkamp, P.P.M., Basu, D.K. and Szerencsei, R.T. (1989) Na^+-Ca^{2+} exchange in bovine rod outer segments requires and transports K^+. *Am. J. Physiol.* **257** (*Cell Physiol.* **26**) C153-C157

Schentkamp, P.P.M., Basu, D.K., Li, X.-B. and Szerencsei, R.T. (1991a) Regulation of intracellular free Ca^{2+} in the outer segments of bovine retinal rods by Na-Ca-K exchange measured with fluo-3. *J. Biol. Chem.* **266**, 22983-22990

Schnetkamp, P.P.M., Li, X.-B., Basu, D.K. and Szerencsei, R.T. (1991b) Regulation of free cytosolic Ca^{2+} concentration in the outer segments of bovine retinal rods by Na-Ca-K exchange measured with fluo-3. *J. Biol. Chem.* **266**, 22975-22982

Schnetkamp, P.P.M., Szerencsei, R.T., and Basu, D.K. (1991c) Unidirectional Na^+, Ca^{2+}, and K^+ fluxes through the bovine rod outer segment Na-Ca-K Exchanger. *J. Biol. Chem.* **266**, 198-206

Schwarz, E.M. and Benzer, S. (1997) *Calx*, a Na-Ca exchanger gene of *Drosophila melanogaster*. *Proc. Natl. Acad. Sci. U.S.A.* **94**, 10248-10254

Schwarzer, A., Kim, T.S.-Y., Hagen, V., Molday, R.S., and Bauer, P.J. (1997) The Na/Ca-K Exchanger of Rod Photoreceptor Exists as a Dimer in the Plasma Membrane. *Bioc.* **36**, 13667-13676

Siegel, L.M. and Monty, K.J. (1966) Determination of molecular weights and frictional ratios of proteins in impure systems by use of gel filtration and density gradient centrifugation. Application to crude preparations of sulfite and hydroxylamine reductases. *Biochim. Biophys. Acta* **112**, 346-362

Shicida, H.(1983) Biochemistry of vision. New York, Academic Press, 20

Shichida, Y., Imai, H., Imamoto, Y., Fukada, Y. and Yoshizawa, T. (1994) Is chicken green-sensitive cone visual pigment a rhodopsin-like pigment? A comparative study of the molecular properties between chicken green and rhodopsin. *Biochemistry* **33**, 9040-9044

Shimizu-Matsumoto, A., Itoh, K., Inazawa, J., Nishida, K., Matsumoto, Y., Kinoshita, S., Matsubra, K., and Okubo, K. (1996) Isolation and chromosomal localization of the human cone cGMP phosphodiesterase gamma cDNA (PDE6H). *Genomics* **32**, 121-124

Shimizu, Y. and Shaw, S. (1993) Cell adhesion. Mucins in the mainstream *Nature*. **366**, 630-1

Shyjan, A.W., De Sauvage, F.J., Gillett, N.A., Goeddel, D.V., and Lowe, D.G. (1992) Molecular cloning of a retina-specific membrane guanylyl cyclase. *Neuron* **9**, 727-737

Sjostrand, F.S., and Kreman, M. (1978) Molecular structure of outer segment disks in photoreceptor cells. *J. Ultrstruc. Res.* **65**, 195-226

Smith, D.B. and Johnson, K.S.(1988) Single-step purification of polypeptides expressed in *Escherichia coli* as fusions with glutathione-S-transferase. *Gene* **67**, 31-40

Sober, H.A., Ed. (1968) *Handbook of Biochemistry*, Chemical Rubber Co., Cleveland, OH.

Spalton, D.J., Hitchings, R.A., and Hunter, P.A. eds. (1994) Atlas of clinical ophthalmology. 2nd ed. Wolfe Publishing, London.

Steck, T.L. (1972) Cross-linking the major proteins of the isolated erythrocyte membrane. *J. Mol. Biol.* **66**, 295-305

Stein, W.D. (1990) Carrier mediated transport: Facilitated difusion. In: Channels, carriers and pumps. Stein, W.D. (ed) San Diego, California: Academic Press, 127-169

Steinberg, R.H., Fisher, S.K., and Anderson, D.H. (1980) Disc morphogenesis in vertebrate photoreceptors. *J. Comp. Neurol.* **190**, 501-518

Tanford, C., Nozaki, Y., Reynolds, J.A. and Makino, S. (1974) Molecular characterization of proteins in detergent solutions. **13**, 2369-76

Tate, C.G. and Blakely, R.D. (1994) The effect of N-linked glycosylation on activity of the Na^+ and Cl^--dependent serotonin transporter expressed using recombinant baculovirus in insect cells. *J. Biol. Chem.* **269**, 26303-10

Tovée, M.J. (1996) Sensitivity, acuity and neural wiring. In: An introduction to the visual system. Cambridge, Cambridge University Press, 34-35

Towbin, H., Staehelin, T. and Gordon, J. (1979) Electrophoretic transfer of proteins from polyacrylamide gels to nitrocellulose sheets: procedure and some applications. *Proc. Natl. Acad. Sci. U.S.A.* **76**, 4350-4

Tsoi, M., Rhee, K.-H., Bungard, D., Li, X.-F., Lee, S.-L., Auer, R.N., and Lytton, J. (1998) Molecular cloning of a novel potassium-dependent sodium-calcium exchanger from the rat brain. *J. Biol. Chem.* **273**, 4155-4162

Tucker, J.E., Winkfein, R.J., Cooper, C.B. and Schnetkamp, P.P.M. (1998) cDNA cloning of the human retinal rod Na-Ca+K exchanger: comparison with a revised bovine sequence. *Invest. Ophthal. Vis. Sci.* **39**, 435-440

Turk, E., Kerner, C.J., Lostao, M.P., and Wright, E.M. (1996) Membrane topology of the human Na^+/Glucose cotransporter SGLT1. *J. Biol. Chem.* **271**, 1925-1934

Udovichenko, I.P., Cunnick, J., Gonazalez, K. and Takemoto, D.J. (1994) Funtional effect of phosphorylation of the photoreceptor phosphodiesterase inhibitory subunit by protein kinase C. *J. Biol. Chem.* **269**, 9850-9856

Usukura, J. and Yamada, E. (1981) Molecular organization of the rod outer segment. A deep-etching study with rapid freezing using unfixed frog retina. *Biomed. Res.* **2**, 177-193

Vermuri, R. and Philipson, K.D. (1988) Phospholipid composition modulates the Na-Ca exchange activity of cardiac sarcolemma in reconstituted vesicles. *Biochim. Biophys. Acta.* **937**, 258-268

Wakabayashi, S., Fafournoux, P., Sardet, C. and Pouyssegur, J. (1992) The Na+/H+ antiporter cytoplasmic domain mediates growth factor signals and controls "H^+-sensing". *Proc. Natl. Acad, Sci. U.S.A.* **89**, 2424-8

Weinman, E.J., Steplock, D.A. and Shenolikar, S. (1992) Trypsin digestion increases Na^+-H^+ exchange rates in native rabbit brush border membrane. *Miner. Electrolyte Metab.* **19**, 47-50

Wheeler, L.P., and Hinkel, P.C. (1981) Kinetic properties of the reconstituted glucose transporter from human erythrocytes. *J. Biol. Chem.* 256, 8907-8914

Worthington Enzyme Manual (1993) Worthington Biochemical Corp., Freehold, NJ.

Yang, R.B. and Garbers, D.L. (1997) Two eye guanylyl cyclases are expressed in the same photoreceptor cells and form homomers in preference to heteromers. *J. Biol. Chem.* **272**, 13738-42

Yau, K.-W. (1994) Phototransduction mechanism in retinal rods and cones. *Invest. Ophthal. Vis. Sci.* **35**, 9-32

Yau, K.-W. and Nakatani, K. (1984) Electrogenic Na-Ca exchange in retinal rod outer segments. *Nature* **311**, 661-663

Yau, K.-W. and Nakatani, K. (1985) Light-induced reduction of cytoplasmic free calcium in retinal rod outer segment. *Nature* **311**, 661-663

Yee, R., and Liebman, P.A. (1978) Light-activated phosphodiesterase of the rod outer segment. *J. Biol. Chem.* **253**, 8902-8909

Yoshizawa, T. (1994) Molecular basis for color vision. *Biophys. Chem.* **50**, 17-24.

Young, R.W. (1976) Visual cells and the concept of renewal. *Invest. Opthal. Vis. Sci.* **15**, 700-725

Zaleska, M.M and Erecinska, M. (1987) Involvement of sialic acid in high-affinity uptake of dopamine by synaptosomes from rat brain. *Neurosci. Lett.* **82**, 107-112

Zamyatnin, A.A. (1984) Amino acid, peptide, and protein volume in solution. *Annu. Rev. Biophys. Bioeng.* **13**, 145-165

APPENDIX

Partial Specific Volume of the Rod Exchanger

specific volumes of amino acid residues					
	mw	cm3/mol	# of aa	grams	cm3
gly	57.05	35.8	116	6617.8	4152.8
ala	71.07	52	88	6254.2	4576
val	99.13	82.4	80	7930.4	6592
leu	113.16	99.1	101	11429	10009
ile	113.16	99.1	67	7581.7	6639.7
phe	147.18	112.8	35	5151.3	3948
ser	87.08	51.9	94	8185.5	4878.6
thr	101.11	68.4	83	8392.1	5677.2
met	131.2	96.9	33	4329.6	3197.7
cys	103.14	65	6	618.84	390
tyr	163.18	114.7	18	2937.2	2064.6
trp	186.22	135.5	20	3724.4	2710
asp	114.08	65.4	57	6502.6	3727.8
glu	128.11	77.5	142	18192	11005
asn	114.1	69.6	33	3765.3	2296.8
gln	128.13	85.5	36	4612.7	3078
lys	129.18	100.1	51	6588.2	5105.1
arg	157.2	118.9	50	7860	5945
his	137.14	90.4	12	1645.7	1084.8
pro	97.12	72.6	77	7478.2	5590.2
H2O				18	6.6
total			1199	129815	92675
$V_{exchanger}$ (cm3/g)					0.7139

Velocity Sedimentation Calculations

vol of cylinder= tot vol -vol of 0.5 sphere [$V_s = 4/3(\pi)r^3$]

dist of cylinder= (vol of cylinder)/(vol of cylinder 1mm high)

tot dist = dist of cylinder + dist of 0.5 sphere

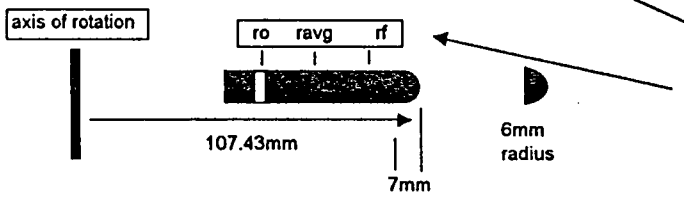

St,m= ([rf-ro]/t)/(revolutions)^{2}x(ravg)

vol at r_{avg} =vol of cylinder+1/2 vol of sphere
=((πr^2)h -7) + 0.5(4/3(π)r^3

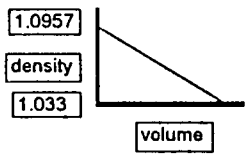

ravg density for H2O
y=mx+b
=[(1.0957-1.0331)/(0-4800)]xravg volume + 1.0957

ravg density for D2O
y=mx+b
=[(1.187-1.141)/(0-4800)]xravg volume + 1.187

% sucrose ravg =[(20-5)/(0-4800)]*ravg volume + 20

Plot ravg of marker proteins versus the viscosity to determine the viscosity of the unknown protein.

			J					
protein	catalase		3					
peak fraction	9.9		4	input				
total volume (µl)	1967.934		5	input				
Vt-Vs.5 (µl)	1559.294		6	J5-408.64				
distance of cylinder (mm)	13.78808		7	J6/113.09				
total distance (mm)	20.78808		8	J7+7				
rf (mm)	86.51192		9	107.3-J8				
r_{origin} (mm)	61.028		10	input				
r_{avg} (mm)	73.76996		11	(J10 + J9)/2				
length of run (h)	6.5		12	input				
time(sec)	23400		13	J12*3600				
speed (rpm)	49000		14	input				
speed (radians)	5131.268		15	(J14) 2π)/60				
$S_{t,m}$ (sec)	5.56E-13		16	(J9-J10)/(6.21e11*J11)				
			17					
volume at r_{avg} (mm)	3409.117		18	((3.1415*36)(107.43-J11)-7)+408.64				
			19					
r_{avg} density (g/cm^3)	1.051239		20	(((1.0957-1.0331)/(0-4800))*J18)+1.0957				
$S_{20,w}$ (sec)	1.13E-12		21	input				
v partial specific vol (cm^3/g)	0.73		22	input				
r_{avg} viscosity (g/(cm sec))	1.751247		23	(J21/J16)*((1-(J22*J20))/(1-(J22*0.9988)))*1.004				
%sucroseravg	9.34651		24	(((20-5)/(0-4800)*J18)+20				
			25					
protein	230K		26					
peak fraction	16.1		27					
total volume (µl)	3303.316		28					
Vt-Vs.5 (µl)	2894.676		29					
distance of cylinder (mm)	25.59622		30					
total distance (mm)	32.59622		31					
rf (mm)	74.70378		32					
r_{origin} (mm)	61.028		33					
r_{avg} (mm)	67.86589		34					
length of run (h)	6.5		35					
time(sec)	23400		36					
speed (rpm)	49000		37					
speed (radians)	5131.268		38					
$S_{t,m}$ (sec)	3.24E-13		39					
			40					
volume at r_{avg} (mm)	4076.851		41					
			42					
r_{avg} density	1.042531		43	(((1.0957-1.0331)/(0-4800))*J41)+1.0957				
r_{avg} viscosity(linear)	2.046861		44	(J34-31.7557)/17.6417				
%sucrose ravg	7.25984		45	(((20-5)/(0-4800)*J41)+20				

Sedimentation Calculations continued

$V_{complex}$ (ml/g)	0.738	$((S_D)(\eta_{Davg})/(S_H)(\eta_{Havg}))-1/((\rho_{Havg})(S_D)(\eta_{davg})/(S_H)(\eta_{havg}))-\rho_{Havg})$
$S_{20,w}$ (sec)	5.34	$((S_D(\eta_{Davg}/1.004))((1-((V_{complex})(0.9988)))/((1-((V_{complex})(\rho_{Davg})))$
$MM_{complex}$ (g/mol)	213364	$((6\pi)(N_A)(a)(S_{20,w})(\eta_{20,w}))/((1-((V_{complex})(\rho_{20,w})))$
g detergent/g protein	0.0141	$(V_{complex} - V_{protein})/(V_{TX-100} - V_{complex})$
$MM_{protein + carbohydrate}$	186986	$(MM_{complex})/(1 + (g\ detergent/g\ protein))$

Abbreviations:

vol	volume
dis	distance
tot	total
$S_{t,m}$	sedimentation coefficient at x°C in medium y
S_D	sedimentation coefficient in D2O
S_H	sedimentation coefficient in H2O
$S_{20,w}$	sedimentation coefficient in H2O at 20°C
η_{Davg}	viscosity in D2O
η_{Havg}	viscosity in H2O
ρ_{Davg}	density in D2O
ρ_{Havg}	density in H2O
$V_{complex}$	partial specific volume of complex
N_A	Avagadro's number (6.02E+23)
a	Stoke's radius
MM	molecular mass

CALCULATION OF THE [Ca]i

Derivation of the equation

$\overline{G} = G° + RT\ lnC + zF\Psi$ partial molar free energy or chemical potential (some text use the symbol μ)

$\overline{\Delta G} = (\overline{G}$ of ion inside) - ($\overline{G}$ of ion outside)
$\overline{\Delta G} = G° + RTlnC_i + zF\Psi - (G° + RTlnC_o + zF\Psi)$
$\overline{\Delta G} = RT\ (lnC_i - lnC_o) + zF\Delta\Psi$
$\overline{\Delta G} = RT\ (lnC_i/C_o) + zF\Delta\Psi$

To reach equilibrium: $\overline{G_{Ca}} + \overline{G_K} = \overline{G_{Na}}$ 4 Na^+

$RT\ ln[Ca]_i/[Ca]_o + 2F\Delta\Psi + RT\ ln\ [K]_i/[K]_o + 1F\Delta\Psi = 4\ (RT\ ln[Na]_i/[Na]_o + 1F\Delta\Psi)$
$RT\ ln[Ca]_i/[Ca]o = RT\ ln\ [K]_o/[K]_i + 4RT\ ln[Na]_i/[Na]_o + 4F\Delta\Psi - 2F\Delta\Psi - 1F\Delta\Psi$
$RT\ ln[Ca]_i/[Ca]o = RT\ ln\ [K]_o/[K]_i + 4RT\ ln[Na]_i/[Na]_o + F\Delta\Psi$
$ln[Ca]_i/[Ca]o = ln\ [K]_o/[K]_i + 4\ ln[Na]_i/[Na]_o + (F\Delta\Psi)/(RT)$

note $ln\ e = 1$
$e^x = 1/lnx$

ie. $[Ca]i = [Ca]_o([Na]_i/[Na]_o)^4([K]_o/[K]_i)\ exp(\Delta\Psi F/RT)$

If the ionic concentrations were as follows:

$[Na^+]i$ = 10 mM	R (gas constant)	8.314 J K^- mol^-
$[Na^+]o$ = 110 mM	F (Faraday's constant)	96,480 J V^- mol^-
$[K^+]i$ = 110 mM	T (temperature at 25°C)	298 K
$[K^+]o$ = 2.5 mM	z charge of ion	
[Ca]o = 1 mM		
$\Delta\Psi$ = -55 mV		

$[Ca]i = (1)((10)^4(2.5))/((110)^4(110))exp[((-0.055)(9.648x10^4))/((8.314)(298))]$
$[Ca]i = 1.8x10^{-10}$ M
0.18 nM

If an exchange stoichiometry of $3Na^+$ for $1Ca^{2+}$ were used, the [Ca]i would be calculated as follows:

$[Ca]_i = [Ca]_o\ ([Na]_i/[Na]_o)^3\ exp(V_mzF/RT)$

$[Ca]_i = (1)((10)^3(2.5))/((110)^3(110))exp[((-0.055)(9.648x10^4))/((8.314)(298))]$

$[Ca]_i = 8.8x10^{-8}$ M
88 nM